Regulation of the CCAAT-binding complex of *Aspergillus nidulans*

under oxidative stress and iron-depleting conditions

Dissertation
zur Erlangung des akademischen Grades doctor rerum naturalium
(Dr. rer. nat.)

vorgelegt dem Rat der Biologisch-Pharmazeutischen Fakultät
der Friedrich-Schiller- Universität Jena

von

Qusai Al Abdallah

geboren am 31.08.1975 in Kuwait

2008

1. Gutachter:

2. Gutachter:

3. Gutachter:

Datum der öffentlichen Verteidigung:

Abstract

The CCAAT-binding complex is an evolutionarily conserved heterotrimeric transcriptional factor in eukaryotes including fungi, plants and mammals. In *Aspergillus nidulans*, the corresponding complex was designated CBC (CCAAT-binding complex). CBC consists of three subunits HapB, HapC and HapE. Interestingly, only HapC contains three cysteine residues. To study the role of these cysteines on the stability of CBC in *A. nidulans*, the *hapC* gene was mutated, in which all three cysteines were exchanged by serines (*hapC3CS*) and by alanines (*hapC3CA*), and fused to *egfp*. The *hapC3CS*- and *hapC3CA-egfp* gene fusions were transformed in the *A. nidulans ΔhapC* strain. The generated strains recovered the *A. nidulans* wild-type phenotype indicating that HapC3CS and HapC3CA can form CBC with HapB and HapE subunits. However, the HapC3CS- and HapC3CA-EGFP fusion proteins were observed in both the nucleus and the cytoplasm, indicating that HapC cysteines contribute to the formation of a stable CBC.

Furthermore, the redox regulation of HapC under oxidative stress conditions was analyzed *in vivo*. The analysis of a HapC-EGFP fusion protein indicated that the regulation of HapC is dependent on the redox status of the cell. Oxidation of the HapC cysteine residues either by the addition of H_2O_2 to the growth medium or by deletion of the major thioredoxin-encoding gene (*trxA*) in *A. nidulans* led to the accumulation of HapC-EGFP in the cytoplasm. The regulation of HapC by TrxA was confirmed *in vivo* by applying bimolecular complementation (BiFC) assays in *A. nidulans* wild-type and *ΔhapE* strains.

Iron homeostasis is tightly controlled, as iron is both essential and toxic. Therefore, it was interesting to study the interaction of an additional CBC subunit designated HapX with the CBC under iron-depleting conditions. In contrast to CBC, which is functionally independent of iron, HapX mediates a novel mechanism of iron-dependent regulation. Interestingly, using BiFC, the interaction between HapX and HapB was observed under oxidative stress as well, which might be explained by the presence of overlapping and synchronized regulatory mechanisms against iron-limiting and oxidative stress conditions or the possibility of oxidative stress induction via iron starvation.

Finally, HapX possesses three possible TrxA-target CXXC motifs. Therefore, HapX posttranslational regulation by thioredoxin was analyzed in *A. nidulans* wild-type and *ΔhapC* strains using BiFC. The BiFC analysis revealed the possibility of HapX reduction by TrxA during oxidative stress and iron-depleting conditions.

This study provides a further understanding of the regulation of the CBC during oxidative stress and iron-depleting conditions and raises a number of questions concerning the interaction of other proteins with the CBC under different stress conditions.

Zusammenfassung

Der CCAAT-bindende Komplex ist ein heterotrimerer Transkriptionsfaktor und in Eukaryonten von Pilzen und Pflanzen, bis hin zu Säugetieren hoch konserviert. In *Aspergillus nidulans* wird der entsprechende Komplex CBC (CCAAT-binding complex) genannt. Dieser besteht aus den drei Untereinheiten HapB, HapC und HapE. Interessanterweise weist nur die HapC-Untereinheit drei Cysteine auf. Um den Einfluss dieser Cysteinreste auf die CBC-Stabilität zu untersuchen, wurde das *hapC*-Gen dahingehend verändert, dass die zuvor Cystein-kodierenden Codons zu Serin- bzw. Alanin-kodierenden Codons mutiert wurden. Des Weiteren wurden diese beiden mutierten Gene, *hapC3CS* und *hapC3CA* genannt, translational mit dem *egfp*-Gen fusioniert und in einen *A. nidulans hapC*-Deletionsstamm transformiert. Die aus der Transformation hervorgegangenen Stämme zeigten eine Komplementation des Δ*hapC*-Phänotyps im Vergleich zum Wildtyp. Daraus lässt sich schließen, dass die entsprechenden Genprodukte HapC3CS oder HapC3CA zusammen mit HapB und HapE einen funktionalen CBC bilden können. Dennoch konnten beide Fusionsproteine, HapC3CS-EGFP und HapC3CA-EGFP, sowohl im Zellkern, als auch im Zytoplasma lokalisiert werden, was die Schlussfolgerung zulässt, dass die Cysteine an sich schon eine entscheidende Rolle in Bezug auf die Stabilität des CBC spielen.

Weiterhin wurde die Redoxregulation von HapC unter oxidativem Stress *in vivo* untersucht. Lokalisationsstudien mit einem HapC-EGFP Fusionsprotein deuteten darauf hin, dass die Funktion von HapC, nämlich mit HapE und HapB einen funktionellen Transkriptionskomplex zu bilden, vom zellulären Redoxstatus abhängig sein könnte. So führte die Oxidation der Thiolgruppen der HapC-Cysteine durch die Zugabe von Wasserstoffperoxid zum Wachstumsmedium, oder die Deletion des Thioredoxin A (TrxA) codierenden Gens (*trxA*) in *A. nidulans* zu einer Anreicherung des HapC-EGFP-Fusionsproteins im Zytoplasma. Die Redoxregulation von HapC durch Thioredoxin A konnte sowohl in einem *A. nidulans* Wildtypstamm als auch in einem Δ*hapE*-Stamm mit Hilfe von bimolekularen Fluoreszenz-Komplementationsanalysen (BiFC) bestätigt werden.

Die Eisenverfügbarkeit ist in allen Lebewesen sehr exakt reguliert, da Eisen als Spurenelement zwar lebensnotwendig ist, in hohen Dosen aber auch toxisch sein kann. Aus diesem Grund sollte die Interaktion einer weiteren CBC-Untereinheit, HapX genannt, mit dem Kernkomplex, bestehend aus HapC/E/B, unter Eisenmangel-Bedingungen untersucht werden. Im Gegensatz zum CBC-Kernkomplex, welcher in seiner heterotrimären Form funktional unabhängig von Eisen ist, vermittelt HapX einen neuen eisenabhängigen Regulationsmechanismus im Zusammenspiel mit dem CBC-Kernkomplex. Interessanterweise

konnte in BiFC-Studien sowohl unter Eisenmangel, als auch unter oxidativem Stress eine Interaktion von HapX mit der CBC-Untereinheit HapB nachgewiesen werden. Dies legt die Vermutung nahe, dass die Interaktion von HapX mit HapB unter Eisenmangel und/oder oxidativem Stress auf überlappenden oder gleichen basalen Mechanismen beruht. Auch eine Induktion von oxidativem Stress unter Eisenmangel-Bedingungen kann generell nicht ausgeschlossen werden.

Weiterhin besitzt HapX drei CXXC-Motive, deren Disulfidform von TrxA erkannt werden kann. Aus diesem Grund wurde die posttranslationale Regulation von HapX durch Thioredoxin A in einem *A. nidulans* Wildtypstamm und einem Δ*hapC*-Stamm untersucht. Die BiFC-Ergebnisse deuten dabei auf eine Reduktion von HapX durch TrxA unter oxidativem Stress und unter Eisenmangel-Bedingungen hin.

Somit erweitert diese Arbeit das Verständnis zur Regulation des CBC, speziell unter oxidativem Stress und unter Eisenmangel-Bedingungen. Gleichzeitig wirft sie aber auch neue Fragen bezüglich der Interaktion weiterer Proteine mit dem CBC-Kernkomlex unter verschiedenen Stressbedingungen auf.

Contents

Abbreviations.

A	adenine	kbp	kilobase pairs
A.	*Aspergillus*	kDa	kilodalton
aa	Amino acid	l	Liter
Ala	Alanine (A)	LB	Luria Broth
AMM	*Aspergillus* minimal medium	min	minute
Amp	Ampicillin	mM	millimolar
bp	base pair	mRNA	messenger RNA
BiFC	Bimolecular fluorescence complementation	Mw	molecular weight
C	Cytosine	NF-Y	Nuclear factor Y
Cys	Cysteine (C)	NLS	Nuclear localization signal
°C	degrees Celsius	N-source	Nitrogen source
CBC	*Aspergillus nidulans* CCAAT-binding complex	N-terminal	amino-terminal
cDNA	DNA complementary to mRNA	OD	Optical density
C-source	Carbon source	ORF	open reading frame
C-terminal	carboxyl-terminal	PAGE	polyacrylamide gel electrophoresis
Δ	deletion	PBS	phosphate-buffered saline
Da	Dalton	PCR	polymerase chain reaction
DAPI	4',6-diamidino-2-phenylindole	PEG	polyethylene glycol
DNA	deoxyribonucleic acid	^{R}	resistance
dNTP	deoxyribonucleotide triphosphate	RNA	ribonucleic acid
EDTA	Ethylenediaminetetraacetic acid	ROS	reactive oxygen species
E.	*Escherichia*	rpm	rotations per minute
et al.	and others	SDS	Sodium dodecylsulfate
EMSA	electrophoretic mobility shift assay	Ser	Serine (S)
Fig.	figure	T	thymine
G	guanine	TE buffer	Tris/EDTA buffer
g	gram	U	Unit of enzyme activity
GFP	green fluorescent protein	UV	light ultraviolet light
h	hour	v/v	volume/volume
Hyg	hygromycin	w/v	weight/volume
IPTG	Isopropyl β-D-1-thiogalactopyranoside	wt	wild-type
Kan	kanamycin	YFP	yellow fluorescent protein

1. Introduction

1.1 *Aspergillus nidulans* **as model organism for filamentous fungi.**

Aspergillus nidulans belongs to the class Ascomycotina. The Ascomycotina (the ascomycetes) is the largest class of fungi. The ascomycetes can produce both asexual spores (conidia) and sexual spores (ascospores). They are characterized by having sexual spores, called ascospores, produced within an ascus. They include fungi with wide variation of habitats. Many of them are common as animal and plant pathogens, others are saprophytic and involved in the decomposition of plants and animals (Martinelli, 1994). *A. nidulans* is a saprophytic fungus. It can be isolated from soil and may also occur as mold on food. It is also able to utilize a wide range of different carbon and nitrogen sources (Ward, 1991). In the vegetative (asexual) life cycle of *A. nidulans*, the germinating conidia form a network of multinucleate hyphae. Afterwards, the conidiophore elongates from the footcell, a specialized thick-walled cell within the hyphae that anchors the stalk to the growth substratum. At the tip of the conidiophore, a swollen structure is formed, which is called conidiophore vesicle. The footcell, the conidiophore and the vesicle are unseptated from each other and form a single unit. The vesicle produces primary layer of uninucleate sterigmata (buds) called metulae. The metulae in turn bud twice to produce a second layer of uninucleate sterigmata termed phialides. The phialides produce chains of uninucleate spores called conidia (Fig. 1) (Adams et al., 1998).

Recently, the genome sequence of *A. nidulans* was released by the Broad Institute and (http://www.broad.mit.edu/annotation/fungi/aspergillus/index.html). The size of the *A. nidulans* genome is approximately 30,000 kbp. It has 8 chromosomes containing an estimated 10,000–11,000 gene.
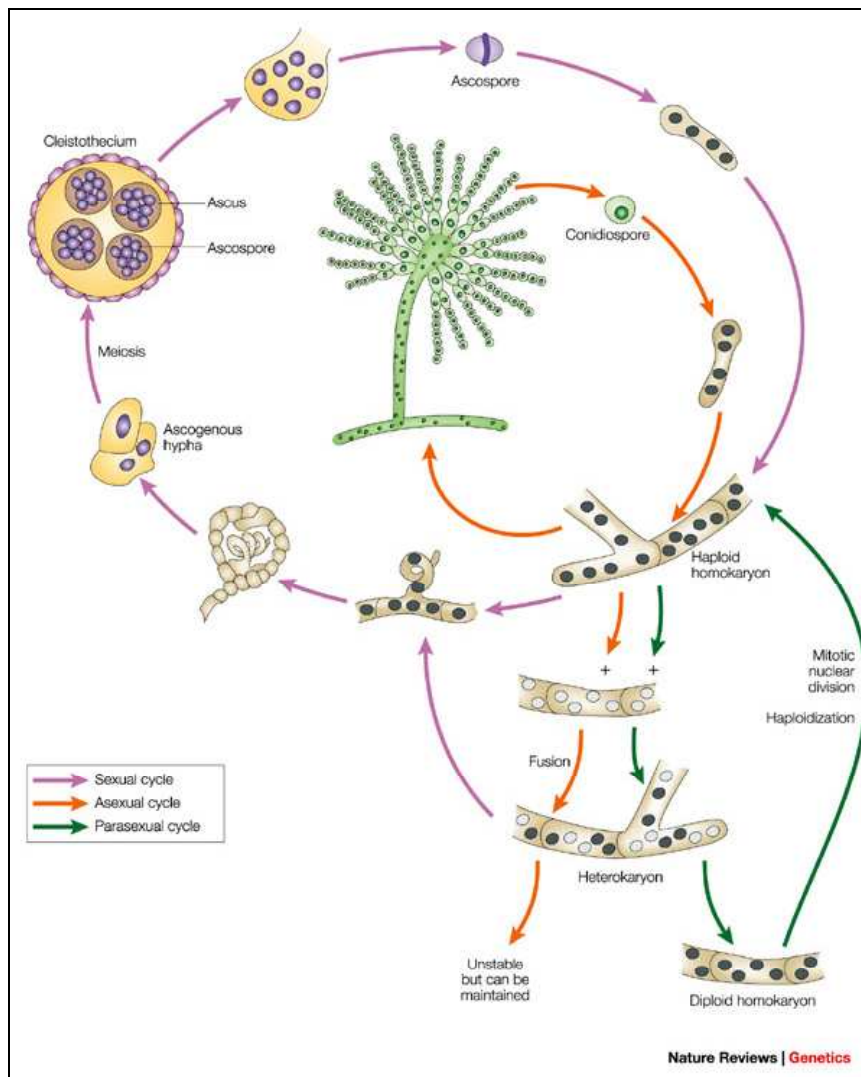
Fig. 1: The life cycle of *Aspergillus nidulans* (after Casselton and Zolan, 2002).

A. nidulans is a model organism for studies of cell biology and gene regulation in filamentous fungi. However, there are many features that *A. nidulans* combines, which made this fungus a good model organism (reviewed in Martinelli, 1994). *A. nidulans* is closely related to other *Aspergillus* species from Deuteromycetes, e.g. *A. fumigatus* which is a common pathogen, *A. niger* and *A. oryzae*, which are used in industry. Unlike the other Aspergilli, which are asexual, *A. nidulans* has a well-characterized and conventional genetic system. The success of several *Aspergillus* species for industrial production of biotechnological products is largely due to the metabolic versatility of this species. The filamentous fungus *A. niger*, for example, is well known to produce organic acids, enzymes, plant growth, and regulators. The industrial importance of *Aspergillus* species is not only dependent on their diverse products but also on the development and commercialization of the new products. This is normally achieved by

understanding of pathways related to secondary metabolism through the tools of genomics, proteomics, and metabolomics.

1.2 CCAAT box and CCAAT-binding complex (CBC) in eukaryotes.

The synthesis of most eukaryotic proteins is regulated at the level of transcription. Although transcription is performed by RNA polymerase, regulation of transcription of most eukaryotic genes is coordinated through sequence-specific binding of proteins to the promoter region located upstream of the gene. Many of these protein-binding sequences have been conserved during evolution and are found in a wide variety of organisms. One such feature is the CCAAT-box element (Gelinas et al., 1985). This motif is found in the promoter region of many eukaryotic genes located between 50 and 300 bp upstream of the transcriptional start point (Bucher 1990) and may operate in either orientation, with possible cooperative interactions with multiple boxes (Tasanen et al., 1992) or other conserved motifs (Muro et al., 1992; Rieping and Schöffl, 1992).

A conserved multimeric protein complex has been identified in different eukaryotes, ranging from lower fungi to human, which binds to the CCAAT box. Its binding consensus motif was determined by band shift assays as RRCCAATC/ARCR (reviewed in Brakhage, 1998). This complex was given different names for different organisms: Hap for *Saccharomyces cerevisiae* (Guarente et al., 1984; McNabb et al., 1995), *Kluyveromyces lactis* (Mulder et al., 1994), and *Arabidopsis thaliana* (Edwards et al., 1998), Php in *Schizosaccharomyces pombe* (McNabb et al., 1997), CBC for *Aspergillus nidulans* (reviewed in Brakhage et al., 1999), CBF in *Xenopus laevis* (Li et al., 1998), and NF-Y in mammals (Hooft van Huijsduijnen et al., 1990; Maity et al., 1990).

Generally, CCAAT binding complex in different organism is made up of three subunits. However, in the yeast *S. cerevisiae*, an additional subunit was identified, termed Hap4p (Forsburg and Guarente, 1989; McNabb et al., 1995). Orothologs of Hap4p have been cloned and characterized only in other yeast species *K. lactis* and *Hansenula polymorpha* until now (Bourgarel et al., 1999; Sybirna et al., 2005). Recently, a novel transcription factor, designated HapX, which interacts with CBC complex in *A. nidulans* was isolated (Tanaka et al., 2002). However, HapX does not seem to be the homologous protein of Hap4p (see 1.2.1.2).

In *Arabidopsis thaliana*, each subunit of the complex is not only represented by one subunit but rather by many subunits (Edwards et al., 1998; Gusmaroli et al., 2001, Yang et al., 2005).

1.2.1 The CBC of different organisms.

1.2.1.1 The Hap complex in yeast.

Proteins that bind to the CCAAT motif were first characterized in the yeast *Saccharomyces cerevisiae* through analysis of mutants with reduced levels of expression of the *CYC1* gene (encoding iso-1-cytochrome *c*) (Guarente et al., 1984; Hahn et al., 1988), termed Hap2p, Hap3p, and Hap5p. The Hap2p/Hap3p/Hap5p heterotrimer has been shown to be sufficient for CCAAT-specific binding at target promoters (McNabb et al., 1995); however, this complex lacks the ability to activate transcription. A fourth subunit of the complex, termed Hap4p, is necessary for transcriptional activation (Forsburg and Guarente, 1989). The yeast Hap4p protein neither binds to the DNA nor it is needed for DNA-binding. Rather, it associates with the Hap2p/3p/5p complex and activates transcription through an acidic domain (Forsburg and Guarente, 1989). Moreover, *HAP4* expression is inducible (DeRisi et al., 1997; Forsburg and Guarente, 1989), i.e. its expression is repressed in the presence of glucose and activated in its absence, while the expression of *HAP2, HAP3*, and *HAP5* is constitutive (DeRisi et al., 1997). Thus, the synthesis and interaction of Hap4p with Hap2p/Hap3p/Hap5p modulates the activity of target genes. Mutations that abolish the function of any of the four Hap subunits result in the inability of yeast to grow on non-fermentable carbon sources (Forsburg and Guarente, 1989; Hahn et al., 1988; McNabb et al., 1995; Pinkham et al., 1987), emphasizing the importance of this protein complex as a global regulator of respiration.

1.2.1.2 The CBC complex in *Aspergillus nidulans* (*syn*. PENR1, AnCP, AnCF, Hap complex).

CBC of *A. nidulans* consists of three subunits designated HapB, HapC and HapE, homologues of the Hap2p, Hap3p, and Hap5p subunits, respectively. The three subunits are encoded by three genes, termed *hapB*, *hapC* and *hapE* respectively. The three subunits are necessary and sufficient for binding of CBC to the DNA. Deletion of one of the *hap* genes resulted in strains (*Δhap* strains) with a characteristic phenotype of slow growth and poor conidiation (Papagiannopoulos et al., 1996; Steidl et al., 1999).

It has been found that CBC binds to the widespread CCAAT sequence present in the promoter regions of a variety of genes in *A. nidulans* including penicillin biosynthesis genes *acvA*, *ipnA* and *aatA* (Then Bergh et al., 1996; Litzka et al., 1996) and the acetamidase-encoding *amdS* (Littlejohn and Hynes, 1992). Using gel mobility shift assays with crude nuclear extracts have shown that CBC is involved in the regulation of the acetamidase gene *amdS*, a gene required for utilizing acetamide as the nitrogen and carbon source (van Heeswijck and Hynes 1991). Consequently, *hap* mutant strains does not grow on acetamide as the sole nitrogen and carbon source indicating that CBC plays a role in regulating *amdS* expression (Papagiannopoulos et al., 1996; Steidl et al., 1999). Deletion or mutagenesis of the CBC binding sites in the promoters of the penicillin biosynthesis genes had opposite effects; the expression of *acvA* increased 8-folds, while the expression of *ipnA* and *aatA* was reduced (Then Bergh et al., 1996; Litzka et al., 1996).

Using yeast two-hybrid screen, a gene encoding a novel transcriptional activator, which interacted with the CBC complex, was isolated from *A. nidulans* and designated HapX (Tanaka et al., 2002). HapX displays no similarity to *S. cerevisiae* Hap4p apart from an N-terminal 17 amino acid-motif, which was shown to be essential for interaction of Hap4p with the *S. cerevisiae* Hap complex (McNabb and Pinto, 2005). Deletion of *hapX* in *A. nidulans* did not result in a slow-growth and weak conidiation phenotype, a typical phenotype for a deletion of any of the three CBC subunit-encoding genes (Steidl et al., 1999). Furthermore, expression of *hapX* in a *Δhap4p* strain of *S. cerevisiae* did not complement the mutant phenotype suggesting that HapX in *A. nidulans* is not the homologous protein of Hap4p.

1.2.1.3 The NF-Y (or CBF) complex in vertebrates.

CCAAT-related motifs have also been identified in the promoters of a variety of vertebrate genes. A range of transcription factors has been shown to bind to different CCAAT boxes, with varying levels of specificity (Dorn et al., 1987; Raymondjean et al., 1988), and each is thought to play a distinct role in gene expression or DNA replication (Santoro et al., 1988). Direct homologues of the yeast HAP complex (called NF-Y or CBF) have been identified in vertebrates (Maity et al., 1990; Becker et al., 1991; Li et al., 1992; Sinha et al., 1995). The individual vertebrate HAP subunits showed a remarkable similarity to the yeast homologue over short domains (Maity et al., 1990; Vuorio et al., 1990), which is sufficient to enable formation of a functional heterologous complex between the human homologue and yeast Hap2p, Hap3p and Hap5p (Becker et al., 1991).

However, outside of the highly conserved core protein motifs associated with DNA binding and subunit interactions, there is considerable divergence. Furthermore, there is no Hap4p homologue. Instead, the vertebrate HAP complex probably interacts with other classes of transcription factors to influence the level of transcription (Bellorini et al., 1997).

1.2.1.4 The Hap complex in plants.

In contrast to yeast, *Aspergillus* and mammals, in which all the subunits are encoded by single copy genes, multiple and distinct genes for each subunits have been identified in plant genomes (Edwards et al., 1998). Yang et al. (2005) identified 30 Hap subunit genes in *Arabidopsis thaliana*, including 10 Hap2p homologues, 10 Hap3p homologues and 10 Hap5p homologues. Moreover, genome analysis of *Oryza sativa* (rice) revealed the presence of 5 Hap2p homologous proteins, 10 Hap3p homologous proteins and 10 Hap5p homologous proteins (Yang et al., 2005).

Northern blot analysis indicated ubiquitous expression for each AtHAP2 and AtHAP5 cDNA in a range of tissues, whereas expression of each AtHAP3 cDNA was under developmental and/or environmental regulation. The unexpected presence of multiple forms of each HAP homologue in *Arabidopsis*, compared with the single genes in yeast and vertebrates, suggests that the HAP2,3,5 complex may play diverse roles in gene transcription in higher plants (Edwards et al., 1998).

1.2.2 Regulation, assembly and nuclear localization of the CBC.

Regulation of the human CCAAT-binding protein (NF-Y) has been studied proposing that the cellular redox environment of mammalian cells is an important posttranscriptional regulator of NF-Y subunit association and DNA binding activities (Nakshatri et al., 1996). However, it has been suggested that highly conserved cysteine residues of NF-YB (human homologue of HapC) play an important regulatory role through protein-protein interaction of NF-YB (human homologue of HapC) with the NF-YC subunit (human homologue of HapE) in response to the redox status of the cell. According to their *in vitro* results, oxidized NF-YB must be reduced by ADF, a human thioredoxin, in order to form a heterodimer with NF-YB as a prerequisite for the heterodimer assembly. Once the NF-YC is reduced, the subsequent NF-Y complex assembly steps can proceed.

Studies made on CBF were used to explain the assembly process of the CCAAT binding complex (Sinha et al., 1996; Kim et al., 1996). Using motif searching method, CBF-A subunit (HapC homologue) and CBF-C subunit (HapE homologue) were identified as containing the histone fold motif, a structural feature common to all four core histones, which is involved in both histone-histone and histone-DNA interactions, in their domains (Baxevanis et al., 1995).

In mammalians, assembly of the CBF complex is achieved through a two-step pathway (Fig. 2-A). The first step in the complex assembly is the formation of heterodimer CBF-A (HapC homologue) and CBF-C (HapE homologue) through the conserved histone-fold motif in their domain (Baxevanis et al., 1995). Dimerization of CBF-A with CBF-C is an essential step in complex formation, in which CBF-B can only bind to the heterodimer but not to its single subunits (Liang and Maity, 1998). However, a study of crystal structure of heterodimer formed by the human NF-YB and NF-YC, found close interactions of the two proteins mediated through the histone fold motifs (Romier et al., 2003).

Subsequently, the second step of the complex formation is binding of CBF-B (HapB homologue) to the heterodimer. In another study, HapB has been found to contain a nuclear localization signal (NLS) in its domain, and HapC and HapE are transported to the nucleus only in a complex with HapB via a piggy back mechanism (Steidl et al., 2004). *In vitro* study showed that the association of CBF-B (HapB homologue) and the heterodimer formed by CBF-A and CBF-C (HapC-HapE heterodimer) is stabilized upon interaction with DNA (Liang and Maity, 1998).

As opposed to mammalian CBF, human NF-Y and *A. nidulans* CBC, yeast Hap complex is assembled via one-step pathway requiring all three subunits (Hap2p, Hap3p and Hap5p) (Fig. 2-B). Hap4p binds to the complex only after the complex has bound to the DNA (McNabb and Pinto, 2005).

1.3 Regulation the redox status of the cell by thioredoxin system.

1.3.1 Oxidative stress and the redox status of the cell.

Reactive oxygen species (ROS), including superoxide radicals (O_2-), hydrogen peroxide (H_2O_2) and hydroxyl radicals ($\cdot OH$), are oxygen containing molecules that possess a stronger reactivity than oxygen itself. ROS can be generated endogenously in many cells as by-products of normal cell activities. ROS can also be formed by exposure of cells to different chemical or environmental stresses. However, ROS are highly reactive modifying various

cellular molecules (proteins, lipids and nucleic acids), and therefore, elevated production of ROS is known to be harmful to the cell.

Cells respond to ROS by activating stress signalling pathways, which act to detoxify ROS or repair the resulting damage. They consist of different proteins such as thioredoxin, thioredoxin peroxidase, thioredoxin reductase, glutathione peroxidase, glutathione reductase, catalase, and superoxide dismutase, and tripeptide glutathione to protect their cellular constituents and maintain cellular redox state. Once the generation of ROS exceeds these scavenging and detoxifying mechanisms, or the cell failed to detoxify the ROS or to repair the resulting demage, oxidative stress occurs and causes damage to the cellular compartments (Jamieson, 1998).
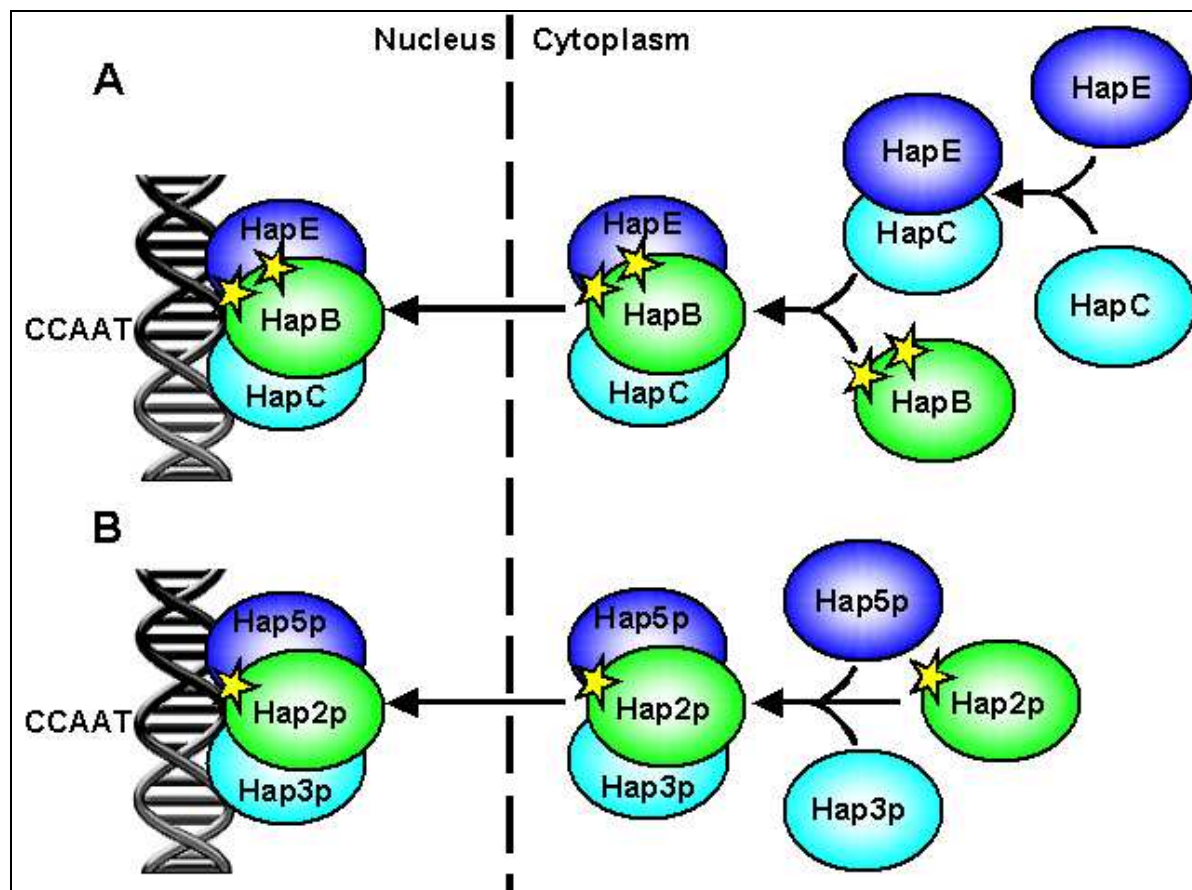
Fig. 2: Assembly and nuclear localization of CCAAT-binding complex. (A) Two-step assembly of CBC in *A. nidulans*. (B) One-step assembly of Hap complex in *S. cerevisiae*. ⭐ : Nuclear Localization Signal (NLS) (modified after Steidl et al., 2004; McNabb and Pinto, 2005).

Cellular proteins, for example, are normally kept in reduced state. They contain many free sulfhydryl (thiol) groups while disulfides (dithiol) are rarely found (Arner and Holmgren, 2000). Upon oxidative stress, proteins are oxidized extensively by reactive oxidative species.

Proteins can undergo different types of oxidation. These include carbonylation (an irreversible process that targets different amino acids) (Stadtman, 1993), nitration of tyrosine and oxidation of methionine to methionine sulphoxide and oxidation of cysteines. Protein cysteines can be oxidized to form different products (Ghezzi, 2005), some of them are reversible (disulphide formation, glutathionylation and S-nitrosylation). This oxidoreduction switch between thiol group and disulfide bridges during oxidative stress is called thio-disulfide exchange reaction. Beside their negative role in protein conformation during oxidative stress, thiol-disulfide exchange reactions, which are rapid and readily reversible, are also ideally suited to control protein function (redox-regulated proteins) via the SH groups. Oxidation of a critical SH group will generally lead to a changed biological function. This mechanism of thiol redox control (Holmgren, 1985) is a major regulatory mechanism in signal transduction.

1.3.2 Thioredoxin and the thioredoxin system.

The thioredoxin system is the major cellular disulfide reductase responsible for maintaining protein in their reduced state. The thioredoxin system, which is made up of thioredoxin (Trx), thioredoxin reductase (TrxR) and NADPH, is ubiquitously distributed from Archea to man.

Thioredoxins are small, heat-stable, oxidoreductase proteins with an approximate molecular mass of 12kDa (Holmgren, 1985). They contain a conserved dithiol/disulfide active site WCGPC (Trp-Cys-Gly-Pro-Cys) (Holmgren, 1989), which is located in a protrusion of the protein with active center sequence. These two cysteine residues are involved in forming the active center disulfide bridge (Tsugita et al., 1983). Thioredoxins, beside their role as the major cellular protein disulfide reductases, act as an intermediate in the posttranslational control of protein activity. First, thioredoxin identifies a change in the redox status of the cell. Second, it responds to that signal by a change in the redox status of thioredoxin (Biswas et al., 2006). Therefore, it also serves as an electron donor for enzymes such as ribonucleotide reductases, thioredoxin peroxidases (peroxiredoxins) and methionine sulfoxide reductases.

In contrast to thioredoxins, thioredoxin reductases are larger, ranging from 70 kDa in bacteria and lower eukaryotes up to 130 kDa in higher eukaryotes, highly specific enzyme only capable of reducing thioredoxin and not any other disulfide bonds in cytoplasmic proteins, and selenium-dependent homodimeric flavoproteins (Arnér and Holmgren, 2000).

The yeast *Saccharomyces cerevisiae* contains two thioredoxin systems; cytoplasmic and mitochondrial. The cytoplasmic is made up of two genes, designated *TRX1* and *TRX2*, encoding thioredoxins (Gan, 1991; Muller, 1991) and one gene (*TRR1*) encoding thioredoxin reductase (Chae et al., 1994). *TRX1* and *TRX2* are closely related. Although the Trx2 protein is one amino acid longer than Trx1, they share 74% and 77% of the coding sequences of the two genes and the two thioredoxin proteins, respectively (Muller, 1991). Deletion of both *TRX1* and *TRX2* results in a prolonged S phase and a shortened G1 interval, a 33% increase in generation time, a significant increase in cell size, and a greater proportion of large budded cells (Muller, 1991).

The mitochondrial system is made up of one thioredoxin gene (*TRX3*) and one thioredoxin reductase (*TRR2*) (Pedrajas et al., 1999). *TRX3* codes for a 14 kDa protein with the typical thioredoxin redox active site, WCGPC. The *TRR2* gene codes for a 37 kDa protein with the putative redox active-site motif (CAVC) as well as binding sites for NADPH and FAD.

A thrioredoxin of *A. nidulans* was also purified and characterized (Le Marechal et al., 1992). When the *A. nidulans* thioredoxin was tested as a substrate for its ability to be reduced by *E. coli* NADPH thioredoxin reductase, it could not serve as a substrate for thioredoxin reductase. Recently, a major thioredoxin system, i.e thioredoxin and thioredoxin reductase, in *A. nidulans* has been identified and characterized (Thön et al., 2007). The 11.6 kDa *A. nidulans* thioredoxin (AnTrxA) protein is encoded by the *trxA* gene and contains the characteristic thioredoxin active site motif (WCGPC). The homodimeric flavoprotein thioredoxin reductase (AnTrxR) is encoded by the *trxR* gene and has a molecular mass of approximately 72.2 kDa. Moreover, a thioredoxin A gene deletion mutant of *A. nidulans* showed decreased growth, an increased catalase activity, and the inability to form reproductive structures like conidiophores or cleistothecia when cultivated under standard conditions. However, lower concentration of glutathione (GSH) led to the development of sexual cleistothecia, in contrast to high GSH levels, which resulted in the formation of asexual conidiophores.

1.4 Objectives of this work.

Biochemical studies on CBF have shown that the histone fold motifs of CBF-C (HapE homologous protein) and CBF-A (HapC homologous protein) are required for heterodimerization (Sinha et al., 1996). However, cysteine residues of CBF-A are located in

the histone fold motif interaction domain required for interaction with CBF-C suggesting the involvement of cysteine residues in the stability of the heterodimer and thus the whole complex. Moreover, biochemical studies suggested that NF-YB (HapC homologous protein) is regulated by the redox status of the cell through reduction of oxidized cysteine residues by thioredoxin (Nakshatri et al., 1996). My first objective was to prove the role of cysteine residues in the redox regulation of HapC and on CBC complex stability *in vivo*, and therefore, to establish methods suitable to study complex stability and protein-protein interaction *in vivo*.

HapX is a transcription factor that was found to bind HapB using the yeast two-hybrid system (Tanaka et al., 2002). The second objective of this work was to analyze *in vivo* the interaction of HapX to HapB and to the CBC complex under iron-depleting conditions and to study the possibility of HapX regulation by the redox status of the cell.

2. Materials and Methods

2.1 Bacterial and fungal strains, plasmids and oligonucleotides used in this study.

Table 1: Bacteria and fungi used in this study.

Strain	Genotype	Reference
E. coli		
BL21 (DE3)	F⁻ *ompT hsd*S$_B$(r$_B^-$m$_B^-$) *gal dcm* (DE3)	Steidl et al., 2001
DH5α	F⁻, φ80d*lacZ*ΔM15, Δ(*lacZYA-argF*)U169, *recA*1, *endA*1, *hsp*R17(r$_k^-$, m$_k^+$), *phoA*, *supE*44, λ⁻, *thi*-1, *gyrA*96, *relA*1	Invitrogen
A. nidulans		
AnTrxAKO	*pyrG89*; *pyroA4*; *riboB2*; *argB2*; Δ*nkuA*::*argB*; Arg⁺; Δ*trxA*::*pyr-4*; PyrG⁺	Thön et al., 2007
AXB4A2	*pyrG89*; *pabaA1*; *argB2*; *fwA1*; *bga0*; *argB2*::pAXB4A (*acvA*p-*uidA*, *ipnA*p-*lacZ*), ArgB⁺	Weidner et al., 1998
Nat24	*pyrG89*; *pabaA1*; *riboB*; Δ*hapC*::*riboB*; RiboB⁺	Papadopoulou, 1999
yC	as AXB4A2; *pyr-4*::pYC-pyr4; PyrG⁺	This study
yCN	as AXB4A2; *pyr-4*::pYC-pyr4; PyrG⁺; pEYFPN	This study
yHapC3CS-N	as AXB4A2; *pyr-4*::pHapC3CS-YC-pyr4; PyrG⁺; pEYFPN	This study
yHapC3CS-TrxA	as AXB4A2; *pyr-4*::pHapC3CS-YC-pyr4; PyrG⁺; pTrxA-YN	This study
yHapC-HapC	as AXB4A2; *pyr-4*::pHapC-YC-pyr4; PyrG⁺; *pabaA1*:: pHapC-YN-paba; Paba⁺	This study
yHapC-HapE	as AXB4A2; *pyr-4*::pHapC-YC-pyr4; PyrG⁺; pHapE-YN	This study
yHapC-HapE-HapB	as yHapC-HapE; *pabaA1*::pHapB-paba; Paba⁺	This study
yHapC-N	as AXB4A2; *pyr-4*::pHapC-YC-pyr4; PyrG⁺; pEYFPN	This study
yHapC-TrxA	as AXB4A2; *pyr-4*::pHapC-YC-pyr4; PyrG⁺; pTrxA-YN	This study
yHapC-TrxAC39S	as AXB4A2; *pyr-4*::pHapC-YC-pyr4; PyrG⁺; pTrxAC39S-YN	This study
yHapC-TrxA-ΔE	as ΔE-89; *pabaA1*::pHapC-YC-paba; Paba⁺; *pyr-4*::pTrxA-YN-pyr4; PyrG⁺	This study

yHapE-C	as AXB4A2; *pyr-4*::pYC-pyr4; PyrG$^+$; pHapE-YN	This study
yHapX-HapB	as AXB4A2; *pyr-4*::pHapX-YC-pyr4; PyrG$^+$; pHapB-YN	This study
yHapX-HapB-HapC^c	as yHapX-HapB-ΔC; *hapC*::pAlcA-HapC; HapC$^+$	This study
yHapX-HapB-ΔC	as Nat24; *pyr-4*::pHapX-HapB-pyr4; PyrG$^+$	This study
yHapX-HapC	as AXB4A2; *pyr-4*::pHapC-YC-pyr4; PyrG$^+$; pHapX-YN	This study
yHapX-HapE	as AXB4A2; *pyr-4*::pHapX-YC-pyr4; PyrG$^+$; pHapE-YN	This study
yHapX-HapX	as AXB4A2; *pyr-4*::pHapX-YC-pyr4; PyrG$^+$; pHapX-YN	This study
yHapX-TrxA	as AXB4A2; *pyr-4*::pHapX-YC-pyr4; PyrG$^+$; pTrxA-YN	This study
yHapX-TrxA-ΔC	as Nat24; *pabaA1*::pHapX-YC-paba; Paba$^+$; *pyr-4*::pTrxA-YN-pyr4; PyrG$^+$	This study
yN	as AXB4A2; *pyr-4*::pYN-pyr4; PyrG$^+$	This study
yNfyB-HapE-ΔC	as Nat24; *pyr-4*::pNfyB-HapE-pyr4; PyrG$^+$	This study
yNfyB-TrxA-ΔC	as Nat24; *pyr-4*::pNfyB-TrxA-pyr4; PyrG$^+$	This study
yTrxA-C	as AXB4A2; *pyr-4*::pYC-pyr4; PyrG$^+$; pTrxA-YN	This study
yTrxAC39S-C	as AXB4A2; *pyr-4*::pYC-pyr4; PyrG$^+$; pTrxAC39S-YN	This study
ΔB-Bgfp	*pyrG89*; *pabaA1*; *argB*; *ΔhapB*::*argB*; ArgB$^+$; pHapB-EGFP; HapB$^+$; *pyr-4*::pKTB1; PyrG$^+$	Steidl, 2001
ΔC-Cgfp	as Nat24; pHapC-EGFP; HapC$^+$; *pyr-4*::pKTB1; PyrG$^+$	Steidl, 2001
ΔC-Cgfp-3CA	as Nat24; *pyr-4*::pKTB1-HapC3CA-EGFP; PyrG$^+$; HapC3CA$^+$	This study
ΔC-Cgfp-3CS	as Nat24; *pyr-4*::pKTB1-HapC3CS-EGFP; PyrG$^+$; HapC3CS$^+$	This study
ΔC-Cgfp-Wt	as Nat24; *pyr-4*::pKTB1-HapC-EGFP; PyrG$^+$; HapC$^+$	This study
ΔC-Egfp	as Nat24; pHapE-EGFP; *pyr-4*::pKTB1; PyrG$^+$	Steidl, 2001
ΔC-Egfp-alcA-3CS	as ΔC-Egfp; *hapC3CS*::pAlcA-HapC3CS; HapC3CS$^+$; *pabaA1*::PabaAnid; Paba$^+$	This study
ΔE-89	*pyrG89*; *pabaA1*; *argB*; *ΔhapE*::*argB*; ArgB$^+$	Steidl, 2001
ΔTrxA-Cgfp	as AnTrxAKO; *pyroA*::pHapC-EGFP-pyro; Pyro$^+$	This study

Table 2: Plasmids used in this study.

Plasmids	Genotype	Reference
p123	Amp^R; *egfp*	Spellig et al., 1996
p3CA-Topo	Amp^R; Kan^R; *hapC3CA*	This study
p3CS-Topo	Amp^R; Kan^R; *hapC3CS*	This study
PabaAnid	Amp^R; pUC 18, 4.1 kb *KpnI* fragment containing *pabaA1* and the flanking regions derived from *A. nidulans*.	Tüncher et al., 2005
pAL4	Amp^R; *pyr-4*; *alcA*p	Waring et al., 1989
pAlcA-HapC	Amp^R; *pyr-4*; *alcA*p-*hapC*	This study
pAlcA-HapC3CS	Amp^R; *pyr-4*; *alcA*p-*hapC3CS*	This study
pCR®2.1	Amp^R; Kan^R; *lacZ*	Invitrogen
pCR2.1-HapC-Bi	Amp^R; Kan^R; *hapC*	This study
pCR2.1-HapX	Amp^R; Kan^R; *hapX*	This study
pET39-AnTrxA(C39S)-H6	Kan^R; T7 promoter-His_6-*trxAC39S*	Thön et al., 2007
pET39-AnTrxA(wt)-H6	Kan^R; T7 promoter-His_6-*trxA*	Thön et al., 2007
pEYFPC	Amp^R; Hyg^R; *eyfpC* terminal part	Hoff and Kück, 2005
pEYFPN	Amp^R; Hyg^R; *eyfpN* terminal part	Hoff and Kück, 2005
pHapB-EGFP	Amp^R; *hapB-egfp*	Steidl, 2001
pHapB-paba	Amp^R; *hapB*; *pabaA1*	This study
pHapB-YN	Amp^R; Hyg^R; *hapB-eyfpN*	This study
pHapC3CA-EGFP	Amp^R; *hapC3CA-egfp*	This study
pHapC3CS-EGFP	Amp^R; *hapC3CS-egfp*	This study
pHapC3CS-YC-pyr4	Amp^R; *pyr-4*; *hapC3CS-eyfpC*	This study
pHapC3CS-YC-Δhyg	Amp^R; *hapC3CS-eyfpC*	This study
pHapC-EGFP	Amp^R; *hapC-egfp*	Steidl, 2001
pHapC-EGFP-pyro	Amp^R; *hapC-egfp*; *pyroA*	This study
pHapC-Topo	Amp^R; Kan^R; *hapC*	Steidl, 2001
pHapC-YC	Amp^R; Hyg^R; *hapC-eyfpC*	This study
pHapC-YC-paba	Amp^R; *pabaA1*; *hapC-eyfpC*	This study
pHapC-YC-pyr4	Amp^R; *pyr-4*; *hapC-eyfpC*	This study
pHapC-YC-Δhyg	Amp^R; *hapC-eyfpC*	This study
pHapC-YN	Amp^R; Hyg^R; *hapC-eyfpN*	This study
pHapC-YN-paba	Amp^R; *pabaA1*; *hapC-eyfpN*	This study
pHapE-EGFP	Amp^R; *hapE-egfp*	Steidl, 2001

pHapE-YN	Amp^R; Hyg^R; *hapE-eyfpN*	This study
pHapE-YN-pyr4	Amp^R; *pyr-4*; *hapE-eyfpN*	This study
pHapX-HapB-pyr4	Amp^R; *pyr-4*; *hapX-eyfpC*; *hapE-eyfpN*	This study
pHapX-YC	Amp^R; Hyg^R; *hapX-eyfpC*	This study
pHapX-YC-paba	Amp^R; *pabaA1*; *hapX-eyfpC*	This study
pHapX-YC-pyr4	Amp^R; *pyr-4*; *hapX-eyfpC*	This study
pHapX-YC-Δhyg	Amp^R; *hapX-eyfpC*	This study
pHapX-YN	Amp^R; Hyg^R; *hapX-eyfpN*	This study
pHELP	Amp^R; *ama1*	Gems and Clutterbuck, 1993
pKTB1	Amp^R; *pyr-4*	Then Bergh, 1997
pKTB1-HapC3CA-EGFP	Amp^R; *pyr-4*; *hapC3CA-egfp*	This study
pKTB1-HapC3CS-EGFP	Amp^R; *pyr-4*; *hapC3CS-egfp*	This study
pKTB1-HapC-EGFP	Amp^R; *pyr-4*; *hapC-egfp*	This study
pMAL-c2X	Amp^R; *malE*; *E. coli* expression vector	New England Biolabs
pMalE-HapC	Amp^R; *malE-hapC*; *E. coli* expression vector	Steidl, 2001
pMalE-HapC3CS	Amp^R; *malE-hapC3CS*; *E. coli* expression vector	This study
pMalE-HapE	Amp^R; *malE-hapE*; *E. coli* expression vector	Steidl, 2001
pNfyB-HapE-pyr4	Amp^R; *pyr-4*; *nf-yb-eyfpC*; *hapE-eyfpN*	This study
pNfyB-TrxA-pyr4	Amp^R; *pyr-4*; *nf-yb-eyfpC*; *trxA-eyfpN*	This study
pNfyB-YC	Amp^R; Hyg^R; *nf-yb-eyfpC*	This study
pNfyB-YC-pyr4	Amp^R; Hyg^R; *pyr-4*; *nf-yb-eyfpC*	This study
pT7-HapBct	Amp^R; T7 promoter-His$_6$-*hapBct* (encoding for aa. 187-369); *E. coli* expression vector	Steidl, 2001
pTopo-MalE-HapC3CS	Amp^R; Kan^R; *hapC3CS*	This study
pTrxAC39S-YN	Amp^R; Hyg^R; *trxAC39S-eyfpN*	This study
pTrxA-YN	Amp^R; Hyg^R; *trxA-eyfpN*	This study
pTrxA-YN-pyr4	Amp^R; *pyr-4*; *trxA-eyfpN*	This study
pYC-pyr4	Amp^R; *pyr-4*; *eyfpC* terminal part	This study
pYC-Δhyg	Amp^R; *eyfpC* terminal part	This study
pYN-pyr4	Amp^R; *pyr-4*; *eyfpN* terminal part	This study
TEV-NF-YB	Amp^R; synthetic gene encoding for NF-YB cloned in pGA4 using *Kpn*I and *Sac*I.	GENEART AG

Table 3: Oligonucleotides used in this study.

Name	Sequence (5' → 3')
3CA-Backward	AGC TTT TTC GGA AGC CTC GCT AGT AAT AAA AGA GAT GAA TTC GCT CAC AGC TTC TTG CAT AGC TTC TTT AG
3CA-Forward	GCT ATG CAA GAA GCT GTG AGC GAA TTC ATC TCT TTT ATT ACT AGC GAG GCT TCC GAA AAA GCT CAA CAG GA
3CS-Backward	AGA TTT TTC GGA AGC CTC GCT AGT AAT AAA AGA GAT GAA TTC GCT CAC AGA TTC TTG CAT AGA TTC TTT AG
3CS-Forward	TCT ATG CAA GAA TCT GTG AGC GAA TTC ATC TCT TTT ATT ACT AGC GAG GCT TCC GAA AAA TCT CAA CAG GA
AnPyro-For	GAG CAG CTG AAG CTT TGC GCG AAA GCG TAA GGA GA
AnPyro-Rev	GAG CAG CTG AAG CTT TCG CAA TCT GAC TTG ACG C
EYFP3'EcoRI(C2)	GGC CGA ATT CTT ACC TCT AAA CAA GTG TAC CTG TGC ATT
EYFP3'KpnI	GGC CGG TAC CTT ACC TCT AAA CAA GTG TAC CTG TGC ATT
EYFP3'BamHI	GTA CAC GAG GAC TGG ATC CAA GAA GGA TTA CCT CTA AAC AA
EYFP3'EcoRI	GCC AGT GCC GAA TTC GCA TGC CTG CAG GTC GAG TG
EYFP5'EcoRI(C2)	TAT AGA ATT CGT ACA GTG ACC GGT GAC TCT TTC TGG C
EYFP5'KpnI	TAT AGG TAC CGT ACA GTG ACC GGT GAC TCT TTC TGG C
EYFP5'BamHI	TTG GGC GAG CTC GGA TCC GTG ACC GGT GAC TCT TT
EYFP5'EcoRI	TTA GAT TGA TTT GAA TTC GGG CGA GCT CTG TAC AGT
eyfpC-For-long	CCG GCC TGC AAG ATC CCG AAC GAC CTG AAA CAG AAG GTC ATG AAC CAC GA
eyfpC-Rev-long	TTA CTT GTA CAG CTC GTC CAT GCC GAG AGT GAT CCC GGC GGC GGT CAC GA
eyfpN-For-long	TCC ATC GCC ACG ATG GTG AGC AAG GGC GAG GAG CTG TTC ACC GGG GTG GT
eyfpN-Rev-long	TTA GGC CAT GAT ATA GAC GTT GTG GCT GTT GTA GTT GTA CTC CAG CTT GT
gpdA-HapB-Rev	CGT GGC GAT GGA GGA TCC TTA GCT GCC ATC TTC ATC
HapB3'NotI	GCG GCC GCT GCC ATC TTC ATC CGA
HapB5'NcoI	CCA TGG AAT ATT CTC CAC AAT ATC AAC AAC AAC
HapC'3NotI625	GCG GCC GCG GGG AGG GTA TCC ATA AGC
HapC3'NcoI	CAG AAA GCC ATG GAA GAT TCG CCA CCA GC
HapC5'BamHI	CCA ACA GCT GGA TCC ATG TCG TCG ACC

HapC-BiFC-For	CCA ACA GCT CCA TGG CAA TGT CGT CGA CC
HapC-BiFC-Rev	AAC CAT GGG AGG GTA TCC ATA AGC TGA GGC
HapC-MalE-antisense	TCT AGA TCA GAA AGC CAT GGA AGA TTC GCC ACC
HapC-MalE-sense	GGA TCC ATG TCG TCG ACC TCT CCC TCC
HapX-3'NotI	GCG GCC GCT TTT GTC GGC AAA TCT TCG
HapX-5'NcoI	CCA TGG CAG CTC AGC CAG CCC TC
HapX-For	CCA TGG CAG CTC AGC CAG CCC T
HapX-Rev	CCA TGG TTT GTC GGC AAA TCT TCG TC
MH10	GAT CGC CAG CCA ATC ACC AGC TAG GCA CCA GCT AAA CCC
MH11	GAT CGG GTT TAG CTG GTG CCT AGC TGG TGA TTG GCT GGC C
NF-YB-For	GCA GAC ATC ACC ATG GAG ATG ACA ATG GAT GGT GA
NF-YB-Rev	CGG GCG GCG GCC GCT TGA AAA CTG AAT TTG CTG AA
TrxBamHI	GGC GGA TCC ATG GGT GCC TCT GAA CAC G
TrxNcoI	GAT CCC CAT GGA AGC AAG CAG AGC CTT G

2.2 Microbiological methods.

All numbers given in % reflect w/v, if not otherwise stated.

2.2.1 Media and supplements.

- LB medium (Miller, 1972): 1% tryptone; 0.5% yeast extract; 1% NaCl, pH 7.5.

- LB agar (Miller, 1972): LB medium; 1.5% agar.

- YEPD medium: 2% yeast extract; 0.1% peptone; 2% glucose.

- *Aspergillus* minimal medium (AMM) (Brakhage and Van den Brulle; 1995): 0.152% KH_2PO_4; 0.052% KCl; 0.6% $NaNO_3$; 1% glucose; 0.05% $MgSO_4$; 1 ml/l trace elements; pH 6.5. If acetamide was used as N source instead of $NaNO_3$, 17 mM or 50 mM of acetamide were employed.

- AMM agar: AMM; 1.5% agar.

- ACM agar (Rowlands and Turner, 1973): 2% malt extract; 0.1% peptone; 2% glucose; 1.5% agar.

2.2.2 Culturing conditions.

2.2.2.1 Growth conditions of *E. coli*.

E. coli cultures were grown overnight at 37°C and 200 rpm in 3 ml LB medium (plus appropriate antibiotic) for miniprep, or in 50 ml LB medium for midiprep (plus appropriate antibiotics).

2.2.2.2 Growth conditions of *Aspergillus nidulans*.

For DNA, RNA or protein isolation, 0.5 ml inoculum of freshly harvested 10^8 spores/ml were grown according to Pontecorvo et al. (1953) at 37°C in 50 ml of AMM, containing glucose as the carbon source and $NaNO_3$ or acetamide as the nitrogen source, in a 250 ml Erlenmeyer flask. Mycelia were harvested by filtration over miracloth and frozen in liquid nitrogen. Frozen mycelia were ground in liquid nitrogen and stored at -20°C.

For fluorescence visualization of mycelia, the fungal strains were grown in 3 ml of AMM supplemented with appropriate supplements at 37°C.

For bimolecular fluorescence complementation (BiFC) analysis under iron depleting (-Fe) and repleting (+Fe) conditions, 10 mM $FeSO_4$ was used as the iron source with the respective supplements to create +Fe conditions while addition of iron was omitted for creating -Fe conditions. Additional treatment with 1 mM deferoxamine mesylate salt for 1 h was essential to cause iron starvation.

For analysis under oxidative stress conditions, GFP subcellular localization and BiFC analysis were performed after growth of fungi at 37°C in AMM supplemented with appropriate supplements. H_2O_2 treatment was used to create oxidative stress conditions.

For induction of the *alcA* promoter, fungal strains were grown in AMM with 6% threonine as the carbon source and for repression conditions, 0.8% glucose was used. For non-inducing/non-repressing conditions 1.6% lactose was used. Cultures were cultivated at 37°C and 180 rpm.

2.2.3 Determination of the dry weight.

Mycelial samples were harvested by filtration over miracloth then dried briefly on paper towels. For the determination of dry weights, samples were dried overnight in an oven at 60°C. Dry weight was plotted against time.

2.2.4. Inhibition zone plate assay.

Conidia of *A. nidulans* strains were harvested from plates and 10^8 spores were added to 20-25 ml AMM agar (48°C) and mixed. The AMM agar was poured in petri dishes and cooled down until it had solidified. In the centre of the agar plate, a 10 mm hole was created, which was filled with different H_2O_2 concentrations. Plates were incubated overnight at 37°C. The diameter of the inhibition zone was measured.

2.3 Molecular genetics methods.

2.3.1 DNA manipulation.

Standard techniques in the manipulation of DNA were carried out as described by Sambrook and Russell (2001) unless it is mentioned otherwise.

2.3.2 Isolation of *E. coli* plasmid DNA.

Miniprep isolation of plasmid DNA from *E. coli* was performed by alkaline lysis, according to Birnboim and Doly (1979). For quicker procedure and purer plasmid DNA, the FastPlasmid Kit (Eppendorf) was used according to the manufacturer's instructions.

Midiprep of plasmid DNA was done using NucleoBond®Xtra purification Kit (Macherey-Nagel) according to the manufacturer's instructions.

2.3.3 Purification of DNA from gel.

DNA recovery from gel carried out using Zymoclean Gel DNA Recovery Kit (Zymo Research) according to the manufacturer's instructions.

2.3.4 Isolation of chromosomal DNA from filamentous fungi.

Chromosomal DNA from *A. nidulans* was prepared either according to the method described previously by Andrianopoulos and Hynes (1988) or using MasterPure™ Yeast DNA Purification Kit (Epicentre Biotechnologies).

2.3.5 Southern blot analysis of the transformants.

For Southern blot analysis, chromosomal DNA of *A. nidulans* was digested using appropriate restriction enzymes. DNA fragments were separated on an agarose gel and blotted onto Hybond N+ nylon membranes (GE Healthcare). Labelling of the DNA probe and detection

were performed using ECL Random Prime Labelling and Detection Kits (GE Healthcare) according to the manufacturer's recommendations.

2.3.6 *In vitro* site-directed mutagenesis of DNA.

Generation of HapC mutant proteins was carried out using the standard procedure from Higuchi et al. (1988). Alternatively, QuikChange II XL Site-Directed Mutagenesis Kit (Stratagene) was applied.

2.3.7 Isolation of RNA from *A. nidulans*.

Total RNA was extracted from mycelia using Plant RNeasy Mini Kit (Qiagen) according to the manufacturer's recommendations.

2.3.8 Northern blot analysis.

For Northern blot analysis, total RNA of *A. nidulans* was separated on a denaturing formaldehyde agarose gel and blotted onto Hybond N+ nylon membranes (GE Healthcare). Preparation of probe was performed using the ECL Random Prime Labelling kit (GE Healthcare). Detection was performed using Gene Images CDP-Star Detection kit (GE Healthcare).

2.3.9 Transformation of *A. nidulans*.

Protoplast preparation and transformation of *A. nidulans* was carried out according to the method described by Balance and Turner (1985).

2.4 Biochemical methods.

2.4.1. Protein extraction from *A. nidulans*.

The mycelia were harvested by filtration over miracloth, and dried on paper towels. Cells were frozen in liquid nitrogen and ground up in a mortar and pestle. For Western blot, lysis buffer (50 mM HEPES (pH 7.5) and 1 mM PMSF) was added to the mycelial powder. Then it was vigorously mixed. Samples were centrifuged for 15 min at 4°C. The supernatant was transferred into a new tube and the protein concentration of the solution was measured (see 2.4.2).

2.4.2 Protein concentration determination.

Protein concentration was determined according to Bradford (1976).

2.4.3 SDS polyacrylamide gel electrophoresis (SDS-PAGE) of proteins.

Protein samples were dissolved in NuPAGE® LDS sample buffer and heated at 95°C for 10 min. SDS-PAGE was performed with NuPAGE 4–12% BisTris Gels using NuPAGE® MES SDS Running Buffer and XCell SureLock™ Mini-Cell (Invitrogen) according to the standard conditions recommended by the manufacturer.

2.4.4 Western blot analysis.

20 µg of each protein sample were electrophoresed through a NuPAGE 4–12% BisTris Gel (Invitrogen) (see 2.4.3) and transferred to nitrocellulose membranes (Schleicher & Schuell). Blots were blocked (25°C, 1 h) with blocking solution (18 ml TBST and 2 ml 10 blocking solution (Invitrogen)). Primary antibodies were diluted 1:5000 and 1:2000 for anti-GFP goat polyclonal antibody (pGFP) (ab5449) and anti-GFP mouse monoclonal antibody (mGFP) (ab 1218), respectively. Blots were then incubated (25°C, 1 h) with the primary GFP antibodies. Blots were washed three times (10 min each) with TBST (50 mM Tris-HCl (pH 8.0), 150 mM NaCl, and 0.05% (v/v) Tween 20). Blots were incubated with either an anti-goat alkaline phosphatase-conjugated antibody (diluted 1:5,000), or an anti-mouse alkaline phosphatase-conjugated antibody (diluted 1:5,000) for 1 h at 25°C.

2.4.5 Overexpression in *E. coli* and purification of recombinant proteins.

Fusion proteins were prepared as described by Steidl et al. (1999). Cultures (200 ml) of *E. coli* harboring plasmid pT7-HapBct, pMalE-HapC, pMalE-HapC3CS or pMalE-HapE were grown to an optical density at 600 nm of ~0.5, and induction was achieved by the addition of 1 mM isopropyl-β-D-thiogalactopyranoside (IPTG). After induction for 3 h at 37°C, cells were harvested, taken up in 15 ml of buffer A (20 mM Tris-Cl, 1 mM EDTA, 1 mM dithiothreitol [DTT], 200 mM NaCl [pH 7.5]), lysed by sonication, and centrifuged at maximum speed for 20 min. The crude cellular extracts were applied to amylose columns (New England Biolabs) and washed with buffer A until the flowthrough optical density at 280 nm was <0.01. The fusion proteins were eluted with buffer A containing 10 mM maltose.

His$_6$-HapBct-containing crude cellular *E. coli* extracts were obtained by the same protocol. The crude cellular extracts were applied to a nitrilotriacetic acid agarose column (Qiagen).

Washing steps were performed according to the supplier. The His$_6$-tagged protein was eluted by a 50 to 500 mM gradient of imidazole in washing buffer.

The purity of all recombinant proteins was examined by SDS-PAGE (see 2.4.3) and Coomassie blue staining.

2.4.6 Electrophoretic mobility shift assay (EMSA).

EMSA was carried out as described by Steidl et al. (2001). As a probe, the *amdS*p-derived CCAAT-containing oligos MH10 and MH11, which after hybridization form 5′ GATC overhangs (Steidl et al., 1999), were used. Labelling of the probe was performed using ECL Random Prime Labelling and Detection Kits (GE Healthcare) according to the manufacturer's recommendations. The labelled probe was incubated with an equal molar concentration of the proteins purified previously (see 2.4.5) and run on non-denaturating polyacrylamide gel. Detection of the probe was carried out using ECL Random Prime Labelling and Detection Kits (GE Healthcare).

2.4.7 Measuring acetamidase specific activity.

Acetamidase can convert acetamide to acetic acid and ammonia. Ammonia reacts further in the presence of α-ketoglutarate with NADPH, which is converted to NADP$^+$ by glutamate dehydrogenase (GDH), to form L-glutamate and water. Acetamidase activity was assayed by measuring the conversion of NADPH to NADP$^+$ at 340 nm.

A. nidulans strains were grown in AMM for 65 h incubation at 37°C. After harvesting, mycelia were frozen in liquid nitrogen and ground with mortar and pestle. Mycelia were suspended in extraction buffer (0.1 M Tris-HCl, pH 8.3). Samples were centrifuged for two times at 4°C and 13,000 rpm for 15 min. The reaction mixture was prepared by mixing 0.2 ml supernatant, which contains total protein, with 0.1 ml of 225 mM α-ketoglutarate, 0.1 ml of 7.5 mM NADPH, and 2.5 ml of extraction buffer. The solution was equilibrated for 5 min. 0.5 ml of the reaction mixture was mixed with 0.5 ml of 1 M acetamide. Enzyme activity was assayed by measuring the decrease in optical density at 340 nm and 25°C. The specific activity of the acetamidase was calculated.

2.5 Fluorescence microscopy

Aspergillus minimal medium (AMM) was inoculated with *Aspergillus* conidia and incubated overnight at 37°C (see 2.2.2.2). For nuclear staining, conidia or mycelia were transferred to

slides and suspended in staining buffer (50 mM sodium phosphate (pH 7.0), 50% glycerol, 0.1% n-propyl gallate) containing 0.1 µg/ml of 4´,6-diamidino-2-phenylindol (DAPI). Then, the cover slip was placed on the slide. *A. nidulans* hyphae were analyzed by light and fluorescence microscopy using Leica DM4500 B digital fluorescence microscope (Leica Microsystems). Leica A filtercube (excitation filter (blue) BP340-380; dichromatic mirror (green) 400, suppression filter (red) LP 425) was applied for DAPI-stained samples. For GFP localization studies, Leica GFP filtercube (excitation filter (blue) BP 470/40; dichromatic mirror (green) 500, suppression filter (red) BP 525/50) was used. BiFC analysis was carried out using Leica YFP filtercube (excitation filter (blue) BP 500/20; dichromatic mirror (green) 515, suppression filter (red) BP 535/30). For documentation, a Leica DFC480 digital camera (Leica Microsystems) was used. Photographs were processed for optimal presentation by Photoshop 7 (Adobe).

3. Results

3.1 The role of HapC cysteine residues in the stability of the CBC complex *in vivo*.

3.1.1 Searching CBC complex subunits for possible cysteine target sites.

Analysis of the amino acid sequence of HapB, HapC and HapE revealed that HapB contains no cysteine residues within its sequence whereas three and one cysteine(s) were found in HapC and HapE, respectively.

3.1.2 Studying the influence of HapC cysteine residues replacement on the stability of the complex *in vivo*.

Baxevanis et al. (1995) and Sinha et al. (1996) showed that the core region of CBF-C (HapE homologous protein) and CBF-A (HapC homologous protein) are required for heterodimer formation, a pre-requisite for CBF-B association and CCAAT binding, indicating that cysteine residues might play a role in the dimerization of CBF-A to CBF-C and influence the stability of the heterodimer. To prove this in *A. nidulans*, we studied the role of the HapC cysteines replacement on the stability of the complex *in vivo* using the subcellular localization analysis of the GFP fusion proteins, phenotypic characterization and complementation analysis of *ΔhapC* mutants.

3.1.2.1 Construction of plasmids and generation of the *A. nidulans* strains.

HapC has three conserved cysteines at positions 74, 78 and 94 representing the three cysteine residues at positions C85, C89 and C105 in NF-YB, the human homologous protein of HapC. To analyze the importance of the HapC conserved cysteines *in vivo*, a mutant carrying all cysteine residues of HapC mutagenized into serine (HapC3CS), was generated.

In order to avoid the possibility of formation of any phosphorylation sites at the generated serines, an additional mutant was generated, which carried a replacement of all three cysteine residues of HapC to alanine (HapC3CA). The two *hapC* mutant proteins were constructed by two-step PCR site-directed mutagenesis (Higuchi et al., 1988) using the plasmid pHapC-EGFP as a template and the primers HapC3'NcoI and HapC5'BamHI to amplify *hapC*. The primer pairs 3CS-Forward and 3CS-Backward, and 3CA-Forward and 3CA-Backward were used to replace all cysteine residues to serine (HapC3CS) and alanine (HapC3CA), respectively. The PCR products were cloned into plasmid pCR®2.1 resulting in the plasmids

p3CS-Topo and p3CA-Topo, respectively. After sequencing, mutated *hapC* genes were cloned into p123 and fused to *egfp* under the control of the *otef* promoter by digestion with *Bam*HI and *Nco*I (Fig. 3-I). The resulting plasmids were called pHapC3CS-EGFP and pHapC3CA-EGFP, which contain the genes *hapC3CS* and *hapC3CA*, respectively.

The *egfp* cassette, including the *otef* promoter, the *hapC3CS-egfp* (or *hapC3CA-egfp*) fusion, and a *nos* terminator, was excised from pHapC3CS-EGFP and pHapC3CA-EGFP by *Cla*I-*Kpn*I digestion and cloned into plasmid pKTB1, which carries the *pyr-4* gene of *N. crassa* as a selectable marker, resulting in the plasmids pKTB1-HapC3CS-EGFP and pKTB1-HapC3CA-EGFP, respectively. To use it as a control, the plasmid pHapC-EGFP (Steidl, 2001), which contains a *hapC-egfp* fusion under the control of the *otef* promoter, was cloned into pKTB1 by *Cla*I-*Kpn*I digestion. The resulting plasmid was designated pKTB1-HapC-EGFP and it contains wild-type *hapC* fused to *gfp* under the control of the *otef* promoter and *pyr-4* gene of *N. crassa* as a selectable marker (Fig. 3-I).

The *A. nidulans* strains were generated by transformation the *ΔhapC* strain Nat24 with the plasmids pKTB1-HapC3CS-EGFP and pKTB1-HapC3CA-EGFP giving the strains ΔC-Cgfp-3CS and ΔC-Cgfp-3CA, respectively. As a control strain, the plasmid pKTB1-HapC-EGFP was transformed into the *ΔhapC* strain resulting in the strain ΔC-Cgfp-Wt, which contains *hapC-egfp* under the control of the *otef* promoter.

3.1.2.2 Phenotypic characterization of the ΔC-Cgfp-3CS and ΔC-Cgfp-3CA mutants.

The idea of this experiment was to transform the *ΔhapC* strain, i.e. Nat24, with mutagenized HapC encoding genes (*hapC3CS* and *hapC3CA*) and characterize the phenotype of transformants. The Nat24 strain is characterized by slow growth, poor conidiation and hardly grows on AMM agar with acetamide as sole N or C source. Recovery of the wild-type phenotype implies that mutagenized HapC complemented *ΔhapC* while the *Δhap* phenotype would indicate the failure of mutagenized HapC to complement *ΔhapC*.

3.1.2.2.1 Complementation analysis of the ΔC-Cgfp-3CS and ΔC-Cgfp-3CA mutants.

The uracil-prototrophic transformants were analyzed by growing the strains ΔC-Cgfp-Wt, ΔC-Cgfp-3CS and ΔC-Cgfp-3CA on AMM agar plates with NaNO$_3$ or acetamide as sole N source. However, all generated *A. nidulans* strains exhibited wild-type morphology when grown either on NaNO$_3$ (Fig. 3-II-1) or acetamide (Fig. 3-II-2) as N source indicating that both HapC mutant proteins recovered the *A. nidulans* wild-type phenotype.
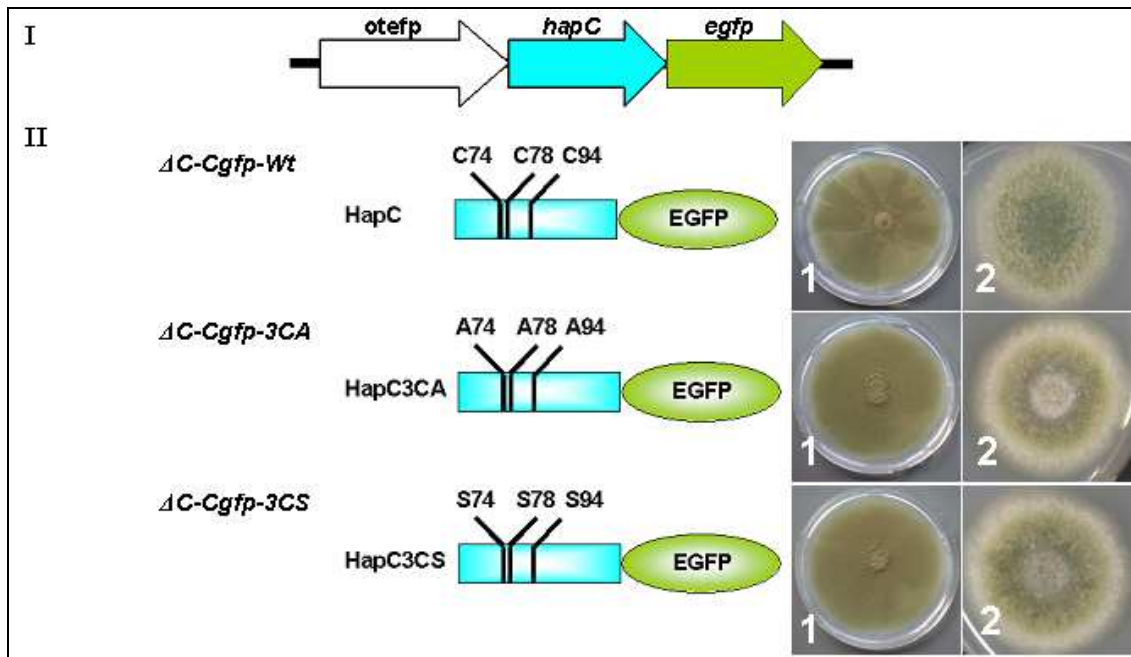
Fig. 3. Analysis of *ΔhapC* strains of *A. nidulans* complemented with the mutagenized *hapC* genes. (I) A schematic map of generated *hapC-*, *hapC3CA-* and *hapC3CS-egfp* gene fusions for complementation a *ΔhapC* strain of *A. nidulans*. The *hapC* wild-type and *hapC* mutant genes were fused in-frame to *egfp* using *Bam*HI and *Nco*I restriction sites under the control of *otef* promoter. (II) Growth of strains ΔC-Cgfp-3CS and ΔC-Cgfp-3CA on AMM agar with NaNO$_3$ (1) or acetamide (2) as N source at 37°C. The wild-type strain ΔC-Cgfp-Wt was used as a positive control. The name of the strains (bold italics) and the depiction of the different HapC-EGFP fusion proteins are indicated on the left side.

3.1.2.2.2 Growth in liquid minimal medium and complete medium.

Transformants were analyzed by growing the strains (10^6 spores/ml final concentration) in AMM and ACM. Samples were collected at 12 h intervals and dried. Dry weight was plotted against time. The result showed that on both media, the growth rate of the ΔC-Cgfp-3CS and ΔC-Cgfp-3CA strains did not differ compared with ΔC-Cgfp-Wt (Fig. 4).
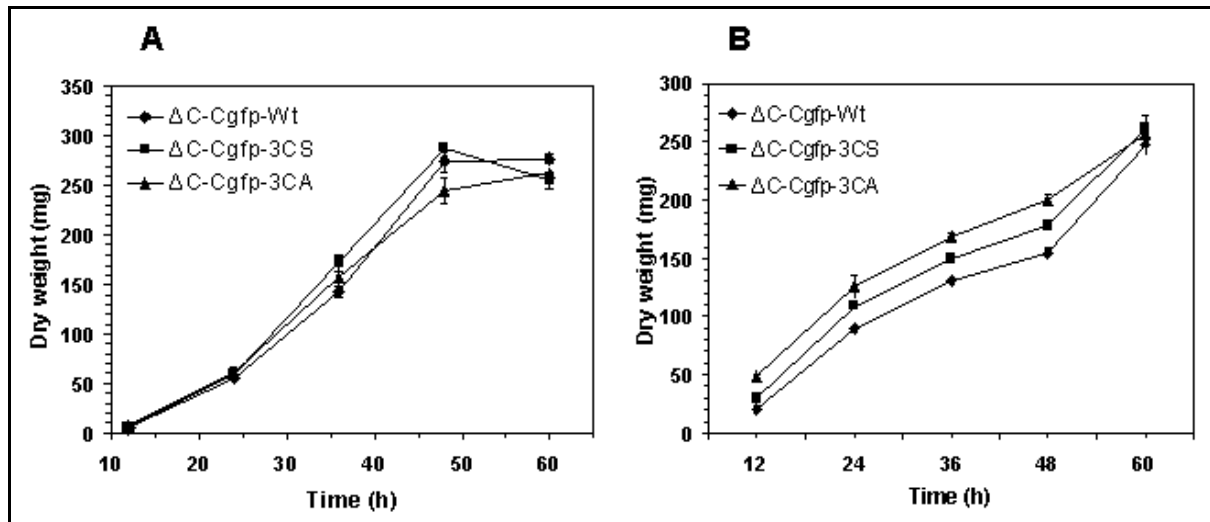
Fig. 4. Growth curve of ΔC-Cgfp-3CS and ΔC-Cgfp-3CA measured by dry weight. The strains were cultivated in AMM (A) and complete medium (B). The wild-type strain ΔC-Cgfp-Wt was used as a positive control.

3.1.2.2.3 Growth on acetamide as sole N source.

Previous study showed that CBC is involved in the regulation of the acetamidase gene *amdS*, which is required for the use of acetamide as the N and C source (van Heeswijck and Hynes, 1991). Consequently, *Δhap* mutant strains hardly grew on acetamide as the sole N and C source, which is characteristic for a *Δhap* phenotype (Papagiannopoulos et al., 1996; Steidl et al., 1999). Therefore, transformants were analyzed by growing the strains ΔC-Cgfp-Wt, ΔC-Cgfp-3CS and ΔC-Cgfp-3CA on AMM agar plates and in AMM with acetamide as sole N source. On AMM agar plates, 2.5 µl of (10^6 spores/ml) were used to inoculate AMM agar plates with 17 mM acetamide as sole N source. The diameter of growth was measured at 12 h intervals. Moreover, in AMM, transformants were analyzed by growing the strains (10^6 spores/ml final concentration) in AMM with 17 mM acetamide as sole N source. Samples were collected at 12 h intervals and dried. Dry weight was plotted against time. Surprisingly, the results showed that the ΔC-Cgfp-3CS and ΔC-Cgfp-3CA strains exhibited higher growth rates than the wild-type strain ΔC-Cgfp-Wt on acetamide as N source (Fig. 5). To investigate this further, the enzymatic activity of acetamidase (AmdS) was measured in the ΔC-Cgfp-3CS and ΔC-Cgfp-3CA strains as well as the wild-type strain ΔC-Cgfp-Wt (refer to 3.1.2.2.4).
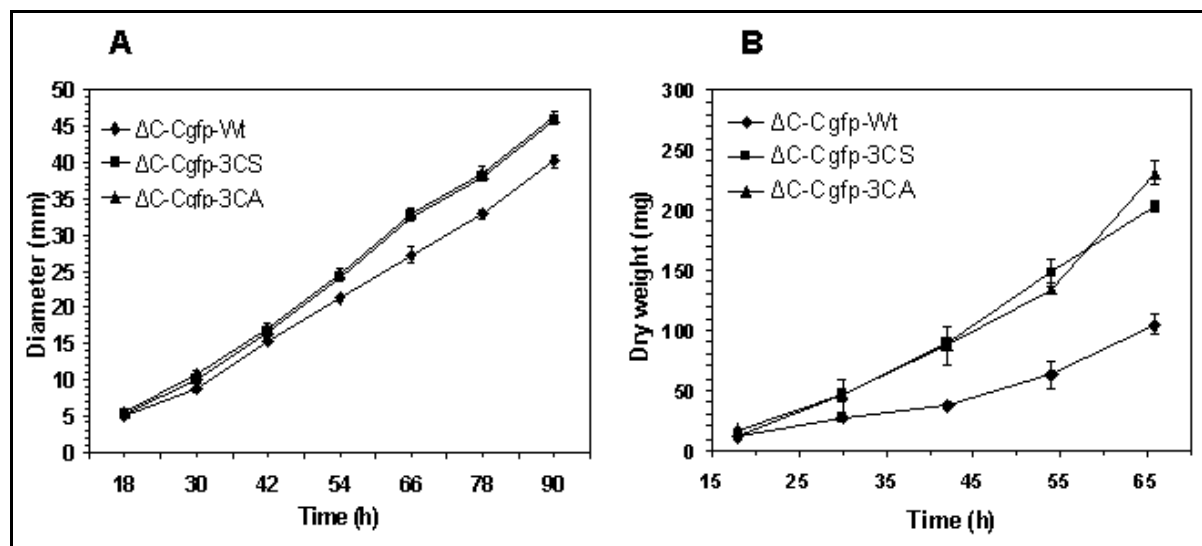
Fig. 5. Growth curve of ΔC-Cgfp-3CS and ΔC-Cgfp-3CA measured by diameter (A) and dry weight (B). The strains were grown on AMM agar plates (A) and in AMM (B) with 17 mM acetamide as sole N source. The wild-type strain ΔC-Cgfp-Wt was used as a positive control.

3.1.2.2.4 Specific enzyme activity of the acetamidase (AmdS).

Amidases catalyze the hydrolysis of amides to the corresponding acids and ammonia. For example, acetamidase (EC 3.5.1.4) catalyzes the hydrolysis of acetamide into acetic acid and ammonia (Kohyama et al., 2007). However, *A. nidulans* can utilize acetamide as both carbon source and nitrogen source by means of an acetamidase (AmdS) enzyme (van Heeswijck and Hynes, 1991). As mentioned above, ΔC-Cgfp-3CS and ΔC-Cgfp-3CA strains showed higher growth rates than the wild-type strain ΔC-Cgfp-Wt on acetamide as N source. Therefore, by measuring the acetamidase activity it should be possible to confirm the higher growth rates of ΔC-Cgfp-3CS and ΔC-Cgfp-3CA strains on acetamide in comparison with the ΔC-Cgfp-Wt. The acetamidase specific activity was measured in the strains ΔC-Cgfp-3CS and ΔC-Cgfp-3CA after 65 h incubation at 37°C in AMM with 17 mM acetamide as N source. The wild-type strain ΔC-Cgfp-Wt was used as a control. As in acetamide growth experiments, the results showed that the acetamidase activity of the ΔC-Cgfp-3CS and ΔC-Cgfp-3CA was higher compared with the wild-type strain ΔC-Cgfp-Wt (Fig. 6), suggesting an unexplained positive involvement of mutagenized HapC proteins (i.e. HapC3CS and HapC3CA) in regulation of the acetamidase gene (*amdS*) in comparison with wild-type HapC.
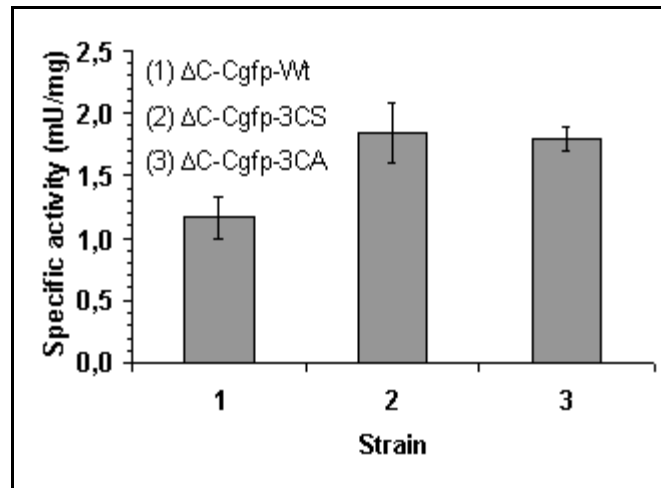
Fig. 6. Specific activity of acetamidase in ΔC-Cgfp-3CS and ΔC-Cgfp-3CA strains of *A. nidulans* cultivated in AMM with acetamide as sole N source. The wild-type strain ΔC-Cgfp-Wt was used as a positive control.

3.1.2.2.5 H_2O_2 susceptibility determined by inhibition zone plate analysis.

In order to compare the H_2O_2 sensitivity of ΔC-Cgfp-3CS and ΔC-Cgfp-3CA strains with the wild-type strain ΔC-Cgfp-Wt, inhibition zone plate analysis was performed using different concentrations of H_2O_2. The results obtained did not show any significant differences between the diameters of the inhibition zone measured for the strains tested at different concentrations (Fig. 7).
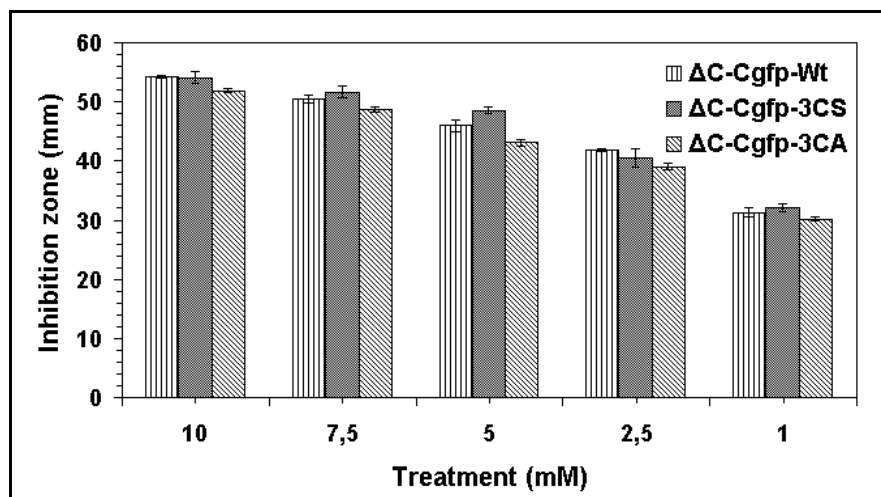
Fig. 7. Sensitivity of ΔC-Cgfp-3CS and ΔC-Cgfp-3CA strains to H_2O_2. Susceptibility was measured as the zone of growth inhibition after overnight growth on AMM agar plates. The wild-type strain ΔC-Cgfp-Wt was used as a positive control.

3.1.2.3 Visualization of the stability of the complex using GFP fusions.

HapC has dual subcellular localizations depending on the stage of CBC complex formation. HapC does not carry any nuclear localization signal (NLS). When HapC forms a heterodimer with HapE, it is localized in the cytoplasm. However, when HapB, which carries an NLS, binds the HapC-HapE heterodimer, it localizes in the nucleus (Steidl et al., 2004). Therefore, the stability of the complex was studied *in vivo* by visualizing the localization of HapC-EGFP. In the stable complex, the HapC-EGFP fusion is becoming part of CBC and it enters the nucleus while the less stable complex gets disassembled causing HapC-EGFP to localize in the cytoplasm.

Here, GFP fusions were used to monitor the localization in the two strains ΔC-Cgfp-3CS and ΔC-Cgfp-3CA. It is expected that mutagenized HapCs (HapC3CS and HapC3CA) form a less stable complex in comparison with the complex formed by wild-type HapC. Consequently, the complexes with mutagenized HapCs very likely localize in the cytoplasm. As shown in Fig. 8-A, unlike the strain ΔC-Cgfp-Wt, the strains ΔC-Cgfp-3CS and ΔC-Cgfp-3CA showed strong fluorescence in the cytoplasm (Fig. 8-B and –C), indicating that mutagenized HapC might form a less stable complex with other CBC subunits, which disassembles later on.
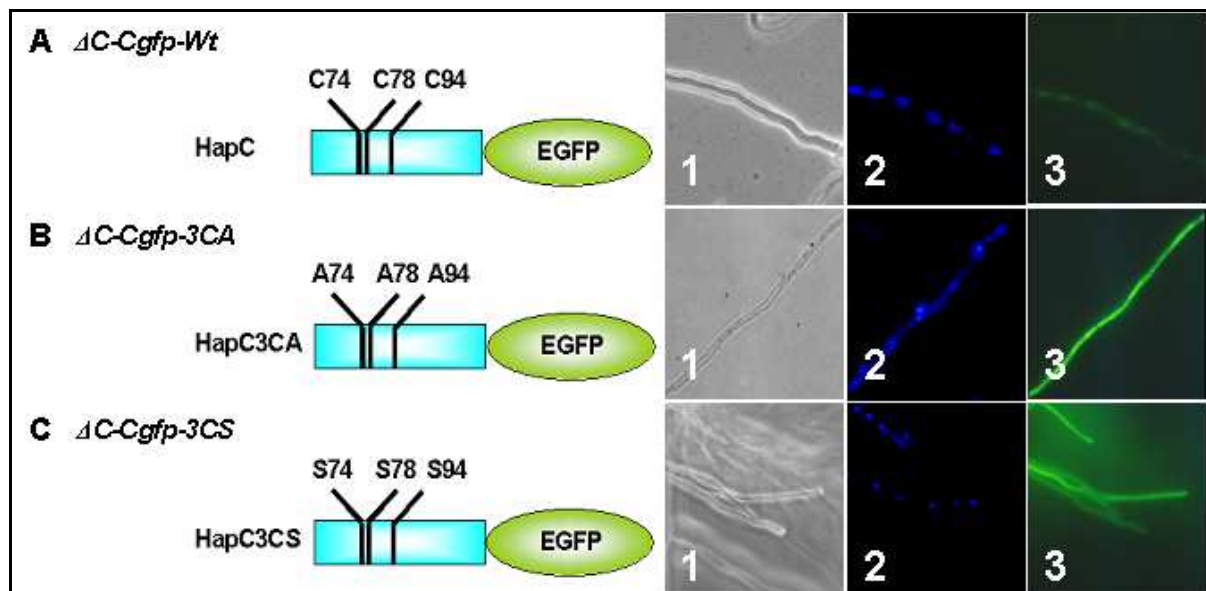
Fig. 8. Cellular localization of HapC3CS and HapC3CA mutant proteins. Cellular localization of HapC3CA-EGFP and HapC3CS-EGFP fusion protein (panels 3), to monitor the localization of HapC3CS- and HapC3CA in the strains ΔC-Cgfp-3CS and ΔC-Cgfp-3CA, respectively. The wild-type strain ΔC-Cgfp-Wt was used as a positive control. Samples were analyzed by light microscopy (panels 1) and fluorescence microscopy (panels 2 for DAPI staining of nuclei and panels 3 for EGFP localization). The name of the strains (bold italics) and the depiction of the different HapC-EGFP fusion proteins are indicated on the left side. The cysteine residues and the amino acids replacing these cysteines are labelled by letters and numbers.

3.1.2.4 Analyzing the stability of the complex *in vitro* using electrophoretic mobility shift assay (EMSA).

To confirm the idea that localization of HapC3CS and HapC3CA in the cytoplasm is due to the lower stability of the formed complex, EMSA was performed using the CBC complex formed by HapC3CS, HapB and HapE. DNA binding of this complex was compared with the complex formed by the wild-type HapC, HapB and HapE.

The *hapC3CS* gene was amplified by PCR using HapC-MalE-sense and HapC-MalE-antisense primers and p3CS-Topo plasmid as a template. The PCR product was cloned into pCR®2.1 resulting in plasmid pTopo-MalE-HapC3CS. After sequencing, the correct plasmid was digested with *Bam*HI and *Xba*I and the 660 bp band of *hapC3CS* was ligated into pMAL-c2X, a vector designed to produce maltose-binding protein (MBP) fusions, where the protein of interest can be cleaved off the MBP with the specific protease factor Xa, resulting in plasmid pMalE-HapC3CS. The plasmid was transformed into *E. coli* DH5α. The *E. coli* overexpression strains for HapB, HapC, and HapE were generated previously (Steidl et al., 1999). To study the *in vitro* reconstitution of a CCAAT-binding complex, HapB, HapC, HapC3CS and HapE were expressed in *E. coli* as fusion proteins and purified by affinity chromatography. HapC (aa 1 to 186), HapC3CS (aa 1 to 186) and HapE (aa 1 to 265) were purified as MalE fusion proteins. HapB was purified as a His_6-tagged truncated protein (HapBct) containing the C-terminal 183 aa of HapB (aa 168 to 349), which includes the predicted conserved DNA binding and subunit interaction domains. Induction was done using 0.1 M IPTG/flask and shaken at 27°C. Equal amounts of the recombinant HapB, HapE and HapC, and HapB, HapE and HapC3CS were mixed to reconstitute the CBC complex containing HapC and HapC3CS, respectively. Both CBC complexes were incubated with 700 pmol of the DNA probes MH10 and MH11. The *amdS* promoter-driven MH10 and MH11 probes are complementary oligonucleotides, which form 5′ GATC overhangs after hybridizing with each other (Steidl et al., 1999). Complex reconstitution and DNA binding of the CBC complex formed by HapC3CS, HapB and HapE was analyzed and compared with the complex formed by the wild-type HapC, HapB and HapE.

The results obtained showed that CBC complex formed using HapC3CS binds weaker in comparison with that formed using an equal amount of HapC (Fig. 9). These results support the idea that the mutagenized HapC forms a less stable complex with other CBC subunits, which disassembles later on.
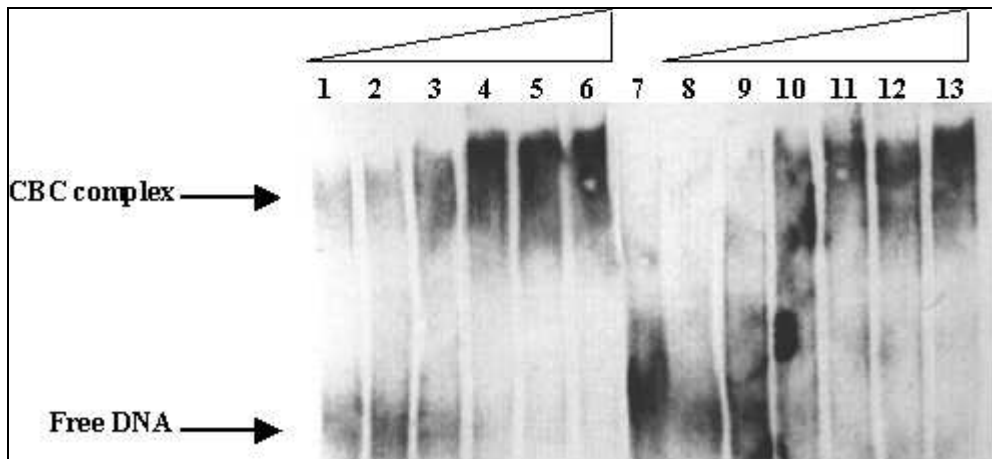
Fig. 9. Stability analysis of the CBC complex formed with HapC3CS by EMSA. EMSA experiments were performed using oligonucleotide duplex mixed with purified recombinant CBC subunits. Lanes 1-6: DNA-CBC complex that contains wild-type HapC, 7: only DNA, 8-13: DNA-CBC complex that contains HapC3CS.

3.1.2.5 Visualization of the nuclear localization of the less stable CBC complex using HapE-EGFP fusion.

As shown previously in 3.1.2.3, both HapC3CS and HapC3CA are able to form a CBC complex with lower stability, which can recover the wild-type phenotype in *ΔhapC* mutants. However, to prove that the less stable CBC complex, which contains HapC3CS (or HapC3CA), localizes in the nucleus, the ΔC-Egfp strain was used. This strain is a *ΔhapC* strain and contains a *hapE-egfp* fusion. The reason for choosing HapE is that HapE does not carry any nuclear localization signal. Therefore, nuclear localization of the HapE-HapC dimer is only possible when the CBC complex is formed.

This ΔC-Egfp strain was transformed with *hapC3CS* under the control of the inducible *alcA* promoter (Fig. 10-I). The plasmid, which carries *hapC3CS* under the control of the inducible *alcA* promoter, was constructed by digestion of p3CS-Topo with *Bam*HI and *Xba*I. The resulting DNA fragment, which contains *hapC3CS* and 51 bp after the stop codon, was ligated into the pAL4 plasmid. The resulting plasmid was designated pAlcA-HapC3CS. The *A. nidulans* strain ΔC-Egfp was co-transformed with the plasmids pAlcA-HapC3CS and PabaAnid. The resulting strain, which was derived from co-transformation of the ΔC-Egfp strain with the plasmids pAlcA-HapC3CS and PabaAnid, was designated ΔC-Egfp-alcA-HapC3CS. This strain was incubated in AMM at 37°C and 180 rpm overnight. The localization of HapE-EGFP was visualized under inducing conditions (threonine), repressing conditions (glucose) and under non-inducing/non-repressing conditions (lactose).

Under inducing and non-inducing/non-repressing conditions HapE-EGFP was localized in the nucleus (Fig. 10-II-A and -C) while repressing conditions led to the accumulation of HapE-EGFP in the cytoplasm (Fig. 10-II-B).

These results are consistent with the previous results. They showed that HapC3CS forms a complex with lower stability, which is still able to localize in the nucleus. We proposed that although HapC3CS and HapC3CA form less stable CBC complexes, however, overexpression of the HapC3CS and HapC3CA by the strong *otef* promoter leads to the formation of the less stable CBC complex in high quantities, which are sufficient to recover the wild-type phenotype.
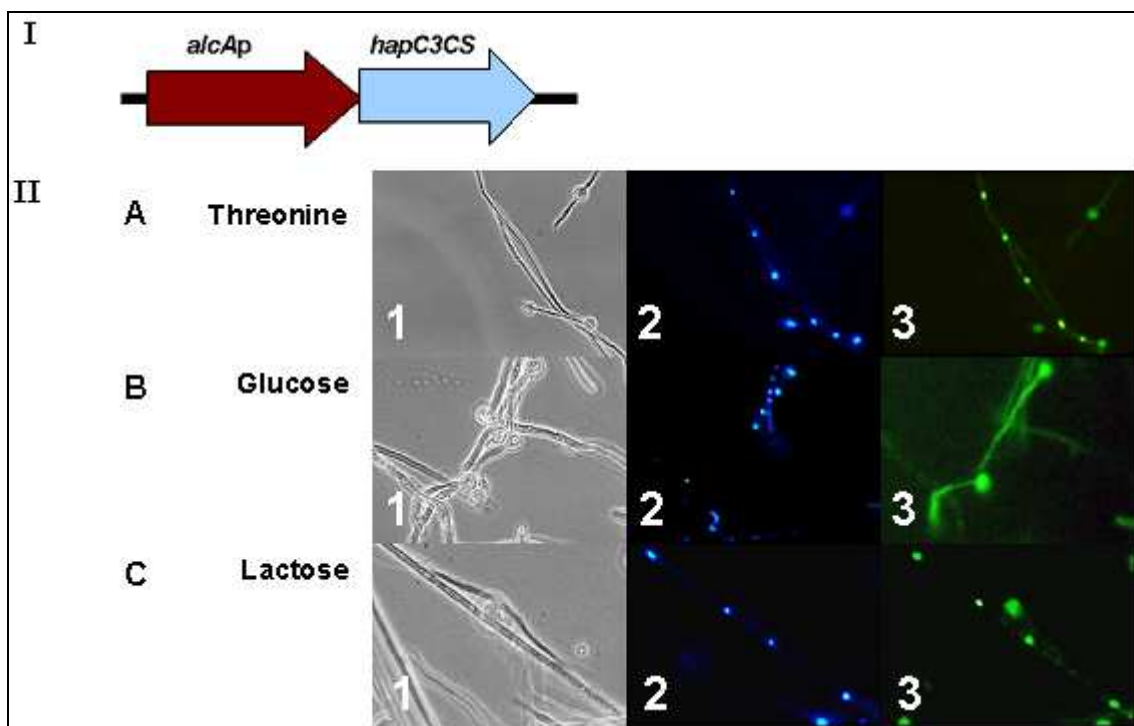
Fig. 10. Cellular localization of CBC complex containing HapC3CS visualized via HapE-EGFP. (I) A schematic map of the generated *alcA*p-*hapC3CS* construct used to transform a *ΔhapC* strain of *A. nidulans*, which contains the *hapE-egfp* fusion under the control of *otef* promoter. (II) Cellular localization of HapE-EGFP fusion protein (panels 3), to monitor the nuclear and cytoplasmic localization of CBC complex under induced (A), inhibited (B) and non-inducing/non-repressing (C) conditions. Samples were analyzed by light microscopy (panels 1) and fluorescence microscopy (panels 2 for DAPI staining of nuclei and panels 3 for EGFP localization).

3.2 Regulation of HapC by the redox status of the cell.

3.2.1 Subcellular localization of *A. nidulans* HapC under oxidative stress conditions.

Subcellular localization is a key functional characteristic of proteins. To cooperate for a common physiological function (metabolic pathway, signal transduction cascade etc.), proteins must be localized in the same cellular compartment. However, the subcellular localization of some proteins might be altered under certain circumstances, e.g. stress conditions.

In this work, I tried to investigate the influence of oxidative stress conditions on the localization of HapC by using an *A. nidulans* strain (ΔC-Cgfp), which carries a HapC-EGFP fusion (Steidl, 2001) under the control of the *otef* promoter (Fig. 11-A). The spores of this strain were grown overnight at 37°C and then exposed to 10 mM H_2O_2 at RT. Then, the subcellular localization of HapC was monitored by visualizing the GFP localization after 15, 30, 45 and 60 minutes post treatment. HapC localization in treated mycelia was compared with the untreated mycelia (-H_2O_2).

Upon H_2O_2 addition, HapC was localized in the cytoplasm up to 30 minutes (Fig. 11-B). However, the subcellular localization of HapC was partially restored back to the nucleus after 45 minutes, in which HapC-EGFP was observed in the nucleus but still visualized in the cytoplasm. After 60 minutes, HapC subcellular localization was restored back to the nucleus (Fig. 11-B).

It is very likely that under oxidative stress conditions, cysteine residues of HapC got oxidized and formed intra- or intermolecular disulfide bridges causing disassembly of the CBC subunits. In order to restore the functional CBC complex, the oxidized form of HapC has to be reduced by an intracellular redox system allowing HapC to become part of the CBC complex.

To confirm the role of cysteine residues in the localization of HapC under oxidative stress, an *A. nidulans* strain (ΔB-Bgfp) was used, which carries a HapB-EGFP fusion (Steidl, 2001) under the control of the *otef* promoter (Fig. 11-A). HapB was used since it contains no cysteine residues (refer to 3.1) and a nuclear localization signal. The conidia of this strain were inoculated overnight at 37°C and the germlings were exposed to 10 mM H_2O_2 at RT. The subcellular localization of HapB was monitored by visualizing GFP localization after 15, 30, 45 and 60 minutes post treatment and compared with untreated mycelia (-H_2O_2).
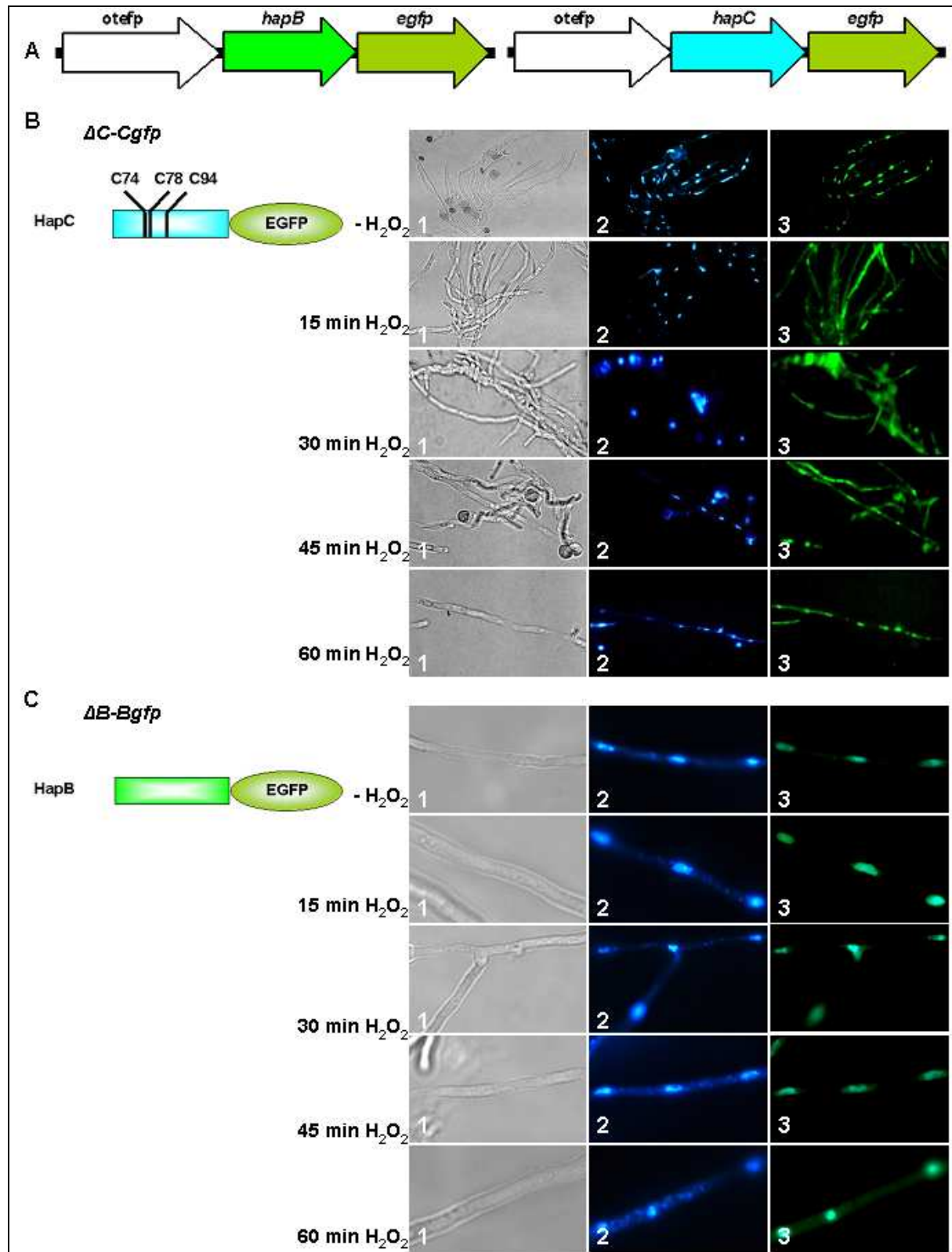
Fig. 11. Visualization of the subcellular localization of HapC and HapB in response to oxidative stress conditions. (A) Schematic map of *hapB-* (left) and *hapC-egfp* (right) gene fusions. (B) Subcellular localization of HapC-EGFP in response to H_2O_2 treatment. (C) Subcellular localization of HapB-EGFP in response to H_2O_2 treatment. Samples were analyzed by light microscopy (panels 1) and fluorescence microscopy (panels 2 for DAPI staining of nuclei and panels 3 for GFP localization). The name of the strains, GFP fusions and the period of H_2O_2 treatment are indicated on the left side.

Unlike HapC, the localization of HapB was not influenced by the treatment with H_2O_2. HapB-EGFP was observed in the nucleus before and after treatment with H_2O_2 (Fig. 11-C).

This further suggests the model that HapC cysteines play a role in the localization of HapC upon treatment with H_2O_2 by forming intra- or intermolecular disulfide bridges causing disassembly of the CBC subunits.

3.2.2 Transcriptional analysis of *A. nidulans trxA*.

The thioredoxin system responds in the cell to oxidative damage and stress by elevated levels of thioredoxin transcripts. Its main function is to keep proteins in the reduced state (Holmgren, 1985). TrxA represents the main thioredoxin of *A. nidulans* (Thön et al., 2007). In this experiment, the response of the cell to oxidative stress was examined by measuring TrxA mRNA steady state level. The change in *A. nidulans trxA* transcripts in response to elevated concentration of H_2O_2 was estimated using the analysis of the *trxA* steady state mRNA levels. The *A. nidulans* strain ΔC-Cgfp was used. The spores of this strain were incubated overnight at 37°C and the germlings were exposed to 10 mM H_2O_2 at RT. The mycelia were harvested after 15, 30, 45 and 60 minutes post treatment. RNA was extracted and the difference in *trxA* transcript levels was visualized by Northern blot using a fluoresceine-labelled probe of the *A. nidulans trxA* gene. The *trxA* transcript levels of treated mycelia were compared with untreated mycelia (0 min).

The probe was prepared by amplifying the *trxA* gene from genomic DNA using the primers (TrxBamHI and TrxNcoI). The 333 bp PCR product was used as a template for generation of a fluoresceine-labelled probe using Gene Images Random Prime Labelling Kit (GE Healthcare).

As expected, under standard conditions hardly any *trxA* mRNA was visible whereas trxA mRNA steady state transcript levels were drastically increased after H_2O_2 exposure (Fig. 12). However, 15 min after addition of H_2O_2 a great amount of *trxA* mRNA was detectable which was reduced after 30 min and not visible anymore after 45 min (Fig. 12). Based on these results, it is very likely that the production of thioredoxin under oxidative stress conditions led to reduction of oxidized HapC.
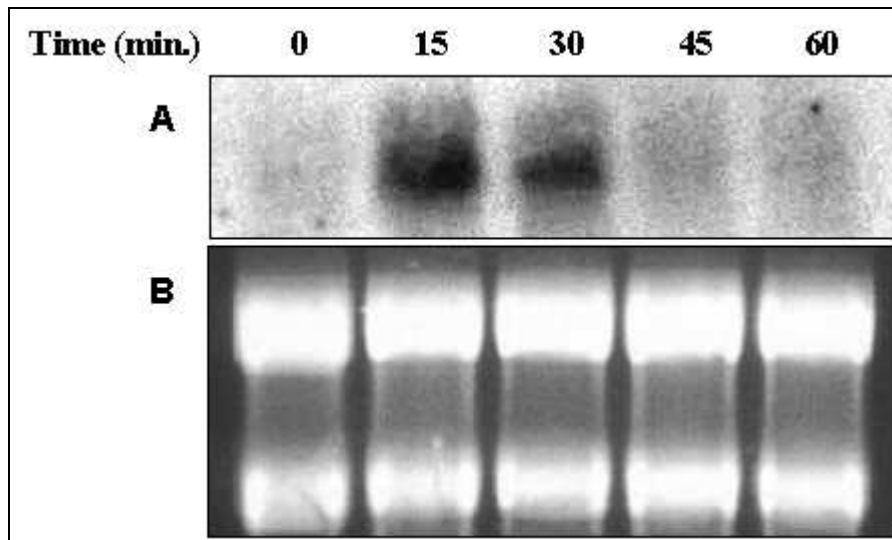
Fig. 12. Response of the cell to oxidative stress measured by *trxA* mRNA steady state level. (A) The mRNA of *A. nidulans* was hybridized with *trxA* specific probe corresponding to 333 bp of *trxA* gene. (B) Photograph of gel stained with ethidium bromide.

3.2.3 Subcellular localization of HapC in a thioredoxin (*trxA*) deletion mutant of *A. nidulans*.

To provide evidence of TrxA involvement in the reduction of oxidized HapC cysteine residues during oxidative stress conditions, a *ΔtrxA A. nidulans* strain (ΔTrxA-Cgfp) was generated, which carries HapC-EGFP fusion under the control of *otef* promoter. The *A. nidulans pyroA* gene, which is required for pyridoxine biosynthesis (Osmani et al., 1999), was amplified by PCR using the primers AnPyro-For and AnPyro-Rev and genomic DNA of the AXB4A2 strain as a template. The 2.5 kbp PCR product, which contains the 1 kbp *pyroA* gene and the 1 kbp of the endogenous promoter and 0.5 kbp of the endogenous terminator, was digested with *Hin*dIII and ligated into pHapC-EGFP. The resulting plasmid, pHapC-EGFP-pyro, carries *pyroA* as a selection marker. The plasmid was transformed into the *ΔtrxA A. nidulans* strain AnTrxAKO (Thön et al., 2007). The resulting strain, which has a *hapC-egfp* fusion and a *trxA* deletion, was designated ΔTrxA-Cgfp. The strain was grown overnight in AMM with 2 mM glutathione at 37°C and microscoped. As expected, HapC was localized in the cytoplasm. The HapC-EGFP was detected mainly in the cytoplasm but some localization of HapC-EGFP was also observed in the nucleus (Fig. 13).

Combining the previous results from points 3.2.1 and 3.2.2, in which we proposed that oxidized HapC forms intra- and intermolecular disulfide bridges causing disassembly of the CBC subunits, with these results provides indirect evidence that TrxA binds to the oxidized HapC and reduces it. This allows reduced HapC to become part of the CBC complex.

However, to provide a direct evidence for TrxA-HapC interaction, bimolecular complementation (BiFC) was applied to visualize TrxA-HapC interaction *in vivo*.

Fig. 13. Visualization of the subcellular localization of HapC-EGFP in a *ΔtrxA A. nidulans* strain (ΔTrxA-Cgfp). Samples were analyzed by light microscopy (panels 1) and fluorescence microscopy (panels 2 for DAPI staining of nuclei and panels 3 for GFP localization). The HapC-GFP fusion is indicated on the left side.

3.2.4 Visualization of the protein-protein interactions *in vivo* using bimolecular fluorescence complementation (BiFC).

BiFC assay was used to study protein-protein interactions in *A. nidulans*. This approach is based on the complementation between two non-fluorescent fragments of the yellow fluorescent protein (YFP) when they are brought together by interactions between proteins fused to each fragment (Fig. 14).

Fungal expression vectors for the bimolecular fluorescence complementation assay were provided by Hoff and Kück (2005). The N-terminus region encoding the 1–154 amino acids (*eyfp*N) and C-terminus region encoding 155– 238 amino acids (*eyfp*C) of the *eyfp* were cloned to fungal plasmid under the control of the *A. nidulans gpdA* promotor. Linker sequences encoding RSIAT and RPACKIPNDLKQKVMNH were inserted in front of *eyfpN and eyfpC*, respectively (Hu et al., 2002). The resulting plasmids were designated pEYFPN and pEYFPC and contain the eyfpN and eyfpC, respectively. Additionally, in both plasmids, the *Nco*I and *Not*I sites were inserted in front of linker sequences to fuse genes of interest (Fig. 15).

Fig. 14. Principle of the bimolecular fluorescence complementation assay (BiFC). (A) Predicted structure of the EYFP protein. The picture is based on the X-ray crystal structure of GFP and generated using the program PyMol (DeLano Scientific LLC, USA). The C- and the N- terminal parts of EYFP are shown in green and yellow, respectively. (B) The EYFP protein is split into non-fluorescent N- and C-terminal parts and fused to two putative interaction proteins; protein X and Y. The interaction between the two proteins facilitates the association of the two EYFP termini and restoration of fluorescence which could be visualized microscopically.

Fig. 15. Schematic overview of the BiFC fusion constructs used to fuse the interacting partners to EYFPC (A) and EYFPN (B). The *A. nidulans gpdA* promoter is indicated in white arrow. Linker sequences encoding RPACKIPNDLKQKVMNH and RSIAT are drawn in grey boxes. The *eyfpC* and *eyfpN* are marked by yellow arrows. In-frame fusion to *eyfpC* or *eyfpN* was performed using *Nco*I and *Not*I.

3.2.4.1 Construction of expression vectors for visualizing protein-protein interactions using BiFC.

3.2.4.1.1 Construction of expression vectors for visualizing protein-protein interactions with HapC.

The *hapC* gene was amplified by PCR using pHapC-EGFP as a template and the primers HapC-BiFC-For and HapC-BiFC-Rev, which carry *Nco*I in their sequences. The resulting fragment had a length of 621 bp and ATG GCA, which encodes for methionine and alanine, in front of the *hapC* translational start codon. The PCR fragment was ligated into pCR®2.1 resulting in a plasmid called pCR2.1-HapC-Bi. The PCR fragment was sequenced and the correct plasmid was cloned afterwards to the plasmid pEYFPC and fused to the C-terminal part of *eyfp* using *Nco*I. The resulting plasmid was designated pHapC-YC. The 1.4 kbp region between the two *Apa*I restriction sites, which contains *trpC*p-*hph*, was removed by digestion with *Apa*I. The resulting plasmid was called pHapC-YC-Δhyg. This plasmid was digested afterwards with *Xba*I and the 3.8 kbp fragment, which contains *gpdA*p-*hapC-eyfpC-trpC*t, was ligated into pKTB1. The resulting plasmid was designated pHapC-YC-pyr4 and it contains the *pyr-4* gene as a selection marker.

The 2.6 kbp fragment, which contains *gpdA*p-*hapC-eyfpC-trpC*t, was also amplified by PCR using the primers EYFP5'BamHI and EYFP3'BamHI. The plasmid pHapC-YC-pyr4 was used as a template. PCR product was digested with *Bam*HI, which resulted in the removal of the *trpC* terminator. The remaining fragment was ligated into PabaAnid. The resulting plasmid, pHapC-YC-paba, carries the *pabaA1* gene as a selection marker.

HapC was also fused to the N-terminal part of YFP. The *hapC* gene was PCR amplified using the primers HapC-BiFC-For and HapC'3NotI625. The plasmid pHapC-YC-pyr4 was used as a template. The PCR product was digested with *Nco*I and *Not*I and ligated into pEYFPN. The resulting plasmid was called pHapC-YN. The 2.78 kbp fragment, which contains *gpdA*p-*hapC-eyfpN-trpC*t, was also amplified by PCR using the primers EYFP5'BamHI and EYFP3'BamHI and using pHapC-YN as a template. The PCR product was digested with *Bam*HI, which led to the removal of the *trpC* terminator. The remaining fragment was ligated into plasmid PabaAnid. The resulting plasmid was designated pHapC-YN-paba. It carries *pabaA1* as a selection marker.

3.2.4.1.2 Construction of expression vectors for visualizing protein-protein interactions with HapC3CS.

The *hapC3CS* gene was amplified by PCR using pHapC3CS-EGFP as a template and the primers HapC-BiFC-For and HapC-BiFC-Rev, which carry *Nco*I in their sequences. The resulting fragment had a length of 621 bp and has ATG GCA in front of *hapC3CS* translational start codon, which encodes for methionine and alanine. The PCR fragment was cloned into pHapC-YC-Δhyg and was thereby fused to the C-terminal part of *eyfp*, after removing *hapC* using *Nco*I. The resulting plasmid was called pHapC3CS-YC-Δhyg. After sequencing, a 3.8 kbp DNA fragment, which contains *gpdA*p-*hapC-eyfpC*-trpCt, was cloned into the plasmid pKTB1 using the *Xba*I site. The resulting plasmid was designated pHapC3CS-YC-pyr4. It contains the *pyr-4* gene as a selection marker.

3.2.4.1.3 Construction of expression vectors for visualizing protein-protein interactions with HapE.

The *hapE* open reading frame was cloned directly by digesting pHapE-EGFP with *Nco*I. The 986 bp *hapE* fragment, which is made up of 795 bp *hapE* encoding four exons separated by 185 bp containing three introns (Fig. 16), was ligated into pEYFPN and thereby fused to the N-terminal part of *eyfp*. The resulting plasmid was pHapE-YN.

Exon1 Exon2 Exon3 *Kpn*I (274) Exon4 *Cla*I (665) *Nde*I (806)
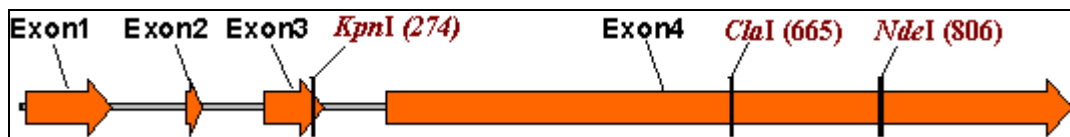
Fig. 16. Schematic overview of the *hapE* used in BiFC. The *hapE* gene used for BiFC analysis contains four exons separated by three introns.

The 3.1 kbp DNA fragment, which contains *gpdA*p-*hapE-eyfpN-trpC*t, was amplified by PCR using the primers EYFP5'EcoRI(C2) and EYFP3'EcoRI(C2) and the plasmid pHapE-YN as a template. The PCR product was digested with *Eco*RI and ligated into pNfyB-YC-pyr4 (refer to 3.2.4.1.8). The resulting plasmid, pNfyB-HapE-pyr4, carries *pyr-4* as a selection marker. The plasmid was afterwards digested with *Xba*I causing removal of a 5.3 kbp DNA fragment, which contains *gpdA*p-*nfyB-eyfpC-trpC*t. The plasmid was then re-ligated resulting in plasmid pHapE-YN-pyr4, which contains only *hapE-eyfpN* under the control of the *gpdA* promoter and has *pyr-4* as a selection marker.

3.2.4.1.4 Construction of expression vectors for visualizing protein-protein interactions with HapB.

The ORF of *hapB* was amplified by PCR using HapB 5'NcoI and HapB 3'NotI primers, which were also used to insert *Nco*I and *Not*I sites at the 5' and 3' ends of the PCR fragment, respectively. The plasmid pHapB-EGFP was used as PCR template for *hapB* amplification. The PCR product was digested with *Nco*I and *Not*I and cloned into pEYFPN. The resulting plasmid, which contains *hapB* fused to the N-terminal part of *eyfp*, was designated pHapB-YN.

The 3.2 kbp DNA fragment, which contains *gpdA*p-*hapB-eyfpN-trpC*t, was amplified by PCR using the primers EYFP5'EcoRI and EYFP3'EcoRI and pHapB-YN as a template. PCR product was digested with *Eco*RI and ligated into pHapX-YC-pyr4 (refer to 3.2.4.1.7). The resulting plasmid was designated pHapX-HapB-pyr4. It carries *pyr-4* as a selection marker.

3.2.4.1.5 Construction of expression vectors for visualizing protein-protein interactions with TrxA.

Amplification of the *trxA* gene was done by PCR using the primers TrxBamHI and TrxNcoI and the plasmid pET39-AnTrxA(wt)-H6 as a template. The PCR product was digested with *Nco*I and ligated into pEYFPN. The resulting plasmid was designated pTrxA-YN, which contains *trxAC* fused to the N-terminal part of *eyfp*. The 2.5 kbp fragment, which contains *gpdA*p-*trxA-eyfpN-trpC*t, was amplified by PCR using the primers EYFP5'KpnI and EYFP3'KpnI. The plasmid pTrxA-YN was used as a template. The PCR product was digested with *Acc*65I (an isoschizomer of *Kpn*I) and ligated into pNfyB-YC-pyr4 (refer to 3.2.4.1.8). The resulting plasmid, pNfyB-TrxA-pyr4, carries *pyr-4* as a selection marker. The plasmid was afterwards digested with *Xba*I causing the removal of a 5.3 kbp DNA fragment, which contains *gpdA*p-*nfyB-eyfpC-trpC*t. The plasmid was then re-ligated resulting in the plasmid pTrxA-YN-pyr4, which contains only *trxA-eyfpN* under the control of *gpdA* promoter and has *pyr-4* as a selection marker.

3.2.4.1.6 Construction of an expression vector for visualizing protein-protein interactions with mutagenized TrxA (TrxAC39S).

Amplification of mutant *trxA* gene (*trxAC39S*) was done by PCR using the primers TrxBamHI and TrxNcoI and the plasmid pET39-AnTrxA(C39S)-H6 as a template. The PCR product was digested with *Nco*I and ligated into pEYFPN. The resulting plasmid was designated pTrxAC39S-YN, which contains *trxAC39S* fused to the N-terminal part of *eyfp*.

3.2.4.1.7 Construction of expression vectors for visualizing protein-protein interactions with HapX.

The *hapX* gene was amplified by PCR using the genomic DNA of the strain AXB4A2. The fragment was amplified by using the primers: HapX-For and HapX-Rev. The resulting PCR fragment had a length of 1.4 kbp and an *Nco*I site at the 5' and 3' ends. The DNA fragment was ligated into pCR®2.1 resulting in a plasmid called pCR2.1-HapX. After sequencing, the *hapX* ORF was amplified by PCR using HapX5'NcoI and HapX3'NotI primers. The PCR product was digested with *Nco*I and *Not*I and *hapX* was ligated into pEYFPC and pEYFPN resulting in the plasmids pHapX-YC and pHapX-YN, which contain *hapX* fused to the *eyfpC* and *eyfpN* termini, respectively.

The 1.4 kbp DNA region in pHapX-YC, which is located between the two *Apa*I restriction sites and contains *trpC*p-*hph*, was removed by digestion with *Apa*I. The resulting plasmid was called pHapX-YC-Δhyg. This plasmid was digested with *Xba*I and the 4.65 kbp DNA fragment, which contains *gpdA*p-*hapX-eyfpC-trpC*t, was ligated into pKTB1. The resulting plasmid was designated pHapX-YC-pyr4. It contains *pyr-4* gene as a selection.

The 3.4 kbp DNA fragment, which contains *gpdA*p-*hapX-eyfpC-trpC*t, was also amplified by PCR using the primers EYFP5'BamHI and EYFP3'BamHI. As a template, the plasmid pHapX-YC-pyr4 was used in the PCR. The PCR product was digested with *Bam*HI, which resulted in the removal of the *trpC* terminator. The remaining fragment was ligated into PabaAnid. The resulting plasmid was designated pHapX-YC-paba. It carries *pabaA1* as a selection marker.

3.2.4.1.8 Construction of expression vectors for visualizing protein-protein interactions with NF-YB.

The ORF of *nf-yB* was amplified by PCR using TEV-NF-YB (P. Hortschansky, pers. communication) as a template and the primers NF-YB-For and NF-YB-Rev, which were also used to insert *Nco*I and *Not*I sites at the 5' and 3' ends of the PCR fragment, respectively. The resulting PCR fragment was 650 bp. It contains ATG GCA, which encodes for methionine and alanine, in front of *nf-yB* translational start codon. The PCR fragment was cloned into the plasmid pEYFPC and fused to the C-terminal part of *eyfp* using *Nco*I and *Not*I. The resulting plasmid was designated pNfyB-YC. After sequencing, the plasmid was digested with *Xba*I and the 5.3 kbp DNA fragment, which contains *gpdA*p-*nfyB*-*eyfpC*-*trpC*t, was ligated into pKTB1. The resulting plasmid was designated pNfyB-YC-pyr4. It contains the *pyr-4* gene as a selection marker.

3.2.4.1.9 Construction of expression vectors for generation of control strains.

The plasmid pEYFPC was digested with *Apa*I thereby removing the 1.4 kbp DNA fragment between the two *Apa*I restriction sites, which contains *trpC*p-*hph*. The resulting plasmid was called pYC-Δhyg. This plasmid was digested with *Xba*I and the 3.2 kbp DNA fragment, which contains *gpdA*p-*eyfpC*-*trpC*t, was ligated into pKTB1. The resulting plasmid was designated pYC-pyr4. It contains *pyr-4* gene as a selection marker.

Using the plasmid pEYFPN as a template, the 2.2 kbp DNA fragment, which contains *gpdA*p-*eyfpN*-*trpC*t, was amplified by PCR using the primers EYFP5'EcoRI(C2) and EYFP3'EcoRI(C2). The PCR product was digested with *Eco*RI and ligated into pKTB1. The resulting plasmid was designated pYN-pyr4. It carries *pyr-4* as a selection marker.

3.2.4.2 Generation of *A. nidulans* strains for BiFC analysis.

Plasmids encoding YFP-fusion partner proteins were co-transformed in *A. nidulans* ectopically together with the autonomously replicating *A. nidulans* vector pHELP consisting of pUC18 and the *ama1* (Gems and Clutterbuck, 1993; Aleksenko and Clutterbuck, 1997). Transformants were tested by PCR using the primer pairs eyfpC-For-long and eyfpC-Rev-long, and eyfpN-For-long and eyfpN-Rev-long, which amplify *eyfpC* and *eyfpN*, respectively. Moreover, transformants were confirmed by Southern blot but were not tested for the copy number integration of the plasmids (not shown).

3.2.4.3 Visualization of the interaction between HapC and HapE under oxidative stress conditions.

3.2.4.3.1 Visualization of HapC-HapE interaction under imbalanced stoichiometric overexpression of HapC and HapE in response to oxidative stress.

We started our BiFC assay by analyzing the well known interaction between HapC and HapE. The plasmids pHapC-YC-pyr4 and pHapE-YN, which carry *hapC-eyfpC* and *hapE-eyfpN* fusions respectively, along with pHELP were constructed and transformed in the AXB4A2 strain, as mentioned above (refer to 3.2.4.1.1, 3.2.4.1.3 and 3.2.4.2). The strain was called yHapC-HapE.

In order to ensure that the observed fluorescence resulted from the specific protein-protein interactions and not from unspecific binding of the two EYFP termini, from background or autofluorescence, several control strains were generated. The strains yC and yN were constructed by transforming the plasmids pYC-pyr4 and pYN-pyr4 (refer to 3.2.4.1.9), respectively, in the AXB4A2 strain. The strain yCN was generated by co-transforming the AXB4A2 strain with pYC-pyr4 and pEYFPN. Moreover, the strain yHapE-C was generated by co-transforming the AXB4A2 strain with pHapE-YN and pYC-pyr4 (refer to 3.2.4.1.3 and 3.2.4.1.9). Finally, the strain yHapC-N was generated by co-transforming the AXB4A2 strain with pHapC-YC-pyr4 (refer to 3.2.4.1.1) and pEYFPN.

Using BiFC, we could visualize the interaction between HapC and HapE in the strain yHapC-HapE (Fig. 17). The interaction between HapC and HapE was mainly in the nucleus. However, since the HapC and HapE subunits were under the control of strong promoters, the interaction was also noticed in the cytoplasm caused by imbalance in the stoichiometry of the complex leading to accumulation of the HapC-HapE dimer in the cytoplasm (Fig. 17, 0 min).

To study the influence of oxidative stress on CBC complex, the yHapC-HapE strain was grown in AMM overnight at 37°C and then exposed to 10 mM H_2O_2. Samples were collected after 15, 30, 45 and 60 minutes and microscoped. Upon treatment with H_2O_2, we noticed strong fluorescence in the cytoplasm after 15 and 30 minutes. After 45 minutes, fluorescence was reduced in the cytoplasm. Finally after 60 minutes, fluorescence was restored again mainly in the nucleus and partially in the cytoplasm (Fig. 17). However, this contradicted our expectation, which is the dissociation of the HapC-HapE dimer upon treatment with H_2O_2. In

the control strains yN, yC, yCN, yHapE-C and yHapC-N, no fluorescence was noticed (Fig. 17).
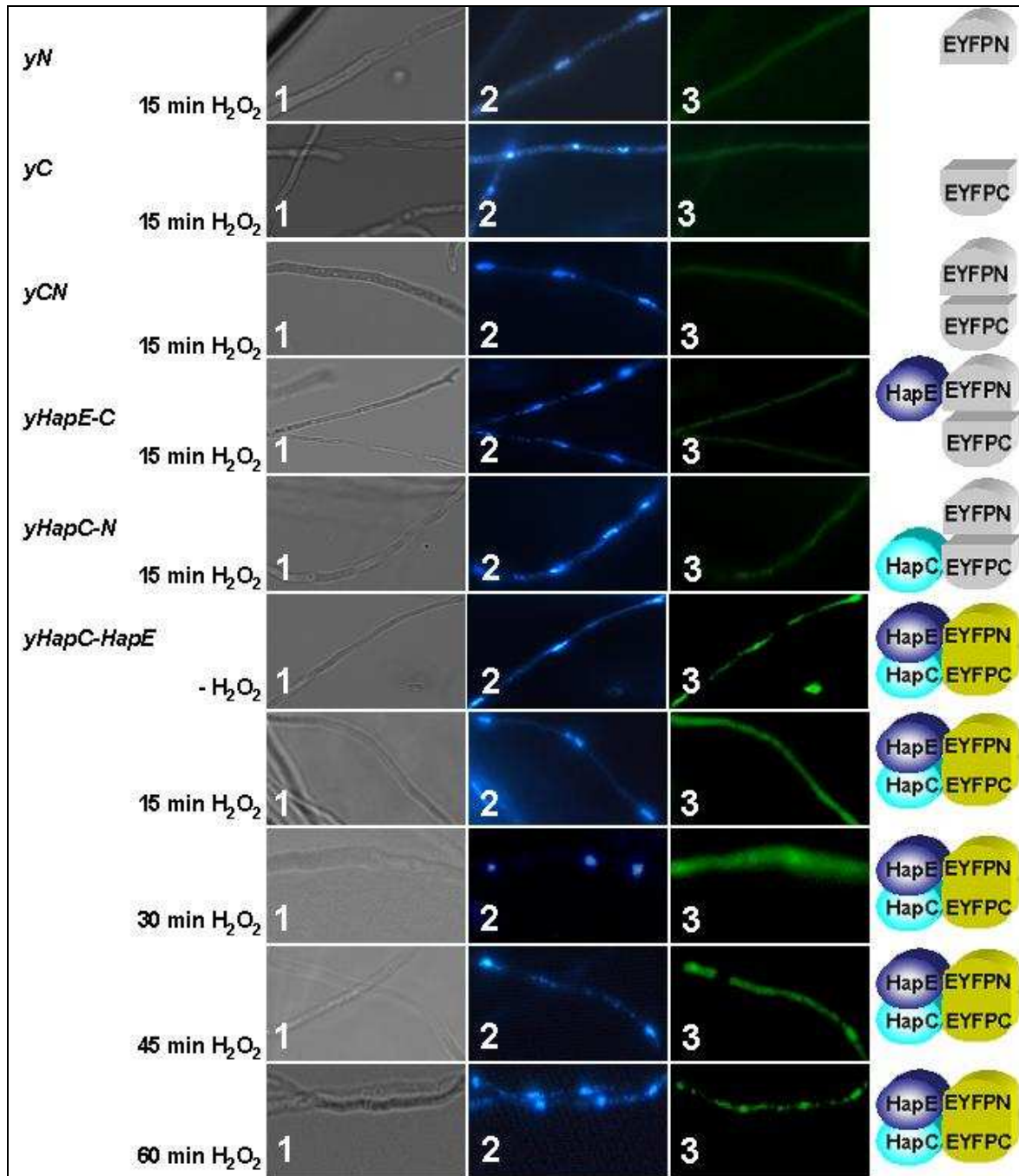
Fig. 17. Visualization of the subcellular localization of HapC-HapE heterodimer in response to oxidative stress under imbalanced stoichiometric overexpression of HapC and HapE. (1) Light microscopy of the mycelia, (2) DAPI staining of the nucleus, (3) fluorescence microscopy of mycelia. The name of the strains (bold italics) and the period of H_2O_2 treatment are indicated on the left side. The interacting partners of BiFC are drawn on the right side.

3.2.4.3.2 Visualization of HapC-HapE interaction under balanced stoichiometric overexpression of all three subunits in response to oxidative stress.

In order to avoid any misinterpretation caused by stoichiometrically imbalanced expression of the CBC subunits, transformation of the yHapC-HapE strain with the *hapB* gene under the control of the strong *gpdA*p promoter was done. The *hapB* gene was amplified by PCR with the primers EYFP5'BamHI and gpdA-HapB-Rev using pHapB-YN as a template. The PCR product was digested with *Bam*HI and cloned into PabaAnid. The resulting plasmid was designated pHapB-paba. The plasmid pHapB-paba was transformed into the strain yHapC-HapE resulting in strain yHapC-HapE-HapB, which restored the stoichiometric imbalance of CBC subunits since they are all under the control of the *gpdA* promoter. Like the strain yHapC-HapE, the strain yHapC-HapE-HapB was treated with H_2O_2 and microscoped, as mentioned above. The HapC-HapE dimer was stable under oxidative stress conditions when the stoichiometric balance of all complex subunits was restored (Fig. 18), since no change or reduction in the fluorescence was noticed upon treatment with H_2O_2.
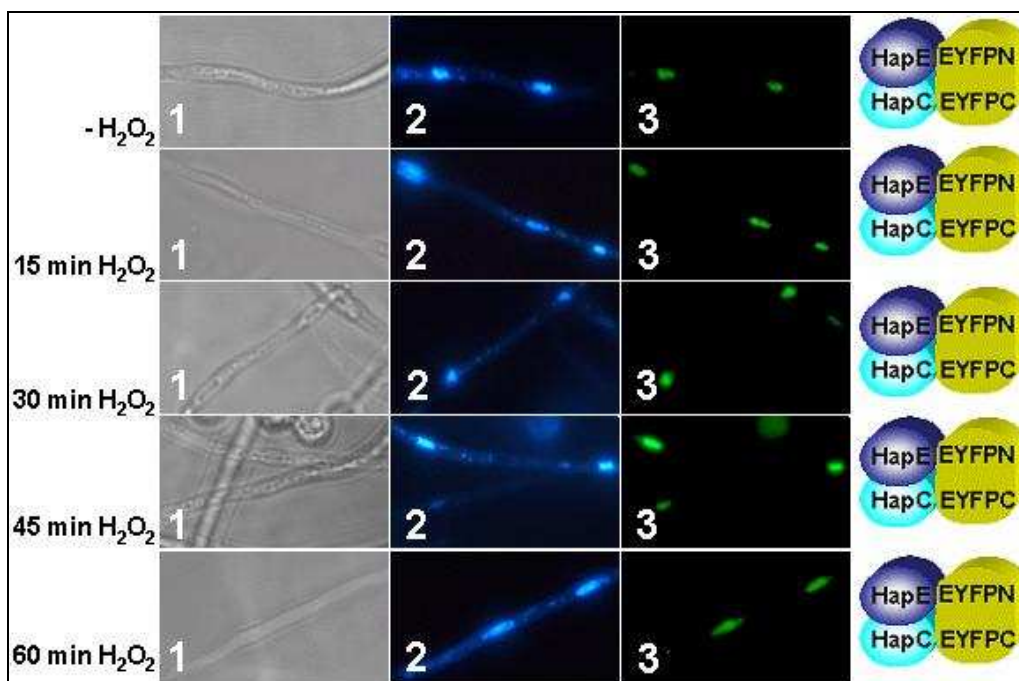
Fig. 18. Visualization of the subcellular localization of HapC-HapE heterodimer in response to oxidative stress under balanced stoichiometric overexpression of all CBC three subunits. (1) Light microscopy of the mycelia, (2) DAPI staining of the nucleus, (3) fluorescence microscopy of mycelia. The period of H_2O_2 treatment is indicated on the left side. The interacting partners of BiFC are drawn on the right side.

3.2.4.4 Visualization of the interaction between HapC and TrxA under oxidative stress conditions.

BiFC assay was employed to analyze the interaction between HapC and TrxA under oxidative stress conditions. Therefore, the analysis was divided into three parts:

1. The interaction between wild-type HapC and wild-type TrxA. In this analysis, we expected to observe transient interaction between HapC and TrxA.

2. The interaction between wild-type HapC and mutagenized TrxA (TrxAC39S). Since the permanent interaction of TrxA with the target protein has been reported when the TrxA cysteine at position 39 was mutagenized to serine (Kallis and Holmgren, 1980; Thön et al., 2007), mutagenized TrxA (TrxAC39S) was used to visualize the permanent interaction between HapC and TrxAC39S.

3. The interaction between mutagenized HapC (HapC3CS) and wild-type TrxA. This interaction served as a negative control. However, we expected that TrxA would not interact with HapC when all HapC cysteines were mutagenized to serine.

3.2.4.4.1 Visualization of the interaction between wild-type HapC and wild-type TrxA under oxidative stress conditions.

An *A nidulans* strain was constructed by co-transformation of the AXB4A2 strain with the plasmids pHapC-YC-pyr4 and pTrxA-YN in addition to pHELP (refer to 3.2.4.1.1, 3.2.4.1.5 and 3.2.4.2). The strain was designated yHapC-TrxA. It contains HapC and TrxA fused to the C- and N- terminal parts of YFP, respectively. To ensure that the fluorescence resulted from specific protein-protein interactions, two control strains were used. The first strain, yHapC-N, was described previously (refer to 3.2.4.3.1), while the second strain yTrxA-C was generated by co-transforming the AXB4A2 strain with pTrxA-YN and pYC-pyr4 (refer to 3.2.4.1.5 and 3.2.4.1.9). To visualize the transient interaction between HapC and TrxA under oxidative stress conditions, two concentrations of H_2O_2 were used, 10 mM (high concentration) and 0.1 mM (low concentration).

To study the interaction between HapC and TrxA under high H_2O_2 concentration, the yHapC-TrxA strain was grown in AMM overnight at 37°C and then exposed to 10 mM H_2O_2. Samples were collected at 0, 15, 30, 45 and 60 minutes post treatment and microscoped. Surprisingly, the interaction between HapC and TrxA was not transient but rather permanent

(Fig. 19). Upon treatment with H_2O_2, fluorescence was noticed in the cytoplasm after 15 and 30 minutes. The fluorescence was extremely weak but slightly stronger than background. After 45 and 60 minutes, strong fluorescence was visualized mainly in the nucleus (Fig. 19).
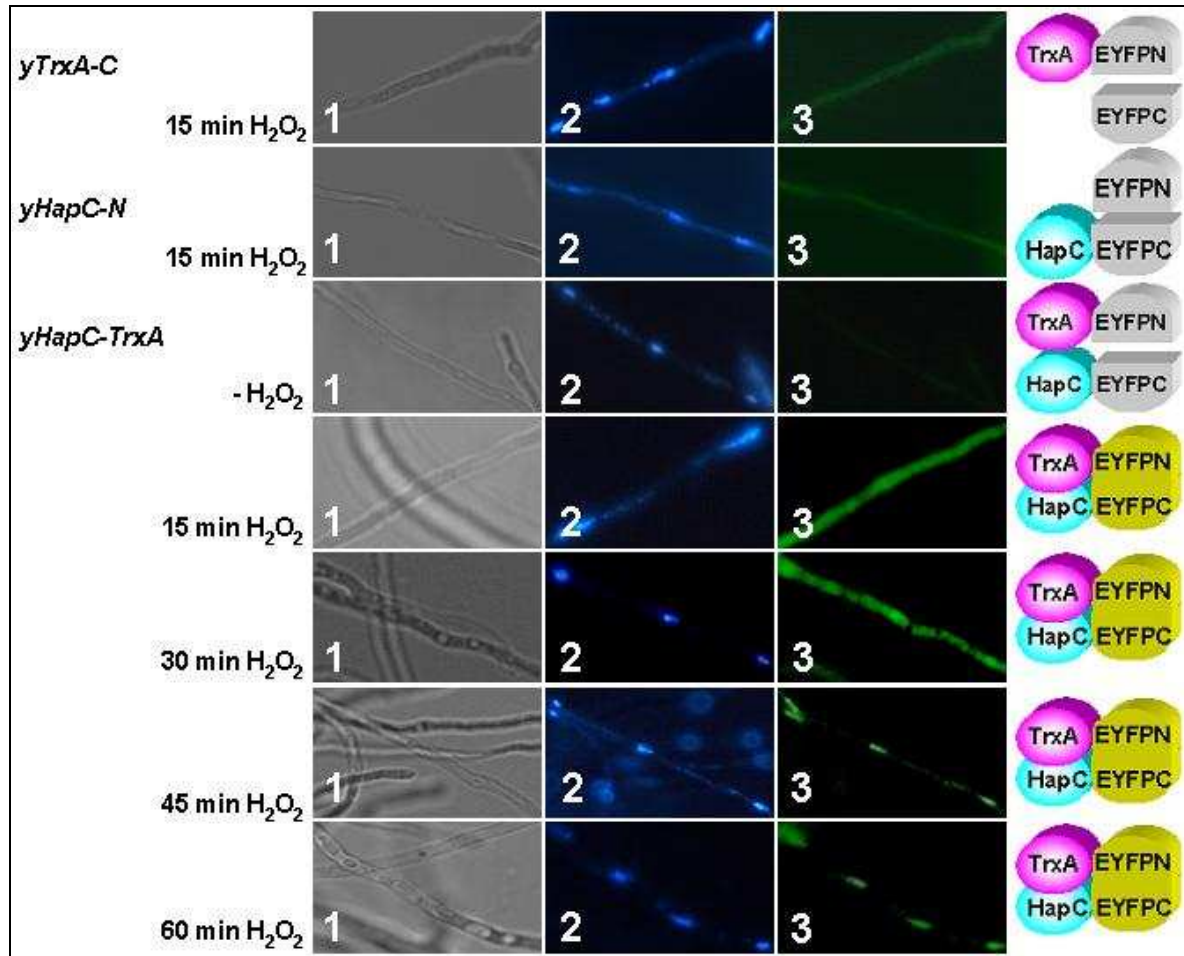
Fig. 19. Visualization of the transient interaction between HapC and TrxA in response to oxidative stress. (1) Light microscopy of the mycelia, (2) DAPI staining of the nucleus, (3) fluorescence microscopy of mycelia. The name of the strains (bold italics) and the period of H_2O_2 treatment are indicated on the left side. The interacting partners of BiFC are drawn on the right side.

Fig. 20. Visualization of the transient interaction between HapC and TrxA in response to oxidative stress. (1) Light microscopy of the mycelia, (2) DAPI staining of the nucleus, (3) fluorescence microscopy of mycelia. The name of the strains (bold italics) and the period of H_2O_2 treatment are indicated on the left side. The GFP fusion and the interacting partners of BiFC are drawn on the right side.

Visualized fluorescence resulting from HapC-TrxA interaction was weaker compared with the constitutive interaction between HapC and HapE. In the control strains yTrxA-C and yHapC-N, no fluorescence was detected (Fig. 19). However, combining these results with the results reported above (points 3.2.1, 3.2.2 and 3.2.3) indicates that under oxidative stress conditions, HapC gets oxidized and forms intra- or intermolecular disulfide bridges. The oxidized form is reduced by TrxA allowing HapC to become part of CBC complex.

To study the interaction between HapC and TrxA under low H_2O_2 concentrations, the yHapC-TrxA strain was grown in AMM overnight at 37°C and then exposed to 0.1 mM H_2O_2. Samples were collected after 15 minutes of H_2O_2 treatment and microscoped. At the same time, the strain ΔC-Cgfp, which carries HapC-EGFP fusion, was also treated with 0.1 mM H_2O_2. Unlike high H_2O_2 concentration, fluorescence resulting from the interaction between HapC and TrxA was noticed in the nucleus directly after 15 minutes, while HapC-EGFP did not accumulate in the cytoplasm (Fig. 20). The fluorescence resulting from HapC-TrxA interaction was also weaker compared with the fluorescence observed for the constitutive interaction between HapC and HapE.

3.2.4.4.2 Visualization of the interaction between wild-type HapC and mutagenized TrxA (TrxAC39S) under oxidative stress conditions.

An *A. nidulans* strain was constructed by co-transformation of the AXB4A2 strain with the plasmids pHapC-YC-pyr4 and pTrxAC39S-YN along with pHELP as mentioned above (refer to 3.2.4.1.1, 3.2.4.1.6 and 3.2.4.2). The strain was designated yHapC-TrxAC39S. It contains HapC and TrxAC39S fused to the C- and N-terminal parts of YFP, respectively. Moreover, two control strains were used. The first strain, yHapC-N, was described previously (refer to 3.2.4.3.1), while the second strain yTrxAC39S-C was generated by co-transforming the AXB4A2 strain with pTrxAC39S-YN and pYC-pyr4 (refer to 3.2.4.1.6 and 3.2.4.1.9).

To visualize the permanent interaction between HapC and TrxAC39S under oxidative stress conditions, the yHapC-TrxAC39S strain was grown in AMM overnight at 37°C and then exposed to 10 mM H_2O_2. Samples were collected at 0, 15, 30, 45 and 60 minutes post treatment and microscoped. The visualized interaction between HapC and TrxAC39S was permanent, as expected. The interaction between HapC and TrxAC39S under oxidative stress conditions followed the same pattern as the interaction between HapC and TrxA. Fluorescence was detected in the cytoplasm after 15 and 30 minutes. The fluorescence was extremely weak but stronger than background. After 45 and 60 minutes, fluorescence was

visualized mainly in the nucleus (Fig. 21). Like the interaction between HapC and TrxA, HapC-TrxAC39S interaction showed extremely weak fluorescence compared with the constitutive interaction between HapC and HapE. In control strains, no fluorescence was detected (Fig. 21).
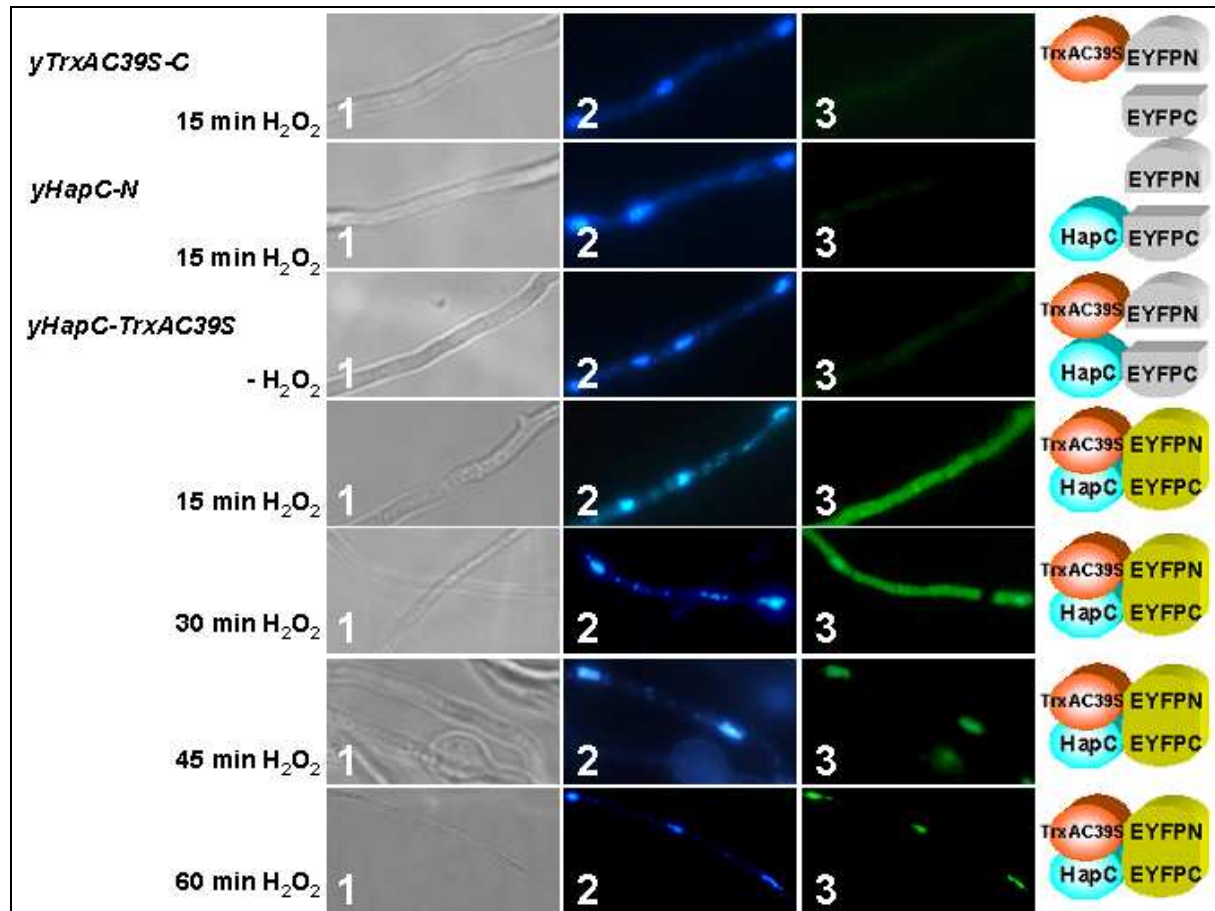
Fig. 21. Visualization of the interaction between HapC and mutant TrxAC39S in response to oxidative stress. (1) Light microscopy of the mycelia, (2) DAPI staining of the nucleus, (3) fluorescence microscopy of mycelia. The name of the strains (bold italics) and the period of H_2O_2 treatment are indicated on the left side. The interacting partners of BiFC are drawn on the right side.

3.2.4.4.3 Visualization of the interaction between mutagenized HapC (HapC3CS) and wild-type TrxA under oxidative stress conditions.

This experiment was used as a control experiment for HapC-TrxA interaction. We expected that there will be no interaction between HapC and TrxA when all HapC cysteines are mutagenized to serine. Therefore, I constructed an *A. nidulans* strain carrying mutagenized HapC, in which all cysteines were exchanged to serine (HapC3CS), fused to the C-terminal part of YFP, and TrxA fused to the N-terminal part of YFP. The strain was constructed by co-transformation of strain AXB4A2 with the plasmids pHapC3CS-YC-pyr4 and pTrxA-YN in

addition to pHELP (refer to 3.2.4.1.2, 3.2.4.1.5 and 3.2.4.2). This strain was called yHapC3CS-TrxA. To study the interaction between HapC3CS and TrxA under oxidative stress conditions, the yHapC3CS-TrxA strain was grown in AMM overnight at 37°C and then exposed to 10 mM H_2O_2. Samples were collected at 0, 15, 30, 45 and 60 minutes post treatment and microscoped.

Surprisingly, the interaction between HapC3CS and TrxA under oxidative stress conditions was visualized in the strain yHapC3CS-TrxA despite mutagenizing all cysteine residues of HapC into serine (Fig. 22). The interaction between HapC3CS and TrxA under oxidative stress conditions followed a different pattern compared with HapC-TrxA interaction. The HapC3CS, which forms less stable but functional CBC complex, tends to interact stronger with TrxA in the cytoplasm since the fluorescence resulting from HapC3CS-TrxA interaction was visualized in the cytoplasm for longer, nearly 45 minutes, than HapC-TrxA interaction. Again, the fluorescence was extremely weak but stronger than background. After 60 minutes, strong fluorescence was visualized mainly in the nucleus (Fig. 22). Visualized fluorescence resulting from HapC3CS-TrxA interaction was weaker compared with the fluorescence observed for the constitutive interaction between HapC and HapE.

3.2.4.5 Visualization of the interaction between HapC and TrxA in an *A. nidulans ΔhapE* strain under oxidative stress conditions.

The reason of using the *ΔhapE* strain is that in the absence of HapE, HapC localizes in the cytoplasm while HapB localizes in the nucleus. This allowed us to visualize the specific interaction between TrxA and HapC *in vivo*. Therefore, an *A. nidulans* strain was constructed by co-transformation using the plasmids pHapC-YC-paba and pTrxA-YN-pyr4 in the *ΔhapE* strain (ΔE-89), as mentioned above (refer to 3.2.4.1.1, 3.2.4.1.5). The strain was designated yHapC-TrxA-ΔE. It contains HapC and TrxA fused to the C- and N-terminal parts of YFP, respectively. To visualize the interaction betw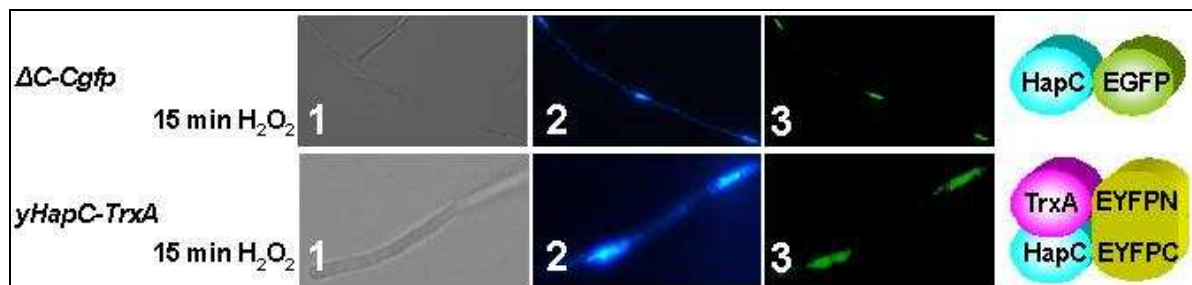een HapC and TrxA under oxidative stress conditions, the yHapC-TrxA-ΔE strain was grown in AMM overnight at 37°C and then exposed to 10 mM H_2O_2. Samples were collected at 0, 15, 30, 45 and 60 minutes post treatment and microscoped. Treatment of mycelia with H_2O_2 induced the interaction between HapC and TrxA (Fig. 23). The interaction was visualized by BiFC fluorescence in the cytoplasm after 15 min and until 60 min (Fig. 23). The results showed that the fluorescence was extremely weak but slightly stronger than background. Visualized fluorescence resulting from HapC-TrxA interaction was weaker compared with the fluorescence observed for the constitutive interaction between HapC and HapE. However, combining these results with the

results above (points 3.2.1, 3.2.2, 3.2.3 and 3.2.4.4.1) shows that TrxA binds precisely to the oxidized HapC and reduces it. This enables HapC to become part of the CBC complex.
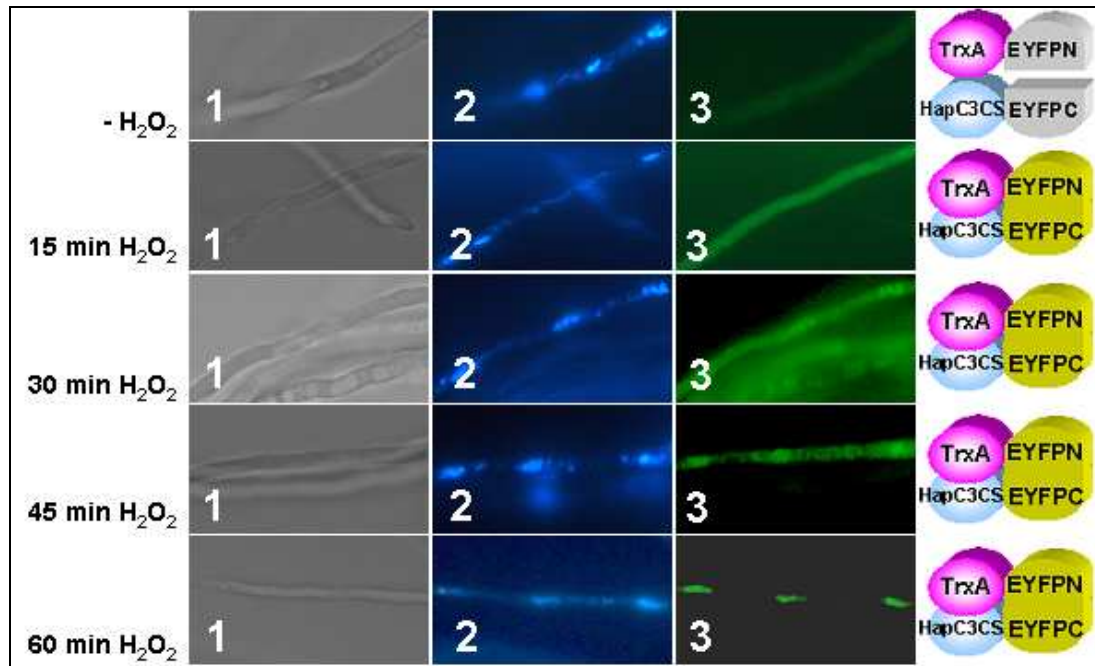
Fig. 22. Visualization of the transient interaction between HapC3CS and TrxA in response to oxidative stress. (1) Light microscopy of the mycelia, (2) DAPI staining of the nucleus, (3) fluorescence microscopy of mycelia. The period of H_2O_2 treatment are indicated on the left side. The interacting partners of BiFC are drawn on the right side.
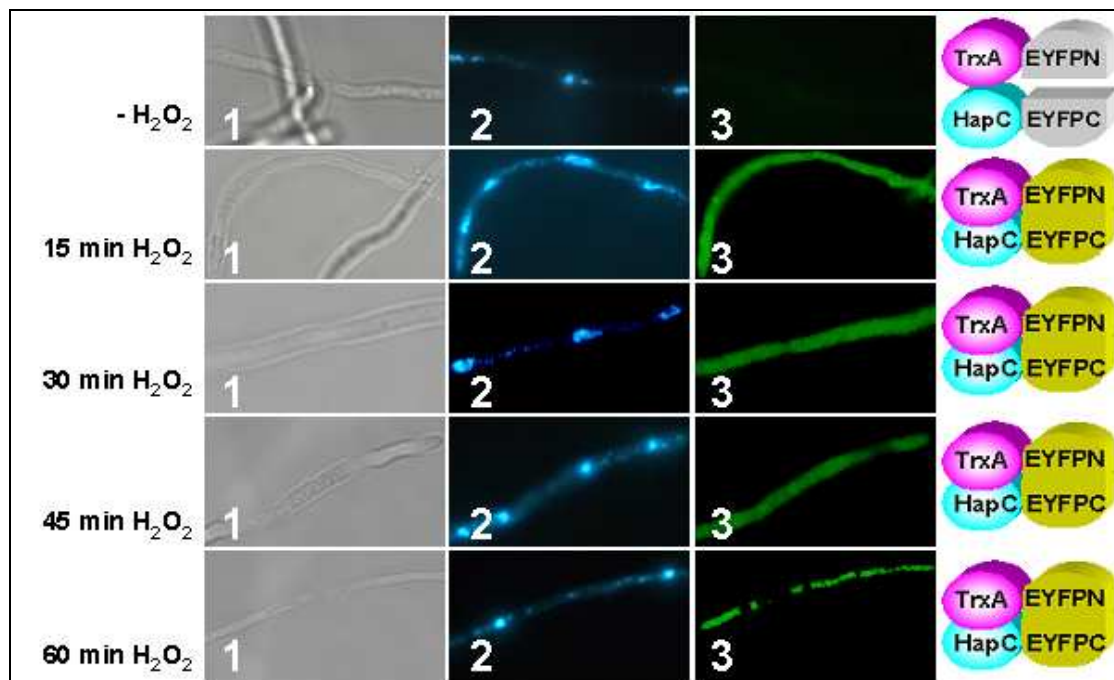
Fig. 23. Visualization of the transient interaction between HapC and TrxA in a *ΔhapE* strain in response to oxidative stress. (1) Light microscopy of the mycelia, (2) DAPI staining of the nucleus, (3) fluorescence microscopy of mycelia. The period of H_2O_2 treatment is indicated on the left side. The interacting partners of BiFC are drawn on the right side.

3.2.4.6 Visualization of the HapC homodimerization in *A. nidulans* under oxidative stress conditions.

An *A nidulans* strain was generated by co-transformation of the AXB4A2 strain with the plasmids pHapC-YC-pyr4 and pHapC-YN-paba as mentioned above (refer to 3.2.4.1.1 and 3.2.4.2). The strain was designated yHapC-HapC. It contains HapC fused to both the C- and N-terminal parts of YFP. To visualize the HapC homodimerization under oxidative stress conditions, the yHapC-HapC strain was grown in AMM overnight at 37°C and then exposed to 10 mM H_2O_2. Samples were collected at 0, 15, 30, 45 and 60 minutes post treatment and microscoped. Surprisingly, fluorescence was observed in the cytoplasm before H_2O_2 treatment and retained after treatment with H_2O_2. The fluorescence was extremely weak but slightly stronger than background (Fig. 24). Visualized fluorescence resulting from HapC homodimerization was weaker compared with the fluorescence observed for the constitutive interaction between HapC and HapE. However, this fluorescence might result form homodimerization of HapC via intramolecular disulfide linkage during oxidative stress. It might also be resulting from unspecific HapC-HapC cross-linking over thiol groups caused by the overexpression of HapC in the cell.

3.2.4.7 Visualization of the interaction between HapC and TrxA under iron-depleting conditions.

To investigate whether other signals are involved in triggering HapC-TrxA interaction, the interaction between TrxA and HapC under iron-deficiency conditions was observed. The strains yHapC-TrxA, yHapC3CS-TrxA and yHapC-TrxAC39S were used. Optimized conditions for studying protein-protein interactions under iron-limiting conditions were applied as described for HapX-HapB interaction (refer to 3.3.1.2), in which the strains were grown overnight at 37°C in AMM in the absence of iron and then treated with 1 mM of deferoxamine. Samples were collected after 60 minutes and microscoped. Unlike high H_2O_2 concentration, fluorescence resulting from the HapC-TrxA and HapC-TrxAC39S interactions under iron-depleting conditions was observed in the nucleus (Fig. 25-B and -F). The HapC3CS-TrxA interaction followed different pattern. The interaction between HapC3CS, which forms a functional but less stable CBC complex, and TrxA was visualized in the cytoplasm as well as the nucleus (Fig. 25-D). This indicates that the interaction between HapC and TrxA could be triggered under iron-deficiency conditions, which could be caused by an overlapping or synchronized regulatory mechanism against iron-limiting and oxidative stress conditions or from iron-induced oxidative stress.

Fig. 24. Visualization of the HapC homodimerization in response to oxidative stress. (1) Light microscopy of the mycelia, (2) DAPI staining of the nucleus, (3) fluorescence microscopy of mycelia. The period of H_2O_2 treatment is indicated on the left side. The interacting partners of BiFC are drawn on the right side.
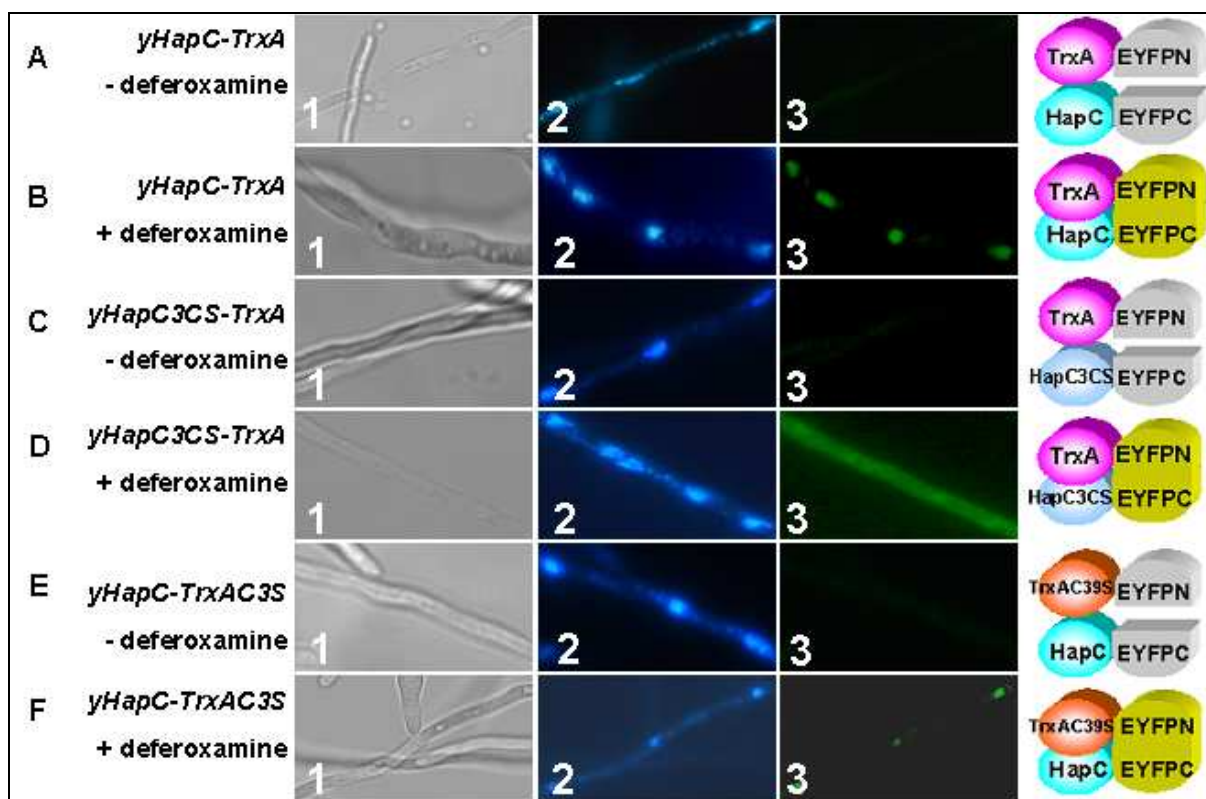
Fig. 25. Visualization of the interaction between HapC and TrxA in response to iron-depleting conditions. (1) Light microscopy of the mycelia, (2) DAPI staining of the nucleus, (3) fluorescence microscopy of mycelia. The name of the strains (bold italics) and type of treatment are indicated on the left side. The interacting partners of BiFC are drawn on the right side.

3.3 Characterization of the transcription factor HapX *in vivo*.

To carry out an analysis of HapX during iron starvation *in vivo* in *A. nidulans*, BiFC was applied. First, the interaction between HapX and CBC under iron limiting conditions was confirmed. Then, the possibility of forming HapX-HapX homodimer was analyzed. Finally the possibility of HapX regulation by TrxA was tested.

3.3.1 HapX interaction with CBC under iron limiting conditions.

In this approach, the physical interaction of HapX with the CBC subunits during iron starvation was analyzed *in vivo*. Therefore, HapX was fused to the C- and N-terminus of YFP. Different CBC subunits were also fused either to the C- or N-terminal part of YFP.

3.3.1.1 Generation of *A. nidulans* strains.

3.3.1.1.1 Generation of an *A. nidulans* strain for studying HapX-HapB interaction.

The plasmids pHapX-YC-pyr4 and pHapB-YN, which carry *hapX-eyfpC* and *hapB-eyfpN* fusions, respectively, were generated and transformed into the AXB4A2 strain, as mentioned above (refer to 3.2.4.1.4, 3.2.4.1.7 and 3.2.4.2). The resulting strain was called yHapX-HapB.

3.3.1.1.2 Generation of an *A. nidulans* strain for studying HapX-HapC interaction.

Plasmids pHapC-YC-pyr4 and pHapX-YN, which carry *hapC-eyfpC* and *hapX-eyfpN* fusions, respectively, were constructed and transformed into the AXB4A2 strain, as mentioned above (refer to 3.2.4.1.1, 3.2.4.1.7 and 3.2.4.2). The resulting strain was called yHapX-HapC.

3.3.1.1.3 Generation of an *A. nidulans* strain for studying HapX-HapE interaction.

Plasmids pHapX-YC-pyr4 and pHapE-YN, which carry *hapX-eyfpC* and *hapE-eyfpN* fusions, respectively, were constructed and transformed into the AXB4A2 strain, as mentioned above (refer to 3.2.4.1.3, 3.2.4.1.7 and 3.2.4.2). The resulting strain was called yHapX-HapE.

3.3.1.2 Optimization of the deferoxamine treatment.

To visualize the interaction between HapX and different subunits of CBC, deferoxamine treatment was optimized. The optimization of deferoxamine treatment for BiFC assay was done using the strain yHapX-HapB, which was employed for the visualization of the recently identified interaction between HapX and HapB (Tanaka et al., 2002). The optimization was

done by using two approaches. First, optimization the concentration of deferoxamine and the time of incubation. Second, influence of iron availability during growth on HapX regulation. In the first approach, deferoxamine treatment was optimized by harvesting spores growing on AMM agar plates containing iron. Spores were then incubated in AMM absent of iron and grown overnight at 37°C. The overnight culture was treated with three concentrations of deferoxamine: 0.1 mM, 0.5 mM and 1 mM. Samples were incubated at RT and microscoped every 15 minutes (Table 4). The higher the concentration of deferoxamine used for treatment of mycelia, the shorter the time required to visualize the fluorescence resulting from the interaction between HapX and HapB. With 0.5 mM and 1 mM of deferoxamine, the same results were obtained.

Table 4. Optimization of the concentration of deferoxamine and the time of incubation.

	1 mM (10 µl in 1 ml AMM)	**0.5 mM (5 µl in 1 ml AMM)**	**0.1 mM (1 µl in 1 ml AMM)**
15 min	No fluorescence	No fluorescence	No fluorescence
30 min	Weak fluorescence	Weak fluorescence	Weak fluorescence
60 min	Strong fluorescence	Strong fluorescence	Weak fluorescence
120 min	Strong fluorescence	Strong fluorescence	Strong fluorescence

In the second approach, spores were harvested from AMM agar plates either containing iron or no iron (Table 5-A). Then, the harvested conidia were grown in two types of AMM, containing and absent of iron (Table 5-B). Finally, the overnight culture was split into two parts, one part was treated with 1 mM of deferoxamine and the other part was not treated (Table 5-C). Samples were incubated at RT and microscopic analysis was carried out every 15 minutes and fluorescence was visualized.

However, there was no grow when the conidia were harvested from agar plates absent of iron and then transferred to AMM absent of iron. Therefore, these treatments were omitted from the table below. On the other hand, mycelia did not show any fluorescence when they were not treated with deferoxamine (Table 5-C).

Table 5. The influence of iron availability in the AMM on HapX-HapB interaction.

	A	B	C	Observed fluorescence
1	+	+	+	Weak fluorescence after 90 min
2	+	+	-	No fluorescence
3	+	-	+	Weak fluorescence after 30 min
4	+	-	-	No fluorescence
5	-	+	+	Weak fluorescence after 30 min
6	-	+	-	No fluorescence

- **A.** Availability (+) /absence (-) of iron in AMM agar plates.
- **B.** Availability (+) /absence (-) of iron in overnight AMM.
- **C.** Treatment (+) /no treatment (-) of overnight culture with deferoxamine.

3.3.1.3 Visualization of HapX interaction with CBC in an *A. nidulans* wild-type strain under iron-depleting conditions.

Previous study showed using the yeast two-hybrid system that HapX interacts with HapB (Tanaka et al., 2002). To confirm this interaction under iron limiting conditions *in vivo* in *A. nidulans*, BiFC system was applied. The yHapX-HapB, yHapX-HapC and yHapX-HapE strains were grown overnight at 37°C in AMM in the absence of iron and then treated with 1 mM of deferoxamine. Samples were collected after 60 minutes and microscoped. In the strain yHapX-HapB, fluorescence was observed in the nucleus indicating the interaction between HapX and HapB under iron depleting conditions (Fig 26). In the strains yHapX-HapC and yHapX-HapE, no fluorescence was observed (Fig. 26).

3.3.1.4 Visualization of HapX interaction with CBC in an *A. nidulans ΔhapC* strain under iron-depleting conditions.

To investigate whether HapX binds to the whole CBC complex or only to the HapB subunit in *A. nidulans*, BiFC was applied in an *A. nidulans ΔhapC* strain. The reason for using this strain is that in the absence of HapC, HapE localizes in the cytoplasm while HapB localizes in the nucleus, enabling us to visualize the specific interaction between HapX and HapB *in vivo*.

For this purpose, an *A. nidulans* strain was generated by transformation of a *ΔhapC* strain (Nat24) with the plasmid pHapX-HapB-pyr4 (refer to 3.2.4.1.4), which carries *hapX-eyfpC*

and *hapB-eyfpN* fusions, and *pyr-4* as a selection marker. The resulting strain was designated

yHapX-HapB-ΔC.
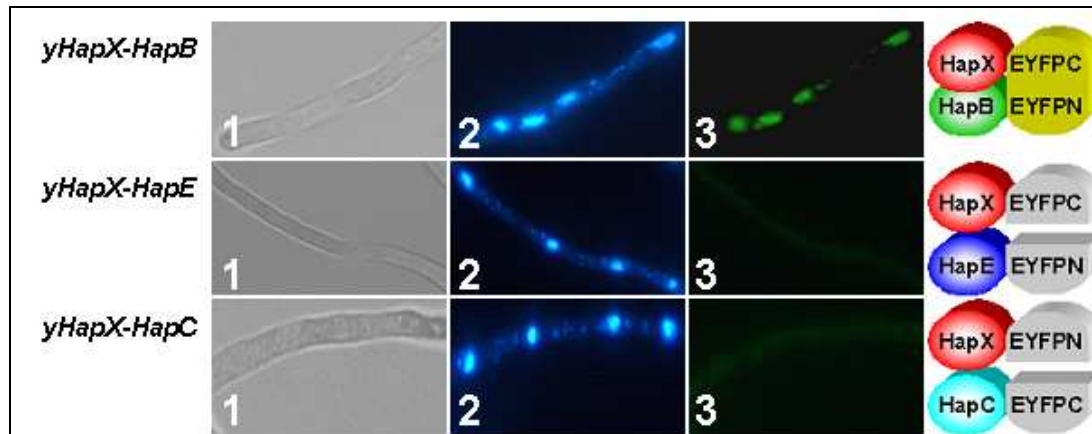
Fig. 26. Visualization of the interaction between HapX and CBC subunits in response to iron-depleting conditions. (1) Light microscopy of the mycelia, (2) DAPI staining of the nucleus, (3) fluorescence microscopy of mycelia. The name of the strains (bold italics) is indicated on the left side. The interacting partners of BiFC are drawn on the right side.
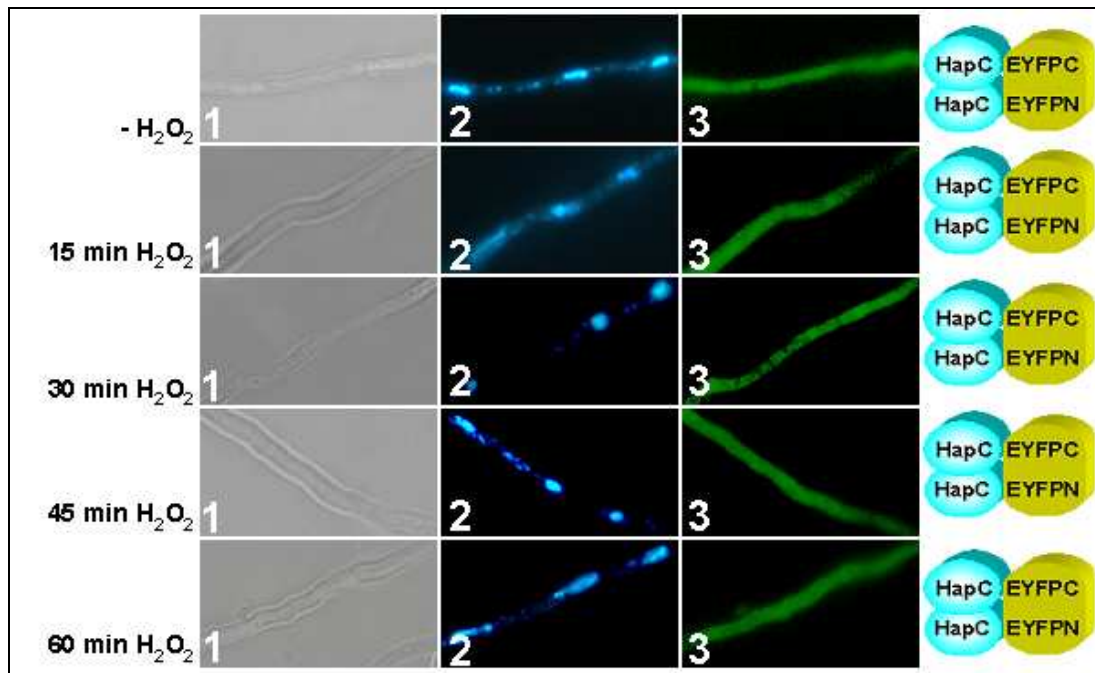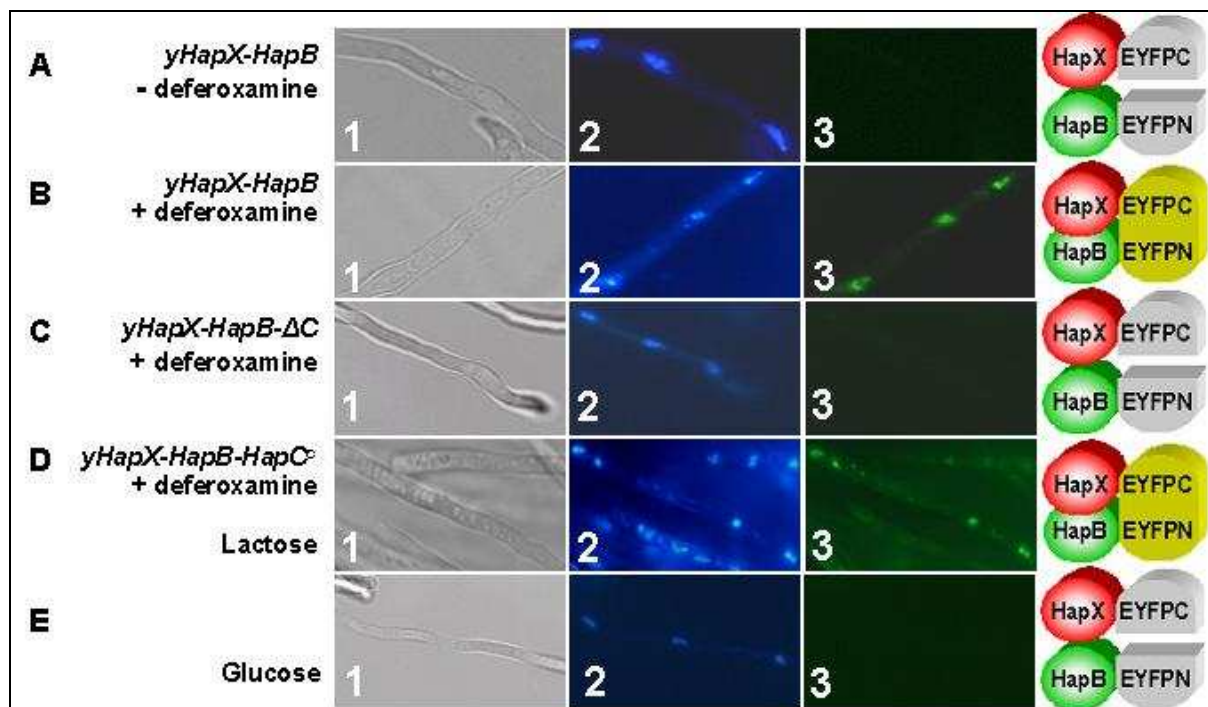

Fig. 27. Visualization of the interaction between HapX and HapB subunit in response to iron-depleting conditions. (1) Light microscopy of the mycelia, (2) DAPI staining of the nucleus, (3) fluorescence microscopy of mycelia. The name of the strains (bold italics) and type of treatment are indicated on the left side. The interacting partners of BiFC are drawn on the right side.

Plasmid pAlcA-HapC was generated by integration of the *hapC*-containing *Bam*HI/*Xba*I fragment from plasmid pHapC-Topo in plasmid pAL4. The yHapX-HapB-ΔC strain was afterwards complemented with *hapC* by transforming the strain with the plasmid pAlcA-HapC using acetamide. The resulting strain was designated yHapX-HapB-HapC[c].

To visualize the interaction between HapX and HapB under iron-depleting conditions, the strains were grown overnight at 37°C in AMM in the absence of iron. The carbon source was switched afterwards from glucose to lactose. The strains were grown for 8 hours in AMM containing lactose as carbon source. The strains were then treated with 1 mM of deferoxamine. Samples were collected after 60 minutes and microscoped.

In the strain yHapX-HapB, BiFC fluorescence was observed between HapX and HapB under iron-depleting conditions (Fig. 27-B) but not under iron-repleting conditions (Fig. 27-A). However, no fluorescence was detected between HapX and HapB in the *ΔhapC* strain yHapX-HapB-ΔC (Fig. 27-C), while it was reconstituted by complementation with the *hapC* gene in strain yHapX-HapB-HapC[c] when *hapC* was induced by lactose (Fig. 27-D) but not when repressed by glucose (Fig. 27-E). These data indicate that the entire CBC is required for *in vivo* interaction with HapX.

To confirm the constitutive expression of the two EYFP split termini, Western blot analysis was employed using anti-GFP mouse monoclonal antibody (mGFP) and anti-GFP goat polyclonal antibody (pGFP). Non of the antibodies tested showed a specific binding to EYFPC terminal part (not shown). As an alternative method, Northern blot analysis confirmed the constitutive expression of the two EYFP split fragment-encoding genes in the used strains (Hortschunsky et al., 2007).

3.3.2 Visualization of the interaction of HapX with HapB in an *A. nidulans* wild-type strain under oxidative stress conditions.

As shown in chapter 3.3.1, HapX interacts with HapB under iron limiting conditions. To investigate whether HapX interacts with HapB under oxidative stress conditions as well, the yHapX-HapB strain was grown in AMM overnight at 37°C and then exposed to 10 mM H_2O_2. Samples were collected at 0, 15, 30, 45 and 60 minutes post treatment and microscoped. Interestingly, an interaction between HapX and HapB was observed upon treatment with H_2O_2. The subcellular localization of interacting HapX and HapB was always visualized in the nucleus (Fig. 28), indicating that the interaction between HapX and HapB tends to take

place under oxidative stress as well. Combining these results with our previous results (refer to 3.2.4.7) implies the presence of an overlapping or a synchronized regulatory mechanism against iron-limiting and oxidative stress conditions or the possibility of oxidative stress induction through iron starvation.

3.3.3 Visualization of HapX homodimerization in *A. nidulans* under iron-depleting conditions.

The members of the bZIP family of transcription factors contain of a basic region, which interacts with DNA through hydrogen bonding, and a leucine zipper region, which is responsible for dimerization. Previous study showed that although HapX possesses no leucine zipper structure, the N-terminal region of HapX exhibits a sequence similar to many members of the bZIP transcription factor family (Tanaka et al., 2002). To investigate whether HapX forms a homodimer, BiFC was applied. An *A. nidulans* strain was generated by transformation of the *A. nidulans* AXB4A2 strain with the plasmid pHapX-YC-pyr4 and pHapX-YN (refer to 3.2.4.1.7), which carry *hapX-eyfpC* and *hapX-eyfpN* fusions, respectively. The resulting strain was designated yHapX-HapX. The yHapX-HapX strain was grown overnight at 37°C in AMM in the absence of iron and then treated with 1 mM of deferoxamine. Samples were collected after 60 minutes and microscoped.

As shown in Fig. 29, no fluorescence was observed indicating that HapX might not form a homodimer under iron-depleting conditions. This should be further confirmed by using the other combinations of HapX fusion to the C- and N-terminal parts of YFP.

3.3.4 Posttranslational regulation of HapX by thioredoxin *in vivo*.

Analysis of the *A. nidulans* HapX amino acid sequence revealed that HapX contains 20 cysteine residues. Sequence alignment of HapX from *A. nidulans* with HapX of other *Aspergilli* showed that 19 of these cysteines are conserved (Fig. 30). Analysis of conserved cysteines in HapX demonstrates that HapX possesses three possible TrxA-targeted CXXC motifs, arising the question whether HapX is also regulated by TrxA. To answer this question, BiFC assay was applied to demonstrate the interaction between TrxA and HapX *in vivo*.
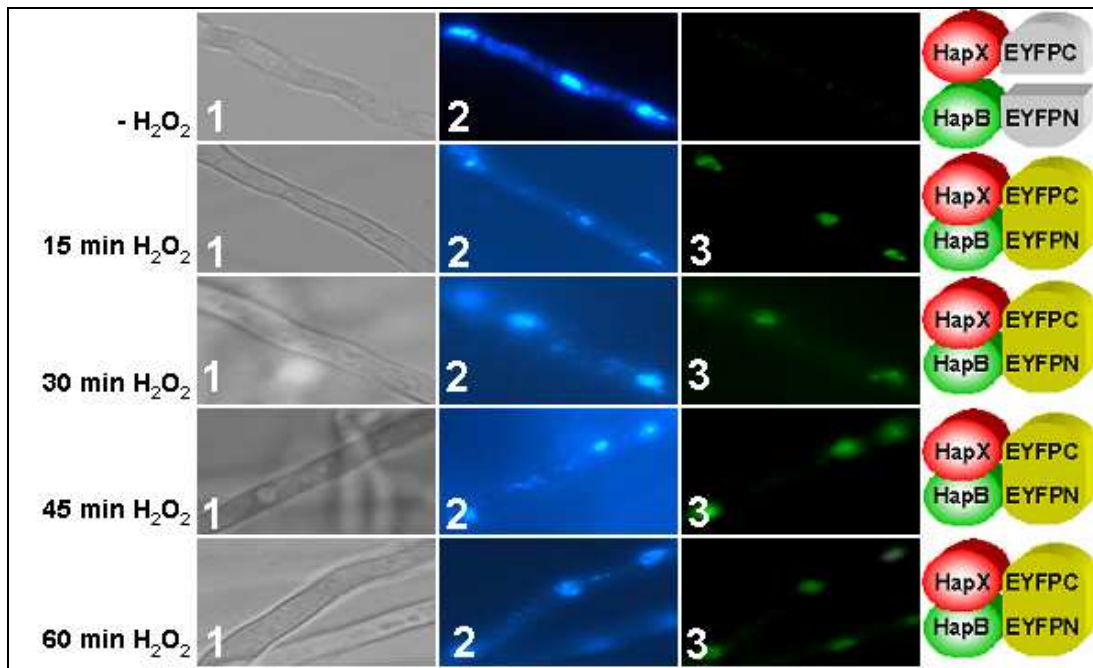
Fig. 28. Visualization of the interaction between HapX and HapB in response to oxidative stress. (1) Light microscopy of the mycelia, (2) DAPI staining of the nucleus, (3) fluorescence microscopy of mycelia. The period of H_2O_2 treatment is indicated on the left side. The interacting partners of BiFC are drawn on the right side.
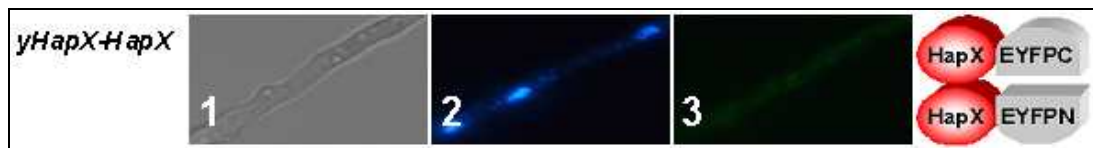
Fig. 29. Visualization of the HapX homodimerization in response to iron-depleting conditions. (1) Light microscopy of the mycelia, (2) DAPI staining of the nucleus, (3) fluorescence microscopy of mycelia. The name of the strain (bold italics) is indicated on the left side. The interacting partners of BiFC are drawn on the right side.

```
                10        20        30        40        50        60        70
          ....|....|....|....|....|....|....|....|....|....|....|....|....|....|
An HapX   MA--AQPALAIAPSAAPLAPALVAKPTVSPSPGPGTPGSVTSKEWIIPPRPKPGRKPATDTPPTKRKAQN
Af HapX   .STP---SI.P..AP--.V...A...AI...........I.....V..................
Afl HapX  ..TPA-.SI.P..TP......IA....I..........V..................
Ao HapX   ..TPA-.SI.P..TP......IA....I..........V..................
Acla HapX .SAP---SM.PT.AP.S.....A...A............I.T...V..................
Ani HapX  ..TP.A.S..P..GP.....A...AI...........V..................

                80        90       100       110       120       130       140
          ....|....|....|....|....|....|....|....|....|....|....|....|....|....|
An HapX   RAAQRAFRERRAARVSELEDQIKCIEDDHEIHVATFKEQIANLSREVEQCRTEMGWWRDRCHALEKEVSV
Af HapX   ...............N...E...K...E....I.A.....T.........S..T.....|.........
Afl HapX  ...............N...K..EE.D....A.....S...H.....N..T.....|.........
Ao HapX   ...............N...K..EE.D....A.....S...H.....N..T.....|.........
Acla HapX ...............N...K...E.D..I.A.....G...C.....S..T.....|....T....
Ani HapX  ...............N......K.......LQL....S...H.....S..A.....|.........

               150       160       170       180       190       200       210
          ....|....|....|....|....|....|....|....|....|....|....|....|....|....|
An HapX   ERAARETLVKELRSSLPEKNTSGTDAVPLP--PRSSRSSRMELEKSSPVDRR----SELGEEVPLGCNRC
Af HapX   ..S.K.AI...F....SDREAVRS.KGLA.LTT--.TPQARSSDRPDNG.ASNNDSG.GR......|.D.
Afl HapX  ..S.K.A....F....SD..APAGR.PLTRVSA.N.G.G.ATN.R...SNANSGSNDDEQ......|PS.
Ao HapX   ..S.K.A....F....SD..APAGR.PLTRVSA.N.G.G.ATN.R...SNANSGSNDDEQ......|PS.
Acla HapX ..S.K.A....F.L..SD..AASS....F.RAT--.SRPENDGVPANNASHDDGHH.DNR......|.D.
Ani HapX  ..S.K.S....F....SD..A.RS.KA..TRI..D.SAAHAAV.NNMHEE.---------......|SN.
                                                                        CXXC

               220       230       240       250       260       270       280
          ....|....|....|....|....|....|....|....|....|....|....|....|....|....|
An HapX   STSHCQCIEDAFG-MPPIEMNRAP------------EPKIKPEPEEMEIDFTTRFAAPHHEEDTAASPVA
Af HapX   ......|..|....T-..GVVAQEQSRR-LDTTKPGLS..Q...D.........S....TQ-QQ.QSPTS.S
Afl HapX  .ST...|..|....A-..GV.S-LHSKR-LSTTGQGRA..E...D...............Q-PQEDN.TA.S
Ao HapX   .ST...|..|....A-..GV.S-LHSKR-LSTTGQGRA..E...D...............Q-PQEDN.TA.S
Acla HapX ......|..|....A-..GVLAQEESRR-PGSTKPGRL..E...D.........A...TMK-PQ.HSPTS.S
Ani HapX  .NV...|..|.....SG..G..RTS.QSKRPDNSSQSHA..E.....................VQ.DTVTN.S

               290       300       310       320       330       340       350
          ....|....|....|....|....|....|....|....|....|....|....|....|....|....|
An HapX   SPPVDPCGFCQDGTPCICAEMAAQEEERRRNSTFESNRLAPIQNISQFTPPPSDSDVRSDNVTLPPISQA
Af HapX   ..A...|..|..S.....|.|............Q.P.RNS..N.........L.........G....-D.........
Afl HapX  ..A...|..|........|.|............Q--.RQS..N.........L.........G....-E....S.N..
Ao HapX   ..A...|..|........|.|............Q--.RQS..N.........L.........G....-E....S.N..
Acla HapX ..A...|..|........|.|............Q..NE.RN...N.........M.........G....-EM...SL...
Ani HapX  ..A...|..|........|.|.............RNS..N.........L.........G....-E.........
                CXXC

               360       370       380       390       400       410       420
          ....|....|....|....|....|....|....|....|....|....|....|....|....|....|
An HapX   TAANPCANGPGTCAACLSDPRRTLFCKTLAASRSASGTPSGCCGGKGRDGGCCQSQSRTSAPRR------
Af HapX   .---..|........|..|Q..A........|.........P.AA...|.....A...|.|..--.NTNVS.GRSGSN
Afl HapX  .---..|........|..|Q..A..KS....|.......VAS..|.....A...|.|..--.S.N.P.---AAA
Ao HapX   .---..|........|..|Q..A..KS....|.......VAS..|.....A...|.|..--.S.N.P.---AAA
Acla HapX .---..|........|..|Q..A...S....|.........AG..|.......|.|..--.S.N.S.SGSTGN
Ani HapX  .---..|........|..|Q..A........|.........P.AA..|.....A.....|.|M.--.N.N.Q.------
                CXXC

               430       440       450       460       470       480       490
          ....|....|....|....|....|....|....|....|....|....|....|....|....|....|
An HapX   --SNTDRSATP-LTLSCADAFTTLSRHPNFSRASDELASWLPKLHTLPNPRDVSQ--TTPASRAAMEVEA
Af HapX   NNTSSGS..A.S.....|....Y.............T...ST........K...FPLT-DRGVP...L....
Afl HapX  AK.TSG..T..S.....|................IST........K..ASP-DRCS....L....
Ao HapX   AK.TSG..T..S.....|................IST........K..ASP-DRCS....L....
Acla HapX AN.IPGP.T..S.....|..........S.T..T.DISN........IPLS-DRGTP.........
Ani HapX  --.GSR.....S.....|.............DIS............SQSQKEVMQ.G....L....
```

```
                    500
                ....|....|....|..
An HapX      ASVMGVLRYFDRRFADK
Af HapX      .................
Afl HapX     .................
Ao HapX      .................
Acla HapX    .................
Ani HapX     .................
```

Fig. 30. Amino acid sequence alignment of HapX with its (hypothetical) homologues from different *Aspergilli*. HapX sequences were extracted from *Aspergillus* Comparative Database (http://www.broad.mit.edu/) after carrying out of blastp (Protein query vs. Protein database). Alignment was done using ClustalW Multiple Alignment option available in BioEdit Sequence Alignment Editor Version 7.0.0. Identical amino acid sequences to the *A. nidulans* HapX are indicated as (**.**) in the sequence. Conserved cysteine residues are boxed. The potential TrxA target motifs are indicated by (CXXC). An HapX: *A. nidulans* HapX (accession number AN8251.3), Af HapX: *A. fumigatus* HapX accession number Afu5g03920), Afl HapX: *A. flavus* HapX (accession number AFL2G_ 09972.2), Ao HapX: *A. oryzae* HapX (accession number AO090102000597), Acla HapX: *A. clavatus* HapX (accession number ACLA_001220), Ani HapX: *A. niger* HapX (accession number est_GWPlus_C_110141).

3.3.4.1 Visualization of the HapX-TrxA interaction in an *A. nidulans* wild-type strain under iron-depleting conditions.

To investigate whether cysteine residues of HapX are targeted by TrxA in *A. nidulans*, BiFC was applied. An *A. nidulans* strain was constructed by co-transformation of pHapX-YC-pyr4 and pTrxA-YN simultaneously with pHELP in the strain AXB4A2, as mentioned above (refer to 3.2.4.1.5, 3.2.4.1.7 and 3.2.4.2). The strain was designated yHapX-TrxA. It contains HapX and TrxA fused to the C- and N-terminal parts of YFP, respectively. To visualize the interaction between HapX and TrxA under iron-depleting conditions, the yHapX-TrxA strain was grown overnight at 37°C in AMM in the absence of iron and then treated with 1 mM of deferoxamine. Samples were collected after 60 minutes and microscoped. Fluorescence, extremely weak but still stronger than background, was observed indicating a possible interaction between HapX and TrxA under iron-depleting conditions (Fig. 31). However, it is still possible that this fluorescence might result from unspecific binding of the two YFP termini caused by the interaction of TrxA with HapC and HapX with HapB at the same time. To analyze this possibility, the interaction between HapX and TrxA was investigated in a *ΔhapC* strain (refer to 3.3.4.2).

3.3.4.2 Visualization of HapX-TrxA interaction in an *A. nidulans ΔhapC* strain under iron-depleting and oxidative stress conditions.

To analyze whether the interaction between HapX and TrxA resulted from specific reduction of the conserved cysteines of HapX by TrxA or from unspecific binding of the two YFP termini caused by the interaction of TrxA with HapC and HapX with HapB at the same time, an *A. nidulans ΔhapC* strain was used. This strain was chosen since it is has been shown that TrxA binds to the HapC subunit of CBC (refer to 3.2.4.4.1 and 3.2.4.5) and HapX does not interact with CBC in a *ΔhapC* strain (refer to 3.3.1.4). Therefore, an *A. nidulans* strain was generated by co-transformation using pHapX-YC-paba and pTrxA-YN-pyr4 in the *ΔhapC A. nidulans* strain Nat24, as mentioned above (refer to 3.2.4.1.5, 3.2.4.1.7 and 3.2.4.2). The strain was designated yHapX-TrxA-ΔC. It contains HapX and TrxA fused to the C- and N-terminal parts of YFP, respectively, in the absence of HapC. To visualize the interaction between HapX and TrxA under iron-depleting conditions, the yHapX-TrxA-ΔC strain was grown overnight at 37°C in AMM, in the absence of iron, then treated with 1 mM of deferoxamine and incubated at RT. Samples were collected after 60 minutes and microscoped.

To observe whether TrxA binds to HapX under oxidative stress conditions, the yHapX-TrxA-ΔC strain was also treated with 10 mM H_2O_2 and microscoped after 60 minutes of treatment. Under both stress conditions, BiFC fluorescence was observed (Fig. 32-B and -D) indicating a possible interaction between HapX and TrxA under iron-depleting and oxidative stress conditions. This might be explained by the possibility of HapX regulation by the redox status of the cell.
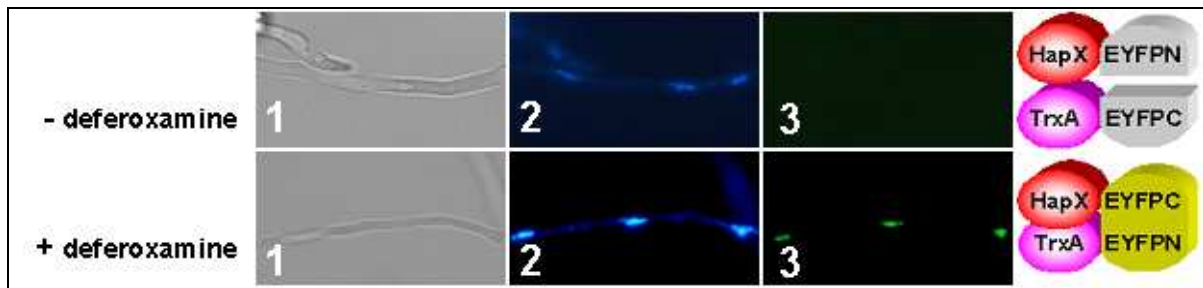
Fig. 31. Visualization of the interaction between HapX and TrxA in the wild-type strain in response to iron-depleting conditions. (1) Light microscopy of the mycelia, (2) DAPI staining of the nucleus, (3) fluorescence microscopy of mycelia. The type of treatment is indicated on the left side. The interacting partners of BiFC are drawn on the right side.
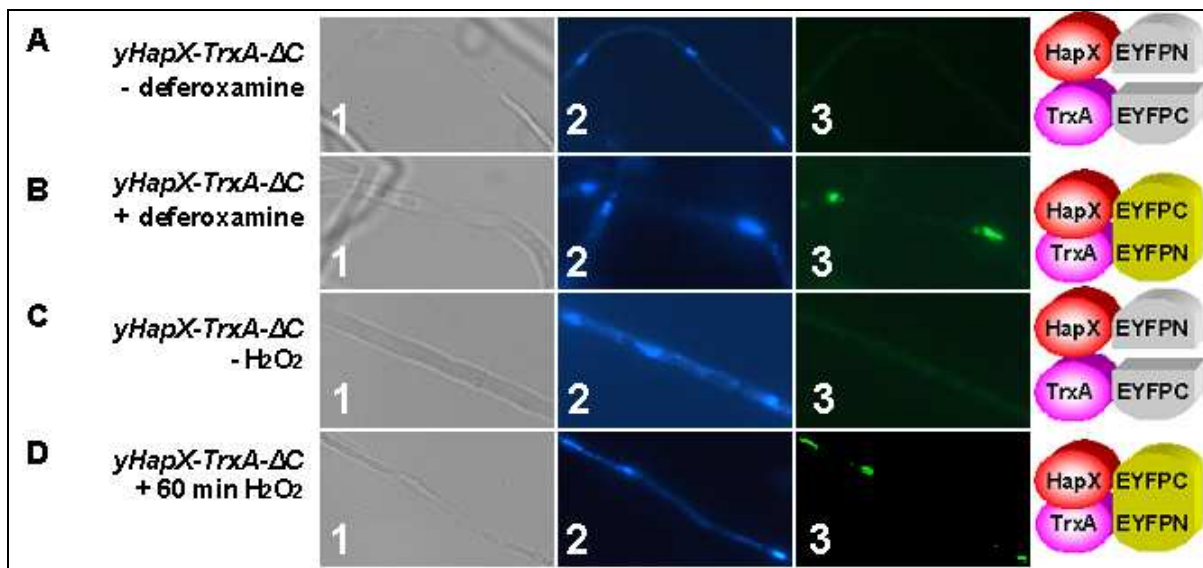
Fig. 32. Visualization of the interaction between HapX and TrxA in a *ΔhapC* strain in response to iron-depleting and oxidative stress conditions. (1) Light microscopy of the mycelia, (2) DAPI staining of the nucleus, (3) fluorescence microscopy of mycelia. The name of the strains and type of treatment are indicated on the left side. The interacting partners of BiFC are drawn on the right side.

3.4 Complementation of HapC by NF-YB in an *A. nidulans ΔhapC* **strain.**

The heterotrimeric CCAAT-binding complex is evolutionarily conserved in eukaryotic organisms, including fungi, plants and mammals. Previous reports have shown that both proteins Hap2p and NF-YA complemented partially the *ΔhapB* strain of *A. nidulans*. This indicated that HapB, Hap2p and NF-YA are interchangeable and that the piggy-back mechanism of nuclear transport found for *A. nidulans* might be conserved in yeast and human (Tüncher et al., 2005).

On the other hand, as shown here, HapC is regulated by the redox status of the cell. To discover whether similar regulation mechanisms for the homologous complex of human exists, and whether there is functional conservation, the functional interchangeability of the human homologous protein of *A. nidulans* HapC was analyzed. The possibility of complementing the *A. nidulans hapC* mutant using the human *nf-yb* gene was tested. For this purpose, the *ΔhapC* strain of *A. nidulans* (Nat24) was complemented with NF-YB by transforming the *ΔhapC* strain Nat24 with the plasmids pNfyB-TrxA-pyr4 (refer to 3.2.4.1.8) and pNfyB-HapE-pyr4 (refer to 3.2.4.1.8), which carry *pyr-4* as a selection marker. This resulted in the strains yNFYB-TrxA-ΔC and yNFYB-HapE-ΔC, respectively. The uracil-prototrophic transformants were analyzed by growing the strains yNFYB-TrxA-ΔC and yNFYB-HapE-ΔC on acetamide as sole N source. However, the strains showed lack of growth on acetamide as sole N source (Fig. 33-B and -C), which is characteristic of the *Δhap* phenotype (Fig. 33-D). By contrast, the presence of the HapC-EGFP fusion in the *ΔhapC* strain (ΔC-Cgfp) led to complementation of the *Δhap* phenotype (Fig. 33-A). Taken together, this data supports that NF-YB did not complement HapC.

To confirm this finding, BiFC was applied to visualize any possible interaction between NF-YB and *A. nidulans* TrxA and heterodimerization of NF-YB and HapE *in vivo* in the strains yNfyB-TrxA-ΔC and yNfyB-HapE-ΔC. Therefore, the strains were grown in AMM overnight at 37°C and then exposed to 10 mM H_2O_2. Samples were collected after 60 minutes and microscoped. However, the BiFC results showed that neither interaction between HapE and NF-YB nor between *A. nidulans* TrxA and NF-YB was observed (Fig. 34) suggesting that HapC and NF-YB are not interchangeable. Nevertheless, it is also possible that the human NF-YB protein is degraded. Therefore, the constitutive expression of the NF-YB in these strains should be confirmed by using Western blot or Northern blot analysis.
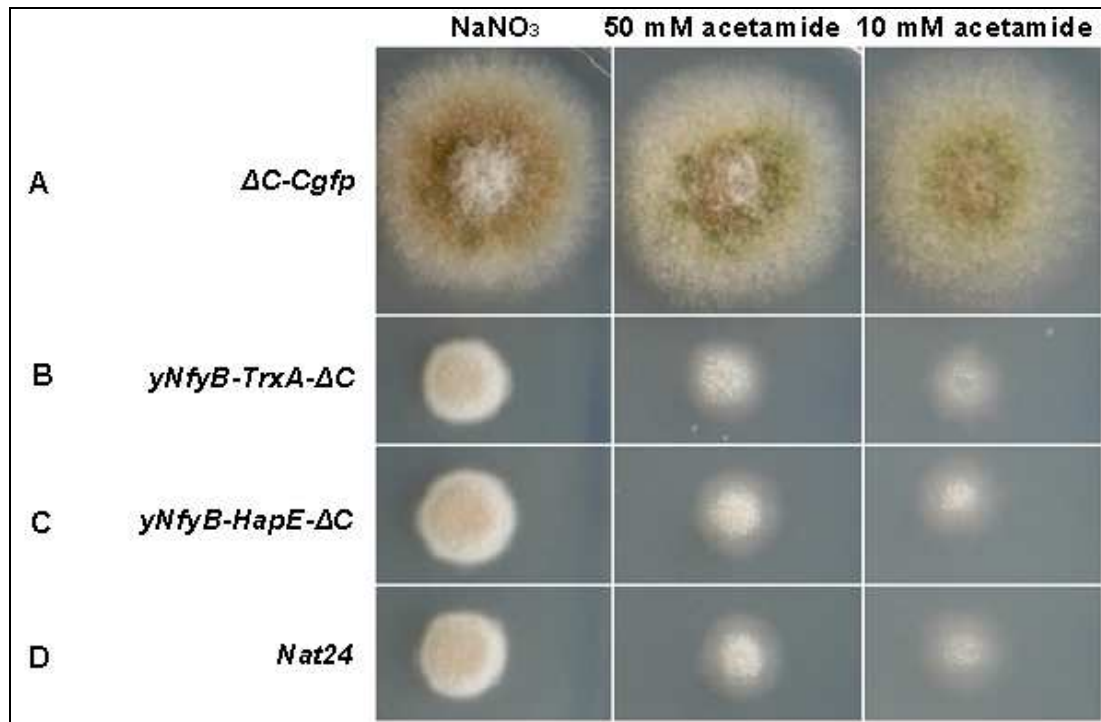
Fig. 33. Analysis of the *hapC* deletion mutants of *A. nidulans* transformed with the *nf-yb* gene. Strains were grown on AMM agar plates at 37°C for 72 hours with 10 mM acetamide, 50 mM acetamide or NaNO₃ as sole N source. The name of the strains (bold italics) is indicated on the left side.
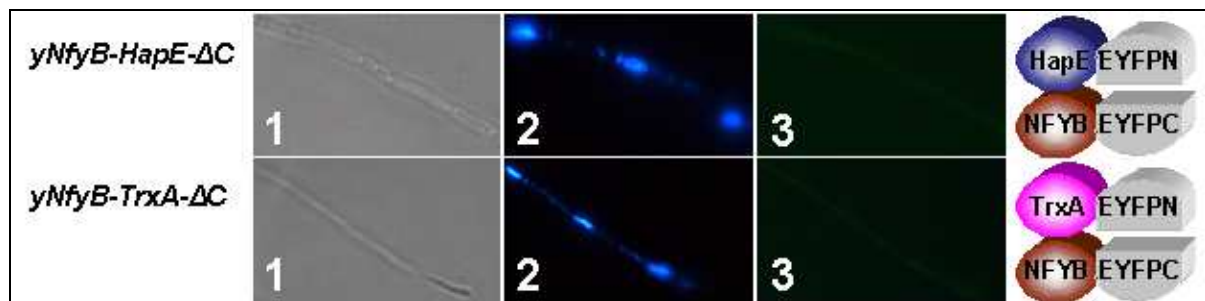
Fig. 34. Visualization of the interaction between NF-YB and HapE and TrxA in a *ΔhapC* strain in response to oxidative stress conditions. (1) Light microscopy of the mycelia, (2) DAPI staining of the nucleus, (3) fluorescence microscopy of mycelia. The name of the strains (bold italics) is indicated on the left side. The interacting partners of BiFC are drawn on the right side.

4. Discussion

In this work, the roles that might be played by HapC cysteine residues on the CBC complex have been studied. Two questions were addressed: (I) Are the HapC cysteine residues essential for CBC complex stability? (II) Are they essential for the regulation of the CBC complex by thioredoxin TrxA *in vivo*?

4.1 Cysteines play a role in the stability of the CBC complex.

The importance of the conserved cysteine residues of HapC on the stability of the CBC complex was shown based on several lines of evidence: First, the ability of the HapC3CS and HapC3CA mutants to recover the wild-type phenotype and to grow on acetamide as sole N source. Second, the subcellular localization of EGFP fusion of both HapC mutants was observed in the cytoplasm as well as in the nucleus. Third, EMSA showed that CBC, which contains HapC3CS, binds with lower affinity to the CCAAT box compared to CBC, which contains the wild-type HapC. In agreement with these results, Baxevanis et al. (1995) and Sinha et al. (1996) showed that CBF-C (HapE homologous protein) and CBF-A (HapC homologous protein) core regions, i.e., amino acids 42-115 of CBF-C and 59–140 of CBF-A, are homologous in sequence to histones H2A and H2B, respectively (Fig. 35). Furthermore, they are required for heterodimerization, a pre-requisite for CBF-B association and CCAAT binding (Sinha et al., 1995; Kim et al., 1996). All three cyteine residues of CBF-A (HapC homologous protein) are located in the H2B. Moreover, cysteines 85 and 89 in CBF-A are located in the CBF-C interaction domain (Fig. 35) indicating that cysteine residues might play a role in the dimerization of CBF-A to CBF-C and influence the stability of the heterodimer. The third cysteine (C105) is located in the H2B but not in the CBF-C interaction domain. Similar to CBF-A, HapC cysteine residues at the positions 74 and 78 are located in the HapE heterodimerization domain, while HapC cysteine residue at the position 94 is located in the H2B but not in the HapE interaction domain (Fig. 35).
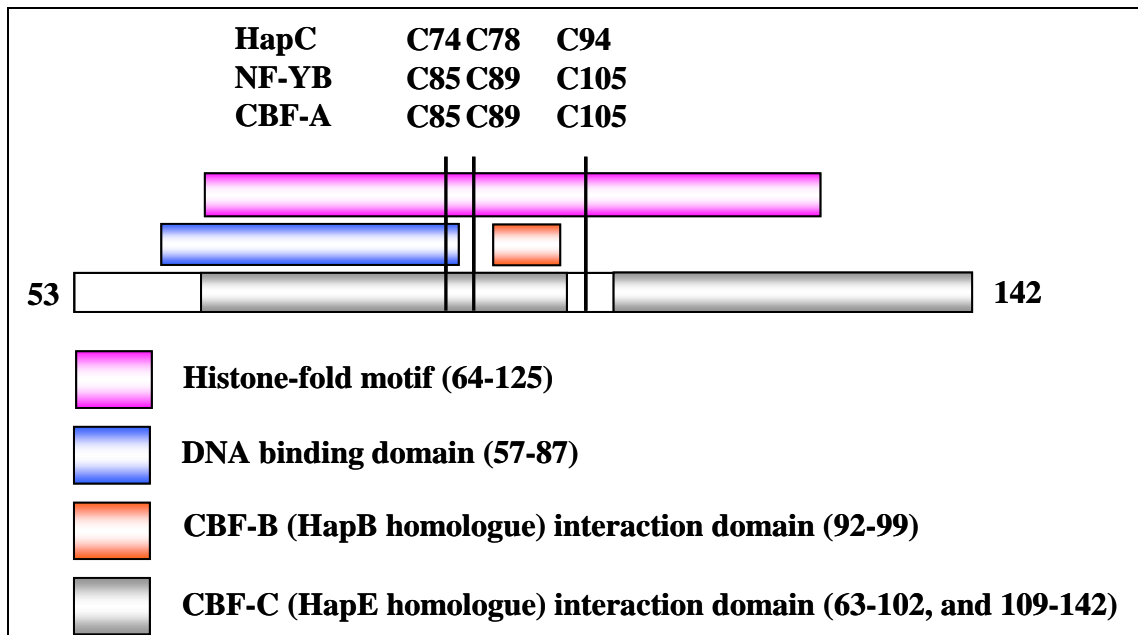
Fig. 35. CBF-A (HapC homologue) core domain analysis indicating the location of the conserved cysteine residues in the different domains (modified after Sinha et al., 1996).

Nakshatri et al. (1996) investigated the role of the highly conserved NF-YB cysteine residues on DNA binding and subunit association activities of the NF-Y complex. Their results suggested that the cysteine residues of NF-YB do not play an obligatory role in the DNA binding activity of NF-Y but do play an important regulatory role in the redox regulation of NF-Y activity through protein-protein interaction with the NF-YC subunit. Mutagenizing the highly conserved cysteine residues at positions 85 and 89 of NF-YB into serine caused the NF-YB to exist only as monomers (Nakshatri et al., 1996). Another *in vitro* analysis of CBC complex assembly in the presence of HapC3CS using BIACORE revealed that HapC3CS forms a less stable heterodimer with HapE compared to the wild-type HapC (P. Hortschansky, pers. communication). When HapB was added, HapC3CS formed a stable complex with HapB and HapE. A reduction in the stability of the CBC complex containing HapC3CS was noticed when the concentration of the CBC subunits was reduced (P. Hortschansky, pers. communication). Combining these *in vitro* results with the *in vivo* data shown in this study indicates that the cysteine residues are essential for the stability of the complex via influencing the heterodimerization of HapC-HapE and the stability of the CBC complex.

4.2 Regulation of CBC complex in response to cell stress.

In eukaryotes, protein-encoding genes are transcribed by RNA polymerase II under the control of short DNA elements located in the promoters, which are recognized by the general transcription machinery and *trans*-acting factors (for review, see Lemon and Tjian, 2000; Workman and Kingston, 1998). Statistical analysis revealed that the CCAAT box is one of the most ubiquitous promoter elements, being present in about 30%-65% of the eukaryotic promoters, ranging from yeast to mammals (Bucher, 1990; Suzuki et al., 2001). In mammals, genes relying on CCAAT elements and therefore controlled by NF-Y, the CBC homologue, include tissue specific (Berry et al., 1992; Ronchi et al., 1996), inducible (Marziali et al., 1997; Roy and Lee, 1995), and cell cycle regulated genes (Caretti et al., 2003), whereas housekeeping genes generally do not rely on CCAAT boxes (Mantovani, 1998). Due to the important functional roles of the CCAAT-binding factor, the characterization of the underlying regulatory mechanism of CBC under different stress conditions is important.

Previous studies showed that HapC and HapE have first to form a heterodimer, which binds to the HapB forming CBC complex (Steidl et al., 2004). HapB, which carries a functional NLS in the C-terminus of the protein outside of the evolutionarily conserved domain, functions as the primary cargo for the complex and transports the heterotrimer to the nucleus via a piggy back mechanism. This enables the cell to provide equimolar concentrations of all subunits to the nucleus (Steidl et al., 2004). The work presented here is a complementary study in order to get an overview about the regulation of CBC during oxidative stress and iron-depleting conditions. The data obtained here contribute to the model that the HapC subunit in *A. nidulans* is regulated by the redox status of the cell and the fully reduced HapC subunit is essential for the heterodimerization to HapE (Fig. 36). On the other hand, binding of HapX to HapB was proven under iron-limiting conditions (Fig. 36). However, the possibility of HapX regulation by thioredoxin needs still to be investigated and the overlap between oxidative stress and iron-depleting stress conditions needs still to be addressed.
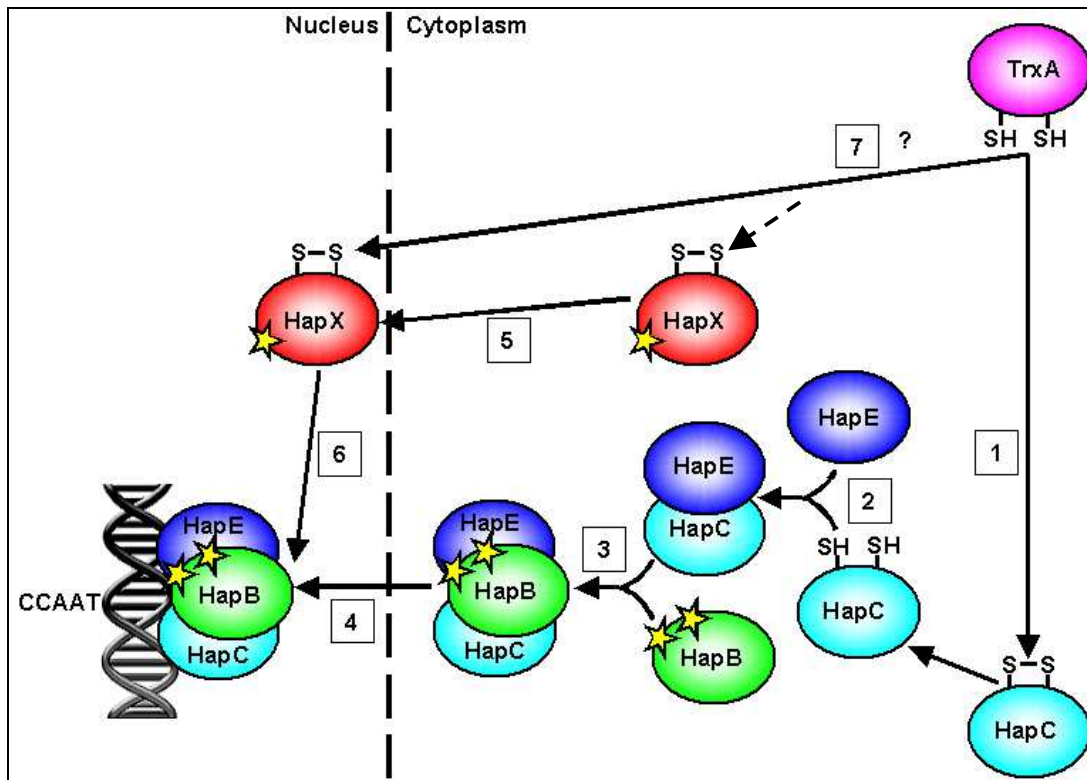
Fig. 38. Model for the CBC regulation under oxidative stress and iron-depleting conditions. (1) Reduction of HapC by TrxA is the first step and a pre-requisite for the assembly of the CBC complex. (2) The reduced HapC forms a heterodimer with HapE, (3) which in turn binds to HapB and forms the CBC complex. (4) The CBC is transported to the nucleus via a piggy back mechanism (Steidl et al., 2004). (5) HapX, which carries an NLS, is transported to the nucleus (6) and binds to the CBC complex under iron-depleting and oxidative stress conditions. (7) HapX might be reduced by TrxA before binding to CBC complex either in the cytoplasm before nuclear translocation or in the nucleus. S-S: Oxidized cysteine residues; SH: Reduced cysteine residue; ☆ : Nuclear Localization Signal (NLS).

4.3 Thioredoxin is the key regulator of the HapC protein during oxidative stress.

Gene expression in eukaryotes is regulated via interactions between DNA and different factors, including DNA-binding proteins, allowing the fine-tuning of essential cellular processes including growth, differentiation, energy metabolism, and stress responses (Ptashne, 1986; Choudhuri, 2004). Redox regulation has now been considered to be one of the important determinants for activity of transcription factors and subsequent gene expression in all eukaryotes (Nordberg and Arnér, 2001; Mustacich and Powis, 2000; Arnér and Holmgren, 2000). Aside from the chemical oxidants/reductants, however, it is important to understand which endogenous factor(s) might be involved in redox regulation of transcription factors. Thioredoxin acts as a potential disulfide reductase for a variety of target proteins (Holmgren, 1985) including several transcription factors directly like NF-kB (Matthews et al., 1992; Okamoto et al., 1992), or indirectly like AP-1 (Hirota et al., 1997). Therefore, in this work,

thioredoxin was suggested as possible posttranslational regulator of the CBC complex in *Aspergillus nidulans*. This assumption was based on *in vitro* results obtained from NF-Y, the human homologue of the CBC complex, where changes in association of NF-Y subunits and DNA binding activity were found to respond to changes in the cellular redox status (Nakshatri et al., 1996). Both CBC and NF-Y complexes share many similarities: (1) Both complexes are heterotrimeric composed of three subunits, all of which are required for CCAAT binding (Sinha et al., 1995). (2) HapB and its human homologue NF-YA are functionally interchangeable: the NF-YA protein-encoding gene partially complemented the *hap* phenotype of a *ΔhapB* strain of *A. nidulans* (Tüncher et al., 2005). (3) Both HapC and its human homologous protein NF-YB contain a core region that is highly conserved and sufficient for subunit interactions and CCAAT binding, whereas the flanking regions, which include the potential activation domains, are less conserved (Coustry et al., 1996; de Silvio et al., 1999). (4) The core region of both HapC and NF-YB proteins contains three conserved cysteine residues (Fig. 35). Therefore, we postulated that the cellular factors that were shown to regulate the activity of the NF-Y complex *in vitro* might also regulate CBC activity in *A. nidulans*. Furthermore, it was also the aim of this study to elucidate the mechanism of CBC regulation *in vivo*. Here, direct and indirect lines of evidence for the regulation of HapC by TrxA are provided. First, oxidation of the HapC cysteine residues either by the addition of H_2O_2 to the growth medium or by deletion of the *trxA* gene in *A. nidulans* led to the accumulation of a HapC-EGFP in the cytoplasm. Second, simulating the oxidative stress by the addition of H_2O_2 to the growth medium increased the levels of *trxA* mRNA in *A. nidulans*. Finally, the ability of TrxA to bind HapC under oxidative stress conditions was proven using BiFC analysis.

4.3.1 Accumulation of the oxidized HapC-EGFP in the cytoplasm.

The HapC cysteine residues are redox-sensitive and located in a region shown to be important for interaction with HapE. Under oxidative stress conditions, intra- or intermolecular disulfide cross-linking between the cysteine residues may occur and alter the conformation of the recognition surface of HapC, and consequently, the functional interaction with HapE is prevented. In this thesis, the importance of the reduced HapC cysteine residues in the heterodimerization with HapE was proven. First, the accumulation of HapC-EGFP in the cytoplasm upon treatment with H_2O_2 in *A. nidulans* wild-type strain indicates that HapC gets oxidized and forms intra- and intermolecular disulfide bridges causing disassembly of the CBC subunits. The oxidized form has to be reduced by an intracellular redox system allowing

HapC to become part of the CBC complex. These results have been shown previously *in vitro* and indicated that the oxidized form of NF-YB fails to associate with NF-YC without treatment with the reducing agent dithiothreitol (DTT) (Nakshatri et al., 1996). Second, the cytoplasmic localization of HapC-EGFP in a *ΔtrxA* strain reveals that the HapC cysteine residues should be reduced in order to become part of the CBC complex. It also shows that the TrxA is the major reducing factor of HapC**.** These results are consistent with previous *in vitro* work, which showed a reduced DNA-binding activity of the NF-Y complex in HeLa cells treated with the thioredoxin reductase inhibitor (1-chloro 2,4-dinitrobenzene (CDNB)) (Nakshatri et al., 1996).

However, using BiFC, it was not possible to visualize the dissociation of the HapC-HapE heterodimer *in vivo*. This finding can be explained by the fact that the BiFC technique has several characteristics that limit its applicability. One limitation is that the formation of the BiFC fluorescence in the cell is irreversible (Kerppola, 2006).

4.3.2 Elevated transcription of *trxA* in response to H$_2$O$_2$ addition.

Cellular life is frequently endangered by adverse conditions and forms of unfavorable changes to which it reacts with various stress responses. A rapid molecular response is induced in all eukaryotic cells to exposure to adverse environments. The response invariably involves changes in the level of gene transcription in response to stress, a complex known as cell signaling (Treisman, 1996; Koerkamp et al., 2002). The thioredoxin system is an important part of this complex. It is involved in cell signaling and the defense against oxidative damage and stress. Its main function is to keep proteins in the reduced state. During this work, induction of the *A. nidulans* main thioredoxin, i.e., TrxA (Thön et al., 2007), was possible by treating growing mycelia with H$_2$O$_2$. Induction of thioredoxins in response to oxidative stress was reported in many studies including *E. coli* (Ritz et al., 2000; Michan et al., 1999; Garrido and Grant, 2002), *Rhodobacter* species (Li et al., 2003a; Li et al., 2003b), *Bacillus subtilis* (Leichert et al., 2003), and *Streptomyces coelicolor* (Kang et al., 1999; Li et al., 2002; Bae et al., 2004). The induction of thioredoxins in the oxidative stress response is expected because of their capability to reduce oxidized proteins. Thioredoxins can also participate in the oxidative stress response by affecting the expression of other genes involved in this response (Gallardo-Madueno et al., 1998; Prieto-Alamo et al., 2000).

Induction of the whole thioredoxin system and glutathione system has been also studied in detail. In a genome-wide expression study of *Saccharomyces cerevisiae*, it has been shown

using DNA microarrays that during transient oxidative stress, there was an increase in the mRNAs encoding proteins, which uphold the redox status of the cell like cytosolic thioredoxin (*TRX2*) and thioredoxin reductase (*TRR1*) (Koerkamp et al., 2002). Increased transcription of the thioredoxin system genes in *Staphylococcus aureus* is observed with diamide, menadione, and t-butyl hydroperoxide but not hydrogen peroxide stress (Uziel et al., 2004). Both thioredoxin reductases (TRR1 and TRR2) are induced in response to H_2O_2 stress in *S. cerevisiae* (Godon et al., 1998; Salmon et al., 2004), while TRR1 is induced with menadione stress in *Schizosaccharomyces pombe* and with peroxide stress in *Kluyveromyces lactis* (Hong et al., 2004; Tarrio et al., 2004).

Induction of thioredoxin in response to oxidative stress seems to be a striking aspect. For example, in *Rhodobacter capsulatus*, it has been found that although both thioredoxins TrxA and TrxC have similar functions in some regards, nevertheless, the two genes respond to changes in oxygen tension in an opposite way. While a reduction in oxygen tension resulted in a significant increase in *trxC* mRNA level, the *trxA* mRNA level decreased (Li et al., 2003a). In *E. coli*, thioredoxins are involved in the response to oxidative stress. The expression of the *trxC* gene is induced by H_2O_2 and *trxC* is under the control of OxyR (Ritz et al. 2000). In contrast, *trxA* expression is not induced by H_2O_2 in *E. coli* and is not under control of OxyR (Michan et al. 1999; Garrido and Grant 2002). Furthermore, there was a remarkable specificity in the choice of expression of genes coding for isoenzymes or isoproteins. Among the thioredoxins, TRX2 was preferred to TRX1 and TRX3, and among the glutaredoxins, GRX2 was preferred to GRX1, GRX3, and GRX4. Thioredoxin reductase 1 (TRR1) was preferred to thioredoxin reductase 2 (TRR2) (Koerkamp et al., 2002).

4.3.3 Visualization of the interaction between HapC-TrxA in the cytoplasm and in the nucleus under oxidative stress conditions using BiFC analysis.

Using BiFC, the interaction between HapC and TrxA was observed *in vivo* under oxidative stress conditions. It was expected that the interaction between TrxA and HapC would occur in the cytoplasm since the treatment of cells with H_2O_2 resulted in localization of HapC-EGFP in the cytoplasm and HapC-EGFP fusion showed cytoplasmic localization in the *ΔtrxA* strain of *A. nidulans*. Surprisingly, the interaction between TrxA and HapC was observed in both the nucleus and the cytoplasm. This finding contradicted the proposed model, in which HapC should be reduced in the cytoplasm to become part of the CBC complex and transported to the nucleus. This obvious failure in the subcellular localization of the TrxA-HapC interaction is explained by the BiFC limitation to visualize reversible interactions in the cell (Kerppola,

2006). Therefore, after reduction of HapC, TrxA detaches from the reduced HapC while the two YFP protein parts seem to remain attached, and consequently, TrxA is transported to the nucleus with the CBC.

In spite of the cytoplasmic localization of thioredoxin, the nuclear localization of thioredoxin has been reported as well. Thioredoxin has no authentic nuclear localization signal (NLS) and the mechanism of the translocation needs to be elucidated. However, many reports showed that the treatment of the cells with H_2O_2 induced the translocation of thioredoxin from the cytoplasm to the nucleus. Previous study on the transcription factor glucocorticoid receptor (GR) demonstrated that TRX directly interacted with the GR in the nucleus, allowing restoration of sequence-specific DNA binding and subsequent transcriptional activation of GR under oxidative conditions (Makino et al., 1999). In another study, UV irradiation resulted in accumulation of TRX into the nucleus in HSC-1 keratinocytes and HeLa cells (Masutani et al., 1996). Similarly, in a mouse Fe-NTA-induced renal tubular damage model, thioredoxin has been largely recovered from nuclear fractions (Tanaka et al., 1997). The nuclear localization of thioredoxin seems to be a part of thioredoxin's role during oxidative stress. Thioredoxin functions as a mediator in response to the damaging effects of oxidative stress. Under oxidative stress conditions, reactive oxygen species (ROS) are formed, initiating a cellular response pathway in the cytoplasm, which triggers the flow of electrons from NADPH to the thioredoxin reductase. Thioredoxin reductase in turn passes the electrons to the oxidized thioredoxin, which is localized in the cytoplasm. The reduced thioredoxin translocates to the nucleus and passes the redox signal to the transcription factors, e.g. the nuclear redox factor-1 protein (Ref-1), which activates AP-1 DNA binding activity and gene transcription (Karimpour et al., 2002; Wei et al., 2000). Taking our results together with previous investigations support the idea that under oxidative stress conditions, HapC might get oxidized in the nucleus and dissociates from CBC. Consequently, TrxA might translocate to the nucleus in response to oxidative stress and might reduce the oxidized HapC in the nucleus. However, it was not possible to detect the oxidized HapC in the nucleus using HapC-EGFP fusion proteins.

4.4 Iron acquisition in *A. nidulans*.

Iron is a trace-substance required for the survival of all organisms. It is essential for the function of some proteins. Some of these proteins are required for crucial cellular processes including respiration and cell division. *A. nidulans* has evolved various strategies, often used in parallel, to adapt to iron starvation. The first strategy is the up-regulation of the iron uptake

by secretion of siderophores (Haas, 2003). The second strategy is down-regulation of many iron-dependent pathways, including proteins involved in the tri-carboxylic acid cycle, respiration and heme biosynthesis (Oberegger et al., 2002a). Fungi produce a variety of siderophores in response to iron-limiting environments because of their high affinities to withdraw iron from protein-iron complexes (Howard, 1999; Ratledge and Dover, 2000). Triacetylfusarinine C is a siderophore common in *Aspergillus* species (Diekmann and Krezdorn, 1975; Eisendle et al., 2003), while ferricrocin is thought to be an important intracellular iron storage compound in fungi such as *A. nidulans* (Eisendle et al., 2003) and *Neurospora crassa* (Matzanke et al., 1987). Ferricrocin is produced by a wide variety of fungi, including *Cenococcum geophilum* (Haselwandter and Winkelmann, 2002), *Phialocephala fortinii* (Bartholdy et al., 2001), and *Colletotrichum gloeosporioides* (Ohra et al., 1995). The repression of the synthesis and uptake of siderophore system under iron-rich conditions in *A. nidulans* is mediated, at least in part, by GATA transcription factor SreA (Oberegger et al., 2001; Oberegger et al., 2002b). In contrast to *A. nidulans*, *S. cerevisiae* does not secrete siderophores, but is able to take up ferric ions by an iron transport system, which is composed of two proteins, the iron permease Ftr1p and the copper-requiring enzyme Fet3p (Stearman et al., 1996; Askwith and Kaplan, 1997).

The second strategy represents oxidative metabolism, which is largely dependent on iron. We showed (Hortschansky et al., 2007) that various iron-dependent pathways are repressed during -Fe conditions by the interaction of HapX with the CBC. Moreover, using BiFC analysis, I could demonstrate the physical interaction between HapX and HapB *in vivo* under iron-limiting conditions. In contrast to CBC, which is functionally independent on iron, HapX has a novel mechanism of iron-dependent regulation. HapX represses the expression of iron-dependent proteins and pathways (e.g., aconitase, and heme biosynthesis) during iron-depleted conditions by physical interaction with the CBC. Extracellular siderophore biosynthesis is activated by CBC-HapX interaction.

4.5 Involvement of iron in the formation of reactive oxygen species (ROS).

Iron homeostasis is important for the cell as iron potentiates the formation of ROS via the Fenton and Haber–Weiss reactions (van Vliet et al., 2002). Thus, iron uptake and assimilation need to be tightly controlled in order to avoid iron-mediated oxidative damage to the cell. Anti-oxidative stress enzymes are used by the cell to detoxify ROS, and therefore, the expression of these enzymes is often coordinated with the expression of iron-transport systems in anticipation of the influx of iron into the cell (Holmes et al., 2005). Iron

overloading provides the ability of iron to participate in reactions that generate ROS and thus, it elicits an adaptive response that may play a major role in the resistance to iron-induced oxidative damage (Pantopoulos and Hentze, 1995; Pantopoulos and Hentze, 1998; Kotamraju et al., 2002).

However, iron deficiency has been shown to induce oxidative stress as well. Many cyanobacteria respond to iron limitation by expressing the *isiA* gene, which is also induced by oxidative stress (Xu et al., 2003; Yousef et al., 2003). Alternatively, iron deficiency caused the accumulation of ROS in *Anabaena* sp. strain PCC 7120 (Latifi et al., 2005). Studies in *Campylobacter jejuni* found that the genes encoding several oxidative stress proteins, including thioredoxin, thioredoxin reductase and a probable thiol peroxidase known as Tpx, were expressed at higher levels in iron-limited conditions (Holmes et al., 2005).

Therefore, observing the interaction between TrxA-HapC and HapX-HapB under the same stress conditions, i.e., oxidative stress and iron-depleting conditions could be explained by the overlap in the triggering signal. This overlap might result from iron-induced oxidative stress or it is caused by synchronized regulatory mechanisms against iron-depleting and oxidative stress conditions. This assumption could be problematic since the function and the regulatory mechanism of HapX are confined to the iron-depleted conditions (Hortschansky et al., 2007).

4.6 Advantages of using BiFC assay to study protein-protein interactions in *A. nidulans*.

The bimolecular fluorescence complementation (BiFC) is a novel promising tool to study protein–protein interactions *in vivo*, which relies on the expression of two proteins of interest as fusion proteins either to the N- or the C-terminal part of YFP (Hu et al., 2002). In this study, the BiFC analysis was used to visualize the interaction *in vivo*. The BiFC analysis was used because it has several advantages compared with other methods for the investigation of protein interactions in cells. These advantages are discussed below.

4.6.1 Visualization protein-protein interactions *in vivo* and in the homologous host system.

One important feature of this method is the ability to visualize the interaction in the homologous host. Using BiFC, the interaction between HapC and TrxA on one side, and between HapB and HapX on the other side was visualized and proven *in vivo* in the homologous host *A. nidulans*. The interaction between HapC and TrxA was proven *in vitro* (M. Thön, pers. communication). Furthermore, the interaction between HapB and HapX was

also studied using two-hybrid system in a heterologous host (Tanaka et al., 2002). In other studies, BiFC was applied to detect protein–protein interactions in living animal cells (Hu et al., 2002; Hu and Kerppola, 2003), plants (Walter et al., 2004) and filamentous fungi (Hoff and Kück, 2005; Blumenstein et al., 2005) by conventional epifluorescence microscopy. Therefore, it is a convenient approach for visualization of protein-protein interactions in many living cells.

4.6.2 Studying different types of protein-protein interactions including permanent as well as transient interactions and the corresponding triggering signal.

Protein-protein interactions can be distinguished based on the half-life of the complex into permanent and transient. Permanent interactions are usually stable and thus exist only in form of a complex. In contrast to permanent interactions, transient interactions carry out cycles of association and dissociation depending on the received signal (Nooren and Thornton, 2003). Transient complexes are more difficult to study, since the proteins or conditions responsible for the transient interaction have to be identified first. Using BiFC, the detection of protein-protein interactions is quite simple and does not require any disruption or stressful treatment of the cells, and therefore, it is suitable for the detection of protein-protein interactions under stress conditions. However, it is important here to mention that when transient interactions are observed, it is expected that such interactions would be observed only elusively. However, using BiFC, transient interactions were observed permanently but emitted weak fluorescence. In this study, BiFC was applied to study both the permanent interaction, e.g HapC-HapE interaction, and the transient interaction, e.g. HapC-TrxA and HapB-HapX interactions. These findings agree with previous studies, which showed the possibility to employ BiFC to study permanent as well as transient protein-protein interactions (Hu et al., 2002; Walter et al., 2004; Hoff and Kück, 2005; Blumenstein et al., 2005; Morell et al., 2007).

4.6.3 Measuring the strength of protein-protein interactions semi-quantitatively.

The strength of protein-protein interactions could be measured semi-quantitatively using the BiFC analysis, allowing discrimination between high- and low-affinity bindings. As previously mentioned, BiFC was applied to visualize the two types of interaction: the permanent interactions and the transient interactions. During this work, it was observed that the permanent interactions are characterized by high fluorescence emission while the transient interactions emitted low fluorescence, a semi-quantitative indicator for the strength of the interaction. This could be also considered as a limiting point for BiFC when BiFC is

compared to other protein-protein interaction detection methods like the BIACORE system, which is a technology that enables the calculation of the interactants affinity in real time.

4.6.4 Determination of the subcellular localization of the interaction.

One of the important advantages of BiFC is the ability to determine subcellular localization of the interaction. However, this is not always applicable using BiFC. Determination the subcellular localization of the interaction is dependent on observing the BiFC fluorescence in the cell, which is influenced by several factors like the strength of the promoter used to control the production of the fusion proteins (discussed in 4.7.1) and the strength of the interaction. Permanent interactions, like that of HapC-HapE, are strong interactions and therefore, it is possible to observe them in the cytoplasm and the nucleus. By contrast, transient protein interactions between HapC and TrxA or HapX and HapB produce weak signals, compared to that produced by a HapC-HapE dimer. This weak signal was detectable in the nucleus and conidial cytoplasm but not in the mycelial cytoplasm. The reason for this is that transient interactions are so weak, and therefore, the fluorescence resulting from transient interactions is harder to observe when distributed over the mycelial cytoplasm in comparison with the nucleus or the compact conidial cytoplasm. This feature could be considered as one of the BiFC limitations.

4.7 Limitations of using BiFC to study protein-protein interactions in *A. nidulans*.

Despite the big advantages of using BiFC to study protein-protein interactions *in vivo* in *A. nidulans*, several limitations have been noticed for this technique. One of the limitations is the incapability of BiFC to detect transient interactions in the mycelial cytoplasm as previously mentioned (refer to 4.6.4). The other limitations are discussed below.

4.7.1 BiFC relies on strong promoters.

Fluorescent proteins must be expressed at high levels to assure that the fluorescence signal is above the cellular background (Remy and Michnick, 2007). Therefore, in this study, strong promoters were used for BiFC assays. However, strong promoters may lead to misinterpretation of subcellular localization of the interacting proteins. They may alter the subcellular localization of the interacting proteins by overexpressing certain subunits. A good example is that HapC-HapE dimers carry no nuclear localization signal (NLS), and thus, they are dependent on HapB in the nuclear localization. Consequently, expression of *hapC* and *hapE*, driven by the strong promoter (*gpdA*p), leads to imbalance in the stoichiometry of the

complex causing accumulation of the HapC-HapE dimer in the cytoplasm. This accumulation was visualized by BiFC as a strong fluorescence in the cytoplasm. However, this would not apply for interacting partners, especially if both of them carried the localization signals or if the interacting partners were transiently interacting. For example, both HapB and HapX carry NLSs and they transiently interact with each other. Therefore, expression of *hapB* and *hapX* was visualized in the nucleus despite of the imbalance in the stoichiometry of the other CBC subunits.

4.7.2 Fluorescence resulting from protein-protein interactions is irreversible.

Visualization of the transient protein-protein interactions using BiFC has been demonstrated to be irreversible (Hu et al., 2002; Kerppola, 2006) which could lead to misinterpretation of the turnover or the localization of the interacting proteins. As consequence, the interaction between HapC and TrxA was observed in the nucleus when it was visualized using BiFC assay. Moreover, the addition of H_2O_2 to the growing mycelia did not cause the disassembly of the HapC-HapE dimer when it was visualized by BiFC analysis. This feature could be also considered as one of the BiFC advantages since it is useful for trapping and visualizing rare complexes using plasmid library screening (Joshi et al., 2007). BiFC can therefore be used to identify novel protein interactions without prior knowledge of the structural basis of the interaction (Hu et al., 2002).

4.7.3 The fluorescence is resulting from binding of the two YFP terminal proteins not from interacting proteins.

Since the achieved signal, e.g. the fluorescence, is dependent on the association of the two terminal parts of EYFP with each other, visualization of fluorescence is dependent not only on the two interacting proteins but also on the two EYFP terminal parts. This point has to be taken into consideration during cloning of genes encoding the studied proteins. If the structural basis of complex formation is not clear, the two interacting proteins should be fused N- and C-terminally to the N- and C- terminal part of YFP. The resulting eight combinations of the fusion proteins should be tested for complementation (Kerppola, 2006). Moreover, the resulting fluorescence should be verified whether the fluorescence is resulting from a specific protein-protein interaction or from unspecific binding of the two YFP termini.

5. References

Adams TH, Wieser JK, and Yu JH (1998). Asexual sporulation in *Aspergillus nidulans*. *Microbiol. Mol. Biol. Rev.* 62:35-54.

Aleksenko A, and Clutterbuck AJ (1997). Autonomous plasmid replication in *Aspergillus nidulans*: AMA1 and MATE elements. *Fungal Genet. Biol.* 21:373-87.

Andrianopoulos A, and Hynes MJ (1988). Cloning and analysis of the positively acting regulatory gene *amdR* from *Aspergillus nidulans*. *Mol. Cell. Biol.* 8:3532–3541.

Arnér E, and Holmgren A (2000). Physiological functions of thioredoxin and thioredoxin reductase. *Eur. J. Biochem.* 267 (20): 6102-6109.

Askwith C, and Kaplan J (1997). An oxidase-permease-based iron transport system in *Schizosaccharomyces pombe* and its expression in *Saccharomyces cerevisiae*. *J. Biol. Chem.* 272:401-405.

Bae JB, Park JH, Hahn MY, Kim MS, and Roe JH (2004). Redox dependent changes in RsrA, an anti-sigma factor in *Streptomyces coelicolor*: zinc release and disulfide band formation. *J. Mol. Biol.* 335:425–435.

Balance DJ, and Turner G (1985). Development of a high-frequency transforming vector for *Aspergillus nidulans*. *Gene* 36:321-331.

Bartholdy BA, Berreck M, and Haselwandter K (2001). Hydroxamate siderophore synthesis by *Phialocephala fortinii*, a typical dark septate fungal root endophyte. *Biometals* 14:33-42.

Baxevanis A, Arents G, Moudrianakis E, and Landsman D (1995). A variety of DNA-binding and multimeric proteins contain the histone fold motif. *Nucleic Acids Res.* 23:2685–2691.

Becker DM, Fikes JD, and Guarente L (1991). A cDNA encoding a human CCAAT-binding protein cloned by functional complementation in yeast. *Proc. Natl. Acad. Sci.USA.* 88:1968-1972.

Bellorini M, Kun Lee D, Dantonel JC, Zemozoumi K, Roeder RG, Tora L, and Mantovani R (1997). CCAAT binding NF-Y-TBP interactions: NF-YB and NF-YC require short domains adjacent to their histone fold motifs for association with TBP basic residues. *Nucleic Acids Res*. 25:2174-2181.

Berry M, Dillon N, and Grosveld F (1992). A single point mutation is the cause of the Greek form of hereditary persistence of fetal hemoglobin. *Nature* 358:499–452.

Birnboim HC, and Doly J (1979). A rapid alkaline extraction procedure for screening recombinant plasmid DNA. *Nucleic Acids Res*. 7:1513-1523.

Biswas S, Chida AS, and Rahman I (2006). Redox modifications of protein–thiols: Emerging roles in cell signalling. *Biochem. Pharmacol.* 71:551-564.

Blumenstein A, Vienken K, Tasler R, Purschwitz J, Veith D, Frankenberg-Dinkel N, and Fischer R (2005). The *Aspergillus nidulans* phytochrome FphA represses sexual development in red light. *Curr. Biol.* 15:1833–1838.

Bourgarel D, Nguyen CC, and Bolotin-Fukuhara M (1999). HAP4, the glucose-repressed regulated subunit of the HAP transcriptional complex involved in the fermentation-respiration shift, has a functional homologue in the respiratory yeast *Kluyveromyces lactis*. *Mol. Microbiol.* 31:1205-1215.

Bradford MM (1976). A rapid and sensitive method for the quantitation of microgram quantities of protein utilizing the principle of protein-dye binding. *Anal. Biochem.* 72:248-254.

Brakhage A A (1998). Molecular regulation of β-lactam biosynthesis in filamentous fungi. *Microbiol. Mol. Biol. Rev.* 62**:**547-585.

Brakhage AA, and Van den Brulle J (1995). Use of reporter genes to identify recessive trans-acting mutations specifically involved in the regulation of *Aspergillus nidulans* penicillin biosynthesis genes. *J. Bacteriol.* 177:2781-2788.

Brakhage AA, Andrianopoulos A, Kato M, Steidl S, Davis MA, Tsukagoshi N, and Hynes MJ (1999). HAP-like CCAAT-binding complexes in filamentous fungi: implications for biotechnology. *Fungal Genet. Biol.* 27:243-252.

Bucher P (1990). Weight matrix descriptions of four eukaryotic RNA polymerase II promoter elements derived from 502 unrelated promoter sequences. *J. Mol. Biol.* 212:563–578.

Caretti G, Salsi V, Vecchi C, Imbriano C, and Mantovani R (2003). Dynamic recruitment of NF-Y and histone acetyltransferases on cell-cycle promoters. *J. Biol. Chem.* 278:30435-30440.

Casselton L, and Zolan M (2002). The art and design of genetic screens: filamentous fungi. *Nature Reviews Genetics* 3:683-697.

Chae HZ, Chung SJ, and Rhee SG (1994). Thioredoxin-dependent peroxide reductase from yeast. *J. Biol. Chem.* 269:27670–27678.

Choudhuri S (2004). Gene Regulation and Molecular Toxicology. *Toxicology Mechanisms and Methods* 15:1-23.

Coustry F, Maity SN, Sinha S, and de Crombrugghe B (1996). The Transcriptional activity of the CCAAT-binding factor CBF is mediated by two distinct activation domains, one in the CBF-B subunit and the other in the CBF-C subunit. *J. Biol. Chem.* 271:14485-14491.

de Silvio A, Imbriano C, and Mantovani R (1999). Dissection of the NF-Y transcriptional activation potential. *Nucleic Acids Res.* 27:2578–2584.

DeRisi J, Iyer V, and Brown P (1997). Exploring the metabolic and genetic control of gene expression on a genomic scale. *Science* 278:680–686.

Diekmann H, and Krezdorn E (1975). Metabolic products of microorganisms. 150. Ferricrocin, triacetylfusigen and other sideramines from fungi of the genus *Aspergillus*, group Fumigatus. *Arch. Microbiol.* 106:191-194. (In German.)

Dorn A, Bollekens J, Staub A, Benoist C, and Mathis D (1987). A multiplicity of CCAAT box-binding proteins.*Cell* 50:863–872.

Edwards D, Murray JAH, and Smith AG (1998). Multiple genes encoding the conserved CCAAT-box transcription factor complex are expressed in *Arabidopsis*. *Plant Physiol.* 117**:**1015–1022.

Eisendle M, Oberegger H, Zadra I, and Haas H (2003). The siderophore system is essential for viability of *Aspergillus nidulans*: functional analysis of two genes encoding 1-ornithine N 5-monooxygenase (*sidA*) and a non-ribosomal peptide synthetase (*sidC*). *Mol. Microbiol.* 49:359-375.

Forsburg SL, and Guarente L (1989). Identification and characterization of HAP4: a 3rd component of the CCAAT-bound HAP2 HAP3 heteromer. *Genes Dev.* 3:1166-1178

Gallardo-Madueno R, Leal JF, Dorado G, Holmgren, Lopez-Barea J, and Pueyo C (1998). *In vivo* transcription of *nrdAB* operon and of *grxA* and *fpg* genes is triggered in *Escherichia coli* lacking both thioredoxin and glutaredoxin 1 or thioredoxin and glutathione, respectively. *J. Biol. Chem.* 273:18382–18388.

Gan ZR (1991). Yeast thioredoxin genes. *J. Biol. Chem.* 266:1692–1696.

Garrido EO, and Grant CM (2002). Role of thioredoxins in the response of *Saccharomyces cerevisiae* to oxidative stress induced by hydroperoxides. *Mol. Microbiol.* 43:993–1003.

Gelinas R, Endlich B, Pfeiffer C, Yagi M, and Stamatoyannopoulos G (1985). G-substitution to A-substitution in the distal CCAAT box of the gamma-globin gene in Greek hereditary persistence of fetal hemoglobin. *Nature* 313:323–325.

Gems DH, and Clutterbuck AJ (1993). Co-transformation with autonomously-replicating helper plasmids facilitates gene cloning from an *Aspergillus nidulans* gene library. *Curr. Genet.* 24:520-524.

Ghezzi P (2005). Oxidoreduction of protein thiols in redox regulation. *Biochem. Soc. Trans.* 33: 1378–1381.

Godon C, Lagniel G, Lee J, Buhler JM, Kieffer S, Perrot M, Boucherie H, Toledano MB, and Labarre J (1998). The H_2O_2 stimulon in *Saccharomyces cerevisiae*. *J. Biol. Chem.* 273:22480-22489.

Guarente L, Lalonde B, Gifford P, and Alani E (1984). Distinctly regulated tandem upstream activation sites mediate catabolite repression of the CYC1 gene of *S. cerevisiae*. *Cell* 36:503-511.

Gusmaroli G, Tonelli C, and Mantovani R (2001). Regulation of the CCAAT-binding NF-Y subunits in *Arabidopsis thaliana*. *Gene* 264:173–185.

Haas H (2003). Molecular genetics of fungal siderophore biosynthesis and uptake: the role of siderophores in iron uptake and storage. *Appl. Microbiol. Biotechnol.* 62:316–330.

Hahn S, Pinkham J, Wei R, Miller R, and Guarente L (1988). The *HAP3* regulatory locus of *Saccharomyces cerevisiae* encodes divergent overlapping transcripts. *Mol. Cell. Biol.* 8:655–663.

Haselwandter K, and Winkelmann G (2002). Ferricrocin—an ectomycorrhizal siderophore of *Cenococcum geophilum*. *Biometals* 15:73-77.

Higuchi R, Krummel B, and Saiki RK (1988). A general method of *in vitro* preparation and mutagenesis of DNA fragments: study of protein and DNA interactions. *Nucleic Acids Res.* 16**:**7351–7367.

Hirota K, Matsui M, Iwata S, Nishiyama A, Mori K, and Yodoi J (1997). AP-1 transcriptional activity is regulated by a direct association between thioredoxin and Ref-1. *Proc. Natl. Acad. Sci. USA.* 94:3633-3638.

Hoff B, and Kück U (2005). Use of bimolecular fluorescence complementation to demonstrate transcription factor interaction in nuclei of living cells from the filamentous fungus *Acremonium chrysogenum*. *Curr. Genet.* 47:132–138.

Holmes K, Mulholland F, Pearson BM, Pin C, McNicholl-Kennedy J, Ketley JM, and Wells JM (2005). *Campylobacter jejuni* gene expression in response to iron limitation and the role of Fur. *Microbiology* 151:243–257.

Holmgren A (1985). Thioredoxin. *Annu. Rev. Biochem.* 54:237-271.

Holmgren A (1989). Thioredoxin and glutaredoxin systems. *J. Biol. Chem.* 264:13963-13966.

Hong SM, Lim HW, Kim IH, Kim K, Park EH, and Lim CJ (2004). Stress-dependent regulation of the gene encoding thioredoxin reductase from the fission yeast. *FEMS Microbiol. Lett.* 234:379-385.

Hooft van Huijsduijnen R, Li XY, Black D, Matthes H, Benoist C, and Mathis D (1990). Co-evolution from yeast to mouse: cDNA cloning of the two NF-Y (CP-1/CBF) subunits. *EMBO J.* 9:3119-3127.

Hortschansky P, Eisendle M, Al-Abdallah Q, Schmidt AD, Bergmann S, Thon M, et al. (2007). Interaction of HapX with the CCAAT-binding complex – a novel mechanism of gene regulation by iron. *EMBO J.* 26:3157–3168.

Howard DH (1999). Acquisition, transport, and storage of iron by pathogenic fungi. *Clin. Microbiol. Rev.* 12:394-404.

Hu CD, and Kerppola TK (2003). Simultaneous visualization of multiple protein interactions in living cells using multicolor fluorescence complementation analysis. *Nat. Biotechnol.* 21:539–545.

Hu CD, Chinenov Y, and Kerppola T K (2002).Visualization of interactions among bZIP and Rel family proteins in living cells using bimolecular fluorescence complementation. *Mol. Cell* 9:789– 798.

Jamieson DJ (1998). Oxidative stress responses of the yeast *Saccharomyces cerevisiae*. *Yeast* 14:1511–1527.

Joshi P, Hirst M, Malcolm T, Parent J, Mitchell D, Lund K, and Sadowski I (2007). Identification of protein interaction antagonists using the repressed transactivator two-hybrid system. *BioTechniques* 42:635-644.

Kallis GB, and Holmgren A (1980). Differential reactivity of the functional sulfhydryl groups of cysteine-32 and cysteine-35 present in the reduced form of thioredoxin from *Escherichia coli*. *J. Biol. Chem.* 255:10261-10265.

Kang JG, Paget MSB, Seok YJ, Hahn MY, Bae JB, Hahn JS, Leanthous C, Buttner MJ, and Roe JH (1999). RsrA, an anti-sigma factor regulated by redox change. *EMBO J.* 18:4292–4298.

Karimpour S, Lou J, Lin LL, Rene LM, Lagunas L, Ma X, Karra S, Bradbury CM, et al. (2002). Thioredoxin reductase regulates AP-1 activity as well as thioredoxin nuclear localization via active cysteines in response to ionizing radiation. *Oncogene* 21:6317–6327.

Kerppola T (2006). Design and implementation of bimolecular fluorescence complementation (BiFC) assays for the visualization of protein interactions in living cells. *Nat. Protoc.* 1:1278-1286.

Kim IS, Sinha S, de Crombrugghe B, and Maity SN (1996). Determination of functional domains in the C subunit of the CCAAT-binding factor (CBF) necessary for formation of a CBF-DNA complex: CBF- B interacts simultaneously with both the CBF-A and CBF-C subunits to form a heterotrimeric CBF molecule. *Mol. Cell. Biol.* 16:4003-4013.

Koerkamp MG, Rep M, Bussemaker HJ, Hardy GP, Mul A, Piekarska K, Szigyarto CA, De Mattos JM, and Tabak HF (2002). Dissection of transient oxidative stress response in *Saccharomyces cerevisiae* by using DNA microarrays. *Mol. Biol. Cell.* 13:2783–2794.

Kohyama E, Dohi M, Yoshimura A, Yoshida T, Nagasawa T (2007). Remaining

acetamide in acetonitrile degradation using nitrile hydratase- and amidase-producing microorganisms. *Appl. Microbiol. Biotechnol.* 74:829-835.

Kotamraju S, Chitambar CR, Kalivendi SV, Joseph J, and Kalyanaraman B (2002). Transferrin receptor-dependent iron uptake is responsible for doxorubicin-mediated apoptosis in endothelial cells: role of oxidant-induced iron signalling in apoptosis. *J. Biol. Chem.* 277:17179–17187.

Latifi A, Jeanjean R, Lemeille S, Havaux M, Zhang C-C (2005). Iron starvation leads to oxidative stress in *Anabaena* sp. strain PCC 7120. *J. Bacteriol.* 187:6596-6598.

Le Marechal P, Hoang BM, Schmitter JM, Van Dorsselaer A, and Decottignies P (1992). Purification, properties and primary structure of thioredoxin from *Aspergillus nidulans. Eur. J. Biochem.* 210:421-429.

Leichert LI, Scharf C, and Hecker M (2003). Global characterization of disulfide stress in *Bacillus subtilis. J. Bacteriol.* 185:1967–1975.

Lemon B, and Tjian R (2000). Orchestrated response: a symphony of transcription factors for gene control. *Genes & Dev.* 14:2551-2569.

Li K, Haertig E, and Klug G (2003a). Thioredoxin 2 is involved in oxidative stress defense and redox-dependent expression of photosynthesis genes in *Rhodobacter capsulatus. Microbiology* 149:419–430.

Li K, Pasternak C, and Klug G (2003b). Expression of the *trxA* gene for thioredoxin 1 in *Rhodobacter sphaeroides* during oxidative stress. *Arch. Microbiol.* 180:484–489.

Li Q, Herrler M, Landsberger N, Kaludov N, Ogryzko VV, Nakatani Y, and Wolffe AP (1998). Xenopus NF-Y pre-sets chromatin to potentiate p300 and acetylation-responsive transcription from the Xenopus hsp70 promoter *in vivo. EMBO J.* 17:6300–6315.

Li W, Stevenson CE, Burton N, Jakimowicz P, Paget MS, Buttner MJ, Lawson DM, and Kleanthous C (2002). Identification and structure of the anti-sigma factor-binding domain of the disulphide-stress regulated sigma factor σ^R from *Streptomyces coelicolor. J. Mol. Biol.* 323:225–236.

Li XY, Mantovani R, Vanhuijsduijnen RH, Andre I, Benoist C, and Mathis D (1992). Evolutionary variation of the CCAAT-binding transcription factor NF-Y. *Nucleic Acids Res.* 20:1087-1091.

Liang SG, and Maity SN (1998). Pathway of complex formation between DNA and three subunits of CBF/NF-Y. Photocross-linking analysis of DNA-protein interaction and characterization of equilibrium steps of subunit interaction and DNA binding. *J. Biol. Chem.* 273**:**31590-31598.

Littlejohn TG, and Hynes MJ (1992). Analysis of the site of action of the *amdR* product for regulation of the *amdS* gene of *Aspergillus nidulans. Mol. & Gen. Genet.* 235, 81-88.

Litzka O, Then Bergh K, and Brakhage AA (1996). The *Aspergillus nidulans* penicillin-biosynthesis gene *aat* (*penDE*) is controlled by a CCAAT-containing DNA element. *Eur. J. Biochem.* 238:675-682.

Maity SN, Vuorio T, and de Crombrugghe B (1990). The B-subunit of a rat heteromeric CCAAT-binding transcription factor shows a striking sequence identity with the yeast HAP2 transcription factor. *Proc. Natl. Acad. Sci. USA.* 87:5378-5382

Makino Y, Yoshikawa N, Okamoto K, Hirota K, Yodoi J, Makino I, and Tanaka H (1999). Direct Association with Thioredoxin Allows Redox Regulation of Glucocorticoid Receptor Function. *J. Biol. Chem.* 274:3182-3188.

Mantovani R (1998). A survey of 178 NF-Y binding CCAAT boxes. *Nucleic Acids Res.* 26:1135–1143.

Martinelli SD (1994). *Aspergillus nidulans* as an experimental organism. *In*: Aspergillus: 50 years on. Eds Martinelli SD and Kinghorn JR. Elsevier, Amsterdam, pp 33-58.

Marziali G, Perrotti E, Ilari R, Testa U, Coccia EM, and Battistini A (1997). Transcriptional regulation of the ferritin heavy-chain gene: the activity of the CCAAT binding factor NF-Y is modulated in heme-treated Friend leukemia cells and during monocyte-to-macrophage differentiation. *Mol. Cell. Biol.* 17:1387-1395.

Masutani H, Hirota K, Sasada T, Ueda-Taniguchi Y, Taniguchi Y, Matsui M, and Yodoi J (1996). Transactivation of an inducible anti-oxidative stress protein, human thioredoxin by HTLV-I Tax. *Immunol. Lett.* 54:67-71.

Matthews JR, Wakasugi N, Virelizier J-L, Yodoi J, and Hay RT (1992). Thiordoxin regulates the DNA binding activity of NF-xB by reduction of a disulphid bond involving cysteine 62. Nucleic Acids Res. 20, 3821-3830

Matzanke BF, Bill E, Trautwein AX, and Winkelmann G (1987). Role of siderophores in iron storage in spores of *Neurospora crassa* and *Aspergillus ochraceus*. *J. Bacteriol.* 169:5873-5876.

McNabb DS, and Pinto I (2005). Assembly of the Hap2p/Hap3p/Hap4p/Hap5p-DNA complex in *Saccharomyces cerevisiae*. *Eukaryot. Cell* 4:1829-1839.

McNabb DS, Tseng KAS, and Guarente L (1997). The *Saccharomyces cerevisiae* HAP5p homolog from fission yeast reveals two conserved domains that are essential for assembly of heterotetrameric CCAAT-binding factor. *Mol. Cell. Biol.* 17:7008–7018.

McNabb DS, Xing YY, and Guarente L (1995). Cloning of yeast HAP5: a novel subunit of a heterotrimeric complex required for CCAAT binding. *Genes Dev.* 9:47-58.

Michan C, Manchado M, Dorado G, Pueyo C (1999). *In vivo* transcription of the *Escherichia coli oxyR* regulon as a function of growth phase and in response to oxidative stress. *J. Bacteriol.* 181:2759–2764.

Miller JH (1972). *In*: Experiments in molecular genetics. Cold Spring Harbor Laboratory, Cold Spring Harbor, New York.

Morell M, Espargaro A, Aviles FX, and Ventura S (2007). Detection of transient protein-protein interactions by bimolecular fluorescence complementation: the Abl-SH3 case. *Proteomics* 7:1023–1036.

Mulder W, Scholten I, de Boer R, Grivell LA (1994). Sequence of the HAP3 transcription factor of *Kluyveromyces lactis* predicts the presence of a novel 4-cysteine zinc-finger motif. *Mol. Gen. Genet.* 245:96-106.

Muller E (1991). Thioredoxin deficiency in yeast prolongs S phase and shortens the G1 interval of the cell cycle. *J. Biol. Chem.* 266:9194–9202.

Muro AF, Bernath VA, and Kornblihtt AR (1992). Interaction of the −170-cyclic AMP response element with the adjacent CCAAT box in the human fibronectin gene promoter. *J. Biol. Chem.* 267:12767–12774.

Mustacich D, and Powis G (2000). Thioredoxin reductase. *Biochem. J.* 346:1-8.

Nakshatri H, Bhat-Nakshatri P, and Currie RA (1996). Subunit association and DNA binding activity of the heterotrimeric transcription factor NF-Y is regulated by cellular redox. *J. Biol. Chem.* 271:28784-28791.

Nooren IM, and Thornton JM (2003). Diversity of protein-protein interactions. *EMBO J.* 22:3486-3492.

Nordberg J, and Arnér E (2001). Reactive oxygen species, antioxidants, and the mammalian thioredoxin system. *Free Radic. Biol. Med.* 31:1287-1312.

Oberegger H, Schoeser M, Zadra I, Abt B, and Haas H (2001). SREA is involved in regulation of siderophore biosynthesis, utilization and uptake in *Aspergillus nidulans*. *Mol. Microbiol.* 41:1077-1089.

Oberegger H, Schoeser M, Zadra I, Schrettl M, Parson W, and Haas H (2002a). Regulation of *freA, acoA, lysF,* and *cycA* expression by iron availability in *Aspergillus nidulans. Appl. Env. Microbiol.* 68:5769-5772.

Oberegger H, Zadra I, Schoeser M, Abt B, Parson W, and Haas H (2002b). Identification of members of the *Aspergillus nidulans* SREA regulon: genes involved in siderophore biosynthesis and utilization. *Biochem. Soc. Trans.* 30:781-783.

Ohra J, Morita K, Tsujino Y, Tazaki H, Fujimori T, Goering M, Evans S, and Zorner P (1995). Production of the phytotoxic metabolite, ferricrocin, by the fungus *Colletotrichum gloeosporioides. Biosci. Biotechnol. Biochem.* 59:113-114.

Okamoto T, Ogiwara H, Hayashi T, Mitsui A, Kawabe T, and Yodoi J (1992). Human thioredoxin/adult T cell leukemia-derived factor activates the enhancer binding protein of human immunodeficiency virus type 1 by thiol redox control mechanism. *Int. Immunol.* 4:811-819.

Osmani A, May G, and Osmani S (1999). The extremely conserved *pyroA* gene of *Aspergillus nidulans* is required for pyridoxine synthesis and is required indirectly for resistance to photosensitizers. *J. Biol. Chem.* 274:23565-23569.

Pantopoulos K, and Hentze MW (1995). Rapid responses to oxidative stress mediated by iron regulatory protein. *EMBO J.* 14:2917–2924.

Pantopoulos K, and Hentze MW (1998). Activation of iron regulatory protein-1 by oxidative stress *in vitro*. *Proc. Natl. Acad. Sci. USA.* 95:10559–10563.

Papadopoulou N (1999). Diplomarbeit, Institut of Microbiology and Genetics, Technical University of Darmstadt. (In German).

Papagiannopoulos P, Andrianopoulos A, Sharp JA, Davis MA, and Hynes MJ (1996). The *hapC* gene of *Aspergillus nidulans* is involved in the expression of CCAAT-containing promoters, *Mol. Gen. Genet.* 251:412-421.

Pedrajas JR, Kosmidou E, Miranda-Vizuete A, Gustafsson J-A, Wright APH, and Spyrou G (1999). Identification and functional characterization of a novel mitochondrial thioredoxin system in *Saccharomyces cerevisiae*. *J. Biol. Chem.* 274:6366–6373.

Pinkham JL, Olesen JT, and Guarente LP (1987). Sequence and nuclear localization of the *Saccharomyces cerevisiae* HAP2 protein, a transcriptional activator. *Mol. Cell. Biol.* 7:578–585.

Pontecorvo G, **Roper JA**, **Hemmons LM**, **MacDonald KD, and Bufton AWJ** (1953). The genetics of *Aspergillus nidulans. Adv. Genet.* 5:141-238.

Prieto-Alamo MJ, Jurado J, Gallardo-Madueno R, Monje-Casas F, Holmgren A, Pueyo C (2000). Transcriptional regulation of glutaredoxin and thioredoxin pathways and related enzymes in response to oxidative stress. *J. Biol. Chem.* 275:13398–13405.

Ptashne M (1986). Gene regulation by proteins acting nearby and at a distance. *Nature* 322:697-701.

Ratledge C, and Dover LG (2000). Iron metabolism in pathogenic bacteria. *Annu. Rev. Microbiol.* 54:881-941.

Raymondjean M, Cereghini S, and Yaniv M (1988) Several distinct CCAAT box binding-proteins coexist in eukaryotic cells. *Proc. Natl. Acad. Sci. USA.* 85:757-761.

Remy I, and Michnick SW (2007). Application of protein-fragment complementation assays in cell biology. *BioTechniques* 42:137-145.

Rieping M, and Schöffl F (1992). Synergistic effect of upstream sequences, CCAAT box elements, and HSE sequences for enhanced expression of chimeric heat-shock genes in transgenic tobacco. *Mol. Gen. Genet.* 231:226–232.

Ritz D, Patel H, Doan B, Zheng M, Aslund F, Storz G, Beckwith J (2000). Thioredoxin 2 is involved in the oxidative stress response in *E. coli*. *J. Biol. Chem.* 275:2502–2512.

Romier C, Cocchiarella F, Mantovani R, Moras D (2003). The NF-YB/NF-YC structure gives insight into DNA binding and transcription regulation by CCAAT factor NF-Y. *J. Biol. Chem.* 278**:**1336–1345.

Ronchi A, Berry M, Raguz S, Imam A, Yannoutsos N, Ottolenghi S, Grosveld F, and Dillon N (1996). Role of the duplicated CCAAT box region in γ-globin gene regulation and hereditary persistence of fetal hemoglobin. *EMBO J.* 15:143–149.

Rowlands RT, and Turner G (1973). Nuclear and extranuclear inheritance of oligomycin resistance in *Aspergillus nidulans*. *Mol. Gen. Genet.* 126:201-216.

Roy B, and Lee AS (1995). Transduction of calcium stress through interaction of the human transcription factor CBF with the proximal CCAAT regulatory element of the grp78/BiP promoter. *Mol. Cell. Biol.* 15:2263-2274.

Salmon TB, Evert BA, Song B, and Doetsch PW (2004). Biological consequences of oxidative stress-induced DNA damage in *Saccharomyces cerevisiae*. *Nucleic Acids Res.* 32:3712-3723.

Sambrook J, and Russell DW (2001). Molecular Cloning: A Laboratory Manual. Cold Spring Harbor Laboratory Press, Cold Spring Harbor, New York.

Santoro C, Mermod N, Andrews PC, Tjian R (1988). A family of human CCAAT-box-binding proteins active in transcription and DNA replication: cloning and expression of multiple cDNAs. *Nature* 334:218-224.

Sinha S, Kim IS, Sohn K-Y, de Crombrugghe B, Maity SN (1996). Three classes of mutations in the A subunit of the CCAAT-binding factor CBF delineate functional domains involved in the three-step assembly of the CBF-DNA complex. *Mol. Cell. Biol.* 16:328-337.

Sinha S, Maity SN, Lu J, and de Crombrugghe B (1995). Recombinant Rat CBF-C, the third subunit of CBF/NFY, allows formation of a protein-DNA complex with CBF-A and CBF-B and with yeast HAP2 and HAP3. *Proc. Natl. Acad. Sci. USA.* 92:1624-1628.

Spellig T, Bottin A, and Kahmann R (1996). Green fluorescent protein (GFP) as a new vital marker in the phytopathogenic fungus *Ustilago maydis*. *Mol. Gen. Genet.* 252:503–509.

Stadtman ER (1993). Oxidation of free amino acids and amino acid residues in proteins by radiolysis and by metal-catalyzed reactions. *Annu. Rev. Biochem.* 62:797-821.

Stearman R, Yuan DS, Yamaguchi-Iwai Y, Klausner RD, and Dancis A (1996). A permease-oxidase complex involved in high-affinity iron uptake in yeast. *Science* 271:1552-1557.

Steidl S (2001). PhD dissertation, Institut of Microbiology and Genetics, Technical

University of Darmstadt. (In German).

Steidl S, Hynes MJ, and Brakhage AA (2001). The *Aspergillus nidulans* multimeric CCAAT binding complex AnCF is negatively autoregulated via its *hapB* subunit gene. *J. Mol. Biol.* 306:643-653.

Steidl S, Papagiannopoulos P, Litzka O, Andrianopoulos A, Davis MA, Brakhage AA, and Hynes MJ (1999). AnCF, the CCAAT binding complex of *Aspergillus nidulans*, contains products of the *hapB*, *hapC*, and *hapE* genes and is required for activation by the pathway-specific regulatory gene *amdR*. *Mol. Cell. Biol.* 19: 99-106.

Steidl S, Tüncher A, Goda H, Guder C, Papadopoulou N, Kobayashi T, Tsukagoshi N, Kato M, and Brakhage AA (2004). A single subunit of a heterotrimeric CCAAT-binding complex carries a nuclear localization signal: piggy back transport of the preassembled complex to the nucleus. *J. Mol. Biol.* 342:515-524.

Suzuki Y, Tsunoda T, Sese J, Taira H, Mizushima-Sugano J, Hata H, Ota T, Isogai T, Tanaka T, Nakamura Y, et al. (2001). Identification and characterization of the potential promoter regions of 1031 kinds of human genes. *Genome Res.* 11:677–684.

Sybirna K, Guiard B, Li YF, Bao WG, Bolotin-Fukuhara M, and Delahodde A (2005). A new *Hansenula polymorpha* HAP4 homologue which contains only the N-terminal conserved domain of the protein is fully functional in *Saccharomyces cerevisiae*. *Curr. Genet.* 47:172-181.

Tanaka A, Kato M, Nagase T, Kobayashi T and Tsukagoshi N (2002). Isolation of genes encoding novel transcription factors which interact with the Hap complex from *Aspergillus* species. *Biochem. Biophys. Acta* 1576:176-182.

Tanaka T, Nishiyama Y, Okada K, Hirota K, Matsui M, Yodoi J, Hiai H, and Toyokuni S (1997). Induction and nuclear translocation of thioredoxin by oxidative damage in the mouse kidney: independence of tubular necrosis and sulfhydryl depletion. *Lab. Invest.* 77:145-155.

Tarrio N, Prado SD, Cerdan ME, and Siso MIG (2004). Isolation and characterization of two nuclear genes encoding glutathione and thioredoxin reductases from the yeast *Kluyveromyces lactis. Biochim. Biophys. Acta* 1678:170-175.

Tasanen K, Oikarinen J, Kivirikko KI, and Pihlajaniemi T (1992). Promoter of the gene for the multifunctional protein disulfide isomerase polypeptide: functional significance of the 6 CCAAT boxes and other promoter elements. *J. Biol. Chem.* 267:11513–11519

Then Bergh K (1997). PhD dissertation, Institute of Genetics and Microbiology, Ludwig-Maximilians-Universität, Munich. (In German).

Then Bergh K, Litzka O, and Brakhage AA (1996). Identification of a major *cis*-acting DNA element controlling the bidirectionally transcribed penicillin biosynthesis genes *acvA* (*pcbAB*) and *ipnA* (*pcbC*) of *Aspergillus nidulans*. *J. Bacteriol.* 178:3908-3916.

Thön M, Al-Abdallah Q, Hortschansky P, and Brakhage AA (2007). The thioredoxin system of the filamentous fungus *Aspergillus nidulans*: Impact on development and oxidative stress response. *J. Biol. Chem.* 282:27259-27269

Treisman R (1996). Regulation of transcription by MAP kinase cascades. *Curr. Opin. Cell Biol.* 8:205-215.

Tsugita A, Maeda K, and Schurmann P (1983). Spinach chloroplast thioredoxins in evolutionary drift. *Biochem. Biophys. Res. Comm.* 115:1-7.

Tüncher A, Sproete P, Gehrke A, and Brakhage AA (2005). The CCAAT-binding complex of eukaryotes: evolution of a second NLS in the HapB subunit of the filamentous fungus *Aspergillus nidulans* despite functional conservation at the molecular level between yeast, *A. nidulans* and human. *J. Mol. Biol.* 352:517-533.

Uziel O, Borovok I, Schreiber R, Cohen G, and Aharonowitz Y (2004). Transcriptional regulation of the *Staphylococcus aureus* thioredoxin and thioredoxin reductase genes in response to oxygen and disulfide stress. *J. Bacteriol.* 186:326-334.

Van Heeswijck R, and Hynes MJ (1991). The *amdR* product and a CCAAT-binding factor bind to adjacent, possibly overlapping DNA sequences in the promoter region of the *Aspergillus nidulans amdS* gene. *Nucleic Acids Res.* 19:2655- 2660.

Van Vliet A, Ketley J, Park S, and Penn C (2002). The role of iron in *Campylobacter* gene regulation, metabolism and oxidative stress defense. *FEMS Microbiol. Rev.* 26:173–186.

Vuorio T, Maity SN, and de Crombrugghe B (1990). Purification and molecular cloning of the A-chain of a rat heteromeric CCAAT-binding protein: sequence identity with the yeast HAP3 transcription factor. *J. Biol. Chem.* 265: 22480-22486.

Walter M, Chaban C, Schütze K, Batistic O, Weckermann K, Näke C, Blazevic D, Grefen C, Schumacher K, Oecking C, et al. (2004). Visualization of protein interactions in living plant cells using bimolecular fluorescence complementation. *Plant J.* 40:428–438

Ward M (1991). *Aspergillus nidulans* and other filamentous fungi as genetic systems. *In*: Modern microbial genetics. Eds Streips UN and Yasbin RE, Wiley-Liss, New York. pp. 355-496.

Waring RB, **May GS**, **Morris NR** (1989). Characterization of an inducible expression system in *Aspergillus nidulans* using *alcA* and tubulin-coding genes. *Gene* 79:119-130.

Wei SJ, Botero A, Hirota K, Bradbury CM, Markovina S, Laszlo A, Spitz DR, Goswami PC, Yodoi J, and Gius D (2000). Thioredoxin nuclear translocation and interaction with redox factor-1 activates the activator protein-1 transcription factor in response to ionizing radiation. *Cancer Res.* 60:6688–6695.

Weidner G, d'Enfert C, Koch A, Mol P, and Brakhage AA (1998). Development of a homologous transformation system for the human pathogenic fungus *Aspergillus fumigatus* based on the *pyrG* gene encoding orotidine 5'-monophosphate decarboxylase. *Curr. Genet.* 33:378–385.

Workman JL, **and Kingston RE** (1998). Alteration of nucleosome structure as a mechanism of transcriptional regulation. *Annu. Rev. Biochem.* 67:545-579.

Xu WL, Jeanjean R, Liu YD, and Zhang CC (2003). *pkn22* (*alr2502*) encoding a putative Ser/Thr kinase in the cyanobacterium *Anabaena* sp. PCC 7120 is induced by both iron starvation and oxidative stress and regulates the expression of *isiA*. *FEBS Lett.* 553**:**179-182.

Yang J, Xie Z, and Glover BJ (2005). Asymmetric evolution of duplicate genes encoding the CCAAT-binding factor NF-Y in plant genomes. *New Phytol.* 165:623–632.

Yousef N, Elfriede K, Pistorius EK, and Michel KP (2003). Comparative analysis of *idiA* and *isiA* transcription under iron starvation and oxidative stress in *Synechococcus elongatus* PCC 7942 wild-type and selected mutants. *Arch. Microbiol.* 180**:**471-483.

Parts of this thesis are included in the following publications:

1. **Al Abdalah Q §**, Thön M **§**, Hortschansky P, Brakhage AA, 2008. Redox regulation of the CCAAT-binding complex is mediated by the thioredoxin system. **In preparation.**

2. Hortschansky P **§**, Eisendle M **§**, **Al Abdallah Q**, Schmidt A, Bergmann S, Thön M, Kniemeyer O, Abt B, Seeber B, Werner E, Kato M, Brakhage AA, Haas H, 2007. Interaction of HapX with the CCAAT-binding complex - a novel mechanism of gene regulation by iron. *EMBO J.* 26: 3157–3168.

3. Thön M, **Al Abdallah Q**, Hortschansky P, Brakhage AA, 2007. The thioredoxin system of the filamentous fungus *Aspergillus nidulans*: Impact on development and oxidative stress response. *J. Biol. Chem.* 37: 27259-27269.

Minireview articles:

1. Brakhage AA, **Al Abdallah Q**, Tüncher A, Spröte P, 2005. Evolution of beta-lactam biosynthesis genes and recruitment of trans-acting factors. *Phytochemistry* 66:1200-1210.

2. Brakhage AA, Spröte P, **Al Abdallah Q**, Gehrke A, Plattner H, Tüncher A., 2004. Regulation of Penicillin Biosynthesis in Filamentous Fungi. *Adv. Biochem. Engin. Biotechnol.* 88: 45–90.

Other publications:

1. Dietrich C **§**, **Al Abdallah Q §**, Lintl L, Pietruszka A, Maiss E, 2007. A chimeric plum pox virus shows reduced spread and cannot compete with its parental wild-type viruses in a mixed infection. *J. Gen. Virol.* 88: 2846-2851.

§ These authors have equally contributed to this work.

Curriculum Vitae

Name: Qusai Al Abdallah

Date of birth: 31.08.1975

Place of birth: Kuwait

Education:

1981-1985	Primary school, Kuwait
1986-1990	Elementary school, Kuwait
1991-1994	Secondary school, Jordan
1994-1998	B.Sc. in Plant protection, University of Jordan, Amman, Jordan
2000-2002	M.Sc. in Plant biotechnology, Leibniz University of Hannover, Hannover, Germany.

Title: A *Plum Pox Virus* (PPV) chimera as a model for a possible recombination event and its use for detection of homologous recombination of PPV.

Supervisor: Prof. Dr. Edgar Maiss

2002-2008   Ph.D. in Microbiology, Leibniz University of Hannover and Friedrich Schiller University, Jena, Germany.

Title: Regulation of the CCAAT-binding complex of *Aspergillus nidulans* under oxidative stress and iron-depleting conditions.

Supervisor: Prof. Dr. Axel Brakhage

Acknowledgements.

Declaration.

I hereby declare that this work is an original piece of work conducted by myself. I have only used the cited materials and technical means. Moreover, this thesis has never been submitted elsewhere.

Jena, 08th February, 2008   …………………..
                                                                 Qusai Al Abdallah